Pôle de Recherche Cardiovasculaire
Institut de Recherche Expérimentale et Clinique
Université Catholique de Louvain
And
Divisions of Cardiology and Cardiothoracic surgery
Clinique Universitaires Saint-Luc
Brussels, Belgium

Prognosis of Right Ventricle Systolic Function Parameters in Patients with Heart Failure and Reduced Ejection Fraction

Laura Houard

Thesis submitted to obtain the degree of
"Docteur en science médicales"

Promotor: Professor Bernhard Lothar Gerber
Co-promotors: Professor Anne-Catherine Pouleur
Professor Sophie Pierard

THESIS COMMITTEE

Promotor:	Professor Bernhard Lothar Gerber Université Catholique de Louvain, Belgium
Co-promotors:	Professor Anne-Catherine Pouleur Université Catholique de Louvain, Belgium
	Professor Sophie Pierard Université Catholique de Louvain, Belgium
President of the Jury:	Professor Fréderic Lecouvet Université Catholique de Louvain, Belgium
Jury:	Professor Agnès Pasquet Université Catholique de Louvain, Belgium
	Professor Stéphane Moniotte Université Catholique de Louvain, Belgium
	Professor Christophe Beauloye Université Catholique de Louvain, Belgium
	Professor Nina Ajmone Marsan Leiden University Medical Center, Netherlands
	Professor Jérôme Garot Cardiovascular institute Paris Sud, France

ACKNOWLEDGEMENTS

This thesis represents an important milestone of my life. I am the kind of person who used to do everything by the book, so doing a PhD was extremely difficult for me at the beginning because I had to figure out on my own success definition and recipe. There were a lot of ups and downs during this journey, but luckily more ups than downs. This PhD ate a significant portion of my time especially my weekends. I spent long hours devouring the entire right ventricle literature in order to make connections, between my emerging data and the theories I was reading. However, I do and will not regret anything. Overall, it was an amazing experience and I learned two important things: great things come from hard work and perseverance and if you want something done right, you have to do it yourself.

I am extremely grateful to my supervisor, Prof. Bernhard Gerber for his invaluable advice, continuous support (including emotional) and patience during my PhD journey. His immense knowledge and comprehensive experience have encouraged me during the entire time of my academic research and daily life. I could not have imagined having a better advisor and mentor for my PhD. I feel privileged to have worked next to him and to have acquired the best non-invasive imaging experience of my career. Thank you, Bernhard! I would also like to thank Prof. Anne Catherine Pouleur and Prof. Pierard Sophie for their constant encouragement throughout this adventure.

I am thankful to the President of my jury, Prof. Frederic Lecouvet, for his strengthening during our annual meetings. I would also like to express my sincere appreciation to all members of my jury (Prof. Stephane Moniotte, Prof. Agnes Pasquet and Prof. Cristophe Beauloye) for their insightful remarks and constant research challenges.
Importantly, I am grateful for the nice feedback of Prof. Nina Ajmone Marsan and Prof. Jerome Garot. I was very honored to have you both as my external jury. Thank you!
Throughout my doctoral years, I felt lucky to work in a dynamic research and human environment. I shared great moments with Christophe de Meester, Mihaela Amzulescu, Alisson Slimani, Sebastian Militaru, Sibille Lejeune, Thomas Paulus, Anais Gauthey and Helene Langet from Philips research team and all the other fellowmates. Thank you for the

stimulating discussions, for the sleepless nights we were working together (scanning study patients or before abstract deadlines) and for all the fun we have had in the last 3 years.
I would also like to extend my special thanks to my new colleagues from the Cardiovascular Diseases Center of UZ Brussel.
My special thoughts go to my dearest friends Lise Charmillot, Carol Walton, Alexandra de Posson, Celine d'Aoust, Franziska Schutte, Tatiana Verstraeten, Lara Van Cauwenberghe, Francesca Severino and all my volunteers for their strong encouragement, good mood and their valuable time spent in an MRI machine!
I would like to thank my family because without them I might not be the person I am today. Importantly, I would like to deeply thank my eldest sister Alessandra for her support not only throughout my doctoral years but throughout my entire life. I will always be deeply grateful for her continuous support and for giving me the best nephew ever, Maximilian.
Finally, this thesis is dedicated to the two loves of my life Jeremy and my daughter Julia.
Jeremy, without your tremendous understanding and encouragement over the past few years, it would have been impossible for me to succeed this way. Thank you also for helping me with all my presentations, my scientific figures and for listening to my presentations at several congresses all around the world.
Julia, you give me every day the strength to face challenges with confidence since the day you were born. I am so proud and lucky to have you and your father in my life. Both of you, remind me of the goodness in this world and inspire me to be the greatest version of myself.

THESIS OUTLINE

The prognostic role of right ventricular (RV) systolic function in left ventricular (LV) heart failure (HF) has been overlooked for many years mainly due to a limited number of imaging techniques available for the RV visualization. However, recent development in cardiac imaging, in particular the development of deformation imaging techniques such as speckle tracking echocardiography (STE) and cardiac magnetic resonance feature tracking (cMR-FT) seems to have changed this situation.

Therefore, the primary objective of our work was to perform a clinical validation of these new modalities bringing out the results on their variability day-to-day and secondly to compare their additional prognostic value with cMR right ventricular ejection fraction (RVEF), in predicting outcome in patients with heart failure and reduced ejection fraction (HF-rEF). Lastly, we performed a clinical validation of the pulmonary transit time assessed by cMR in comparison of cMR-FT and cMR-RVEF in the same type of population.

Chapter I introduces firstly an overview of the right ventricle (RV) anatomy, physiology and physiopathology as well as the notion of myocardial deformation and its relationship with cardiac function and contractility. An important part is dedicated to the detailed description of right heart imaging techniques highlighting the advantages and limitation of each of them and the current problems of intra and inter-modalities inconsistencies in deformation imaging. Thereafter, some clinical considerations on the prognostic applicability of these techniques in HF-rEF patients underlining the importance of RV systolic function in this population.

After staging the aims of this thesis in **Chapter II**, the methods and results are structured in **Chapter III**, comprising three articles. Article 1 reveals with the variability day-to-day of STE and cMR-FT. Article 2 comprises the comparison of RV- STE and RV-FT versus the gold standard of RV systolic function in predicting mortality in HF-rEF patients and finally, article 3 describes the additional prognostic value of pulmonary transit time also in advanced HF.

Finally, a discussion summary and future direction are laid-out on **Chapter IV**.

TABLE OF CONTENTS

I. INTRODUCTION

THE FORGOTTEN CHAMBER, THE RIGHT VENTRICLE

The assessment of right ventricular function by non-invasive cardiac imaging has recently encountered much attention since it has been shown to represents a major parameter impacting the treatment and prognosis of patients with multiple heart pathologies independently of the left ventricular ejection fraction (LVEF) (1) (2).

While attempting to understand and describe right ventricular systolic function, we believe it is essential to understand two relevant points:

1. The normal anatomy of the right ventricle including its structural architecture responsible for the complex contractile mechanism that produces the myocardial deformation.

2. The physiology and physiopathology of the right ventricle.

1.1. OVERVIEW OF THE RIGHT VENTRICLE ANATOMY

The RV, the most anterior cardiac chamber, is a thin-walled crescent-shaped structure coupled to systemic venous return on one side and to the pulmonary circulation on the other. The RV is anatomically and functionally distinct from the LV, and therefore, our knowledge of LV physiopathology cannot be directly extrapolated to the right heart. It is 10% to 15% larger in volume (resulting on a slightly lower ejection fraction) than the LV with a thinner free wall (3 to 5 mm in the adult) as a consequence of the lower ventricular pressures (Laplace's law) and has a muscular mass of only 25% of the LV mass(3). The crescent shape and the thin wall make the RV more compliant than the LV. Accordingly, the RV is well suited as a volume pump, but is prone to failure when faced with an acute pressure challenge. **Table 1** illustrates the principal differences between the RV and the LV.

	Right Ventricle		Left Ventricle
Embryological origin	Primary heart field		Secondary Heart field
Shape	Triangular		Ellipsoid
Trabeculation	Coarse		Fine
AV valve with septal insertion of the chordae	Yes		No
Mass	26 ± 5 gr/m^2	<<	87 ± 12 gr/m^2
Thickness	2 à 5 mm	<<	7 à 11 mm
End diastolic volume	75 ± 13 ml/m^2	>	66 ± 12 ml/m^2
Ventricular Pressure (S/D)	25/4 mmHg	<<	130/8 mmHg
Ejection fraction	> 40 - 45 %	<	> 50 %
Elastance	1.3 ± 0.84 mmHg/ml	<<	5.48 ± 1.23 mmHg/ml
Vascular Resistance	20-130 dyne.s.cm^{-5}	<<	700-1600 dyne.s.cm^{-5}
Indexed ventricular work	8 ± 2 gr/m^2	<<	50 ± 20 gr/m^2
Physiologic pump condition	Low- resistance, low capacitance pump; peristaltic-like motion from inflow to outflow during ejection		High- resistance, high pressure pump; dominant radial thickening and contraction during ejection
Resistance to ischemia	Better resistance		More sensitive
Pathological remodeling	Better for volume overload		Better for pressure overload
Flow characteristics	No or minimal isovolumic periods; hangout periods		Well-defined isovolumic contraction and relaxation; no hangout period.
Other characteristics	Muscular discontinuity between tricuspid and pulmonary valve		Fibrous continuity between mitral and aortic valve.

Table 1 Differences between right ventricle and left ventricle.

AV indicates atrioventricular; S, systolic and D, diastolic.

The RV can be described in terms of three different components: **inlet, apical and outlet** with three walls (anterior, inferior and lateral) (4).

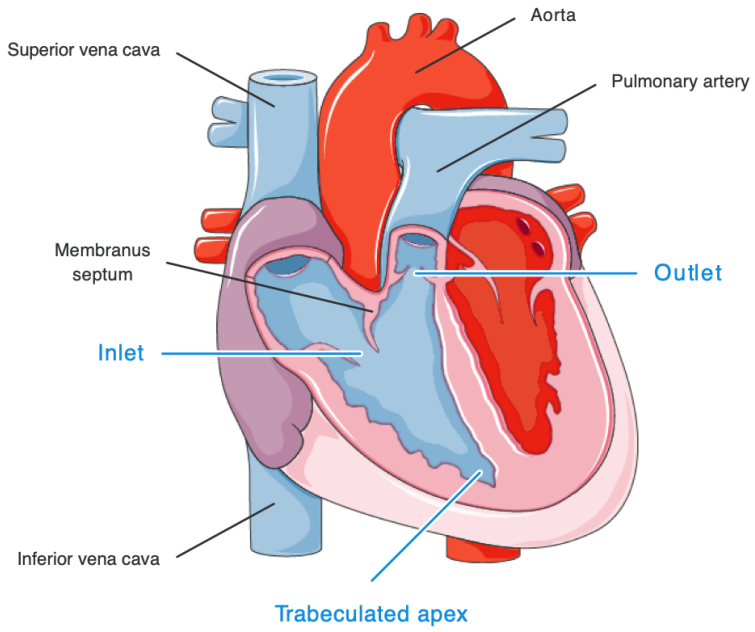

Figure 1 The different components of the right ventricle

1**) The inlet portion** extends from the atrio-ventricular (AV) junction to papillary muscle attachment of the AV valve and contains the tricuspid valve, tendinous chords, and 3 or more papillary muscles.

2) **The trabeculated apex**, often very thin (which may make this portion more susceptible to increased wall stress), is characterized by coarse trabeculations and by the presence of the trabecular septomarginalis (TSM), a prominent Y-shaped muscular strap that proximally is linked with the anterior papillary muscle through the moderator band and distally bifurcates into two limbs, one anterior joining the structural free wall and one posterior lying over the membranous septum. The two limbs of the TSM accommodate the crista supraventricularis which separates the RV inlet and outlet components and, when shortening, it contracts the tricuspid annulus and pulls the free wall toward the septum(5).

3) **The outlet**, infundibulum or conus is a tubular muscular structure that supports the pulmonary valve leaflets.

1.2. MYOARCHITECTURE

There are only 2 distinct myocardial **"layers"** in the RV as compared to the LV which also possesses a 'middle' layer. The **superficial layer** is formed by predominantly **circumferential** myocyte aggregates parallel to the atrioventricular groove that extend from one ventricle to another. The **inner layer** is composed mostly of arranged **longitudinal** myocytes that pass through the apex toward the papillary muscles, tricuspid annulus, RV outflow tract (RVOT) and continue into the superficial layer of fibres of the LV. This binds the ventricles together and represents one of the component of the biventricular functional systolic and diastolic interdependence (6) , together with the sharing of the interventricular septum, and the pericardial by the two ventricles(3). It also explains that both ventricles work as a single unit. Indeed, the LV is an important contributor to RV ejection: in experimental models, LV contraction generates 20% to 40% of both RV stroke volume (SV) and pulmonary flow(7).

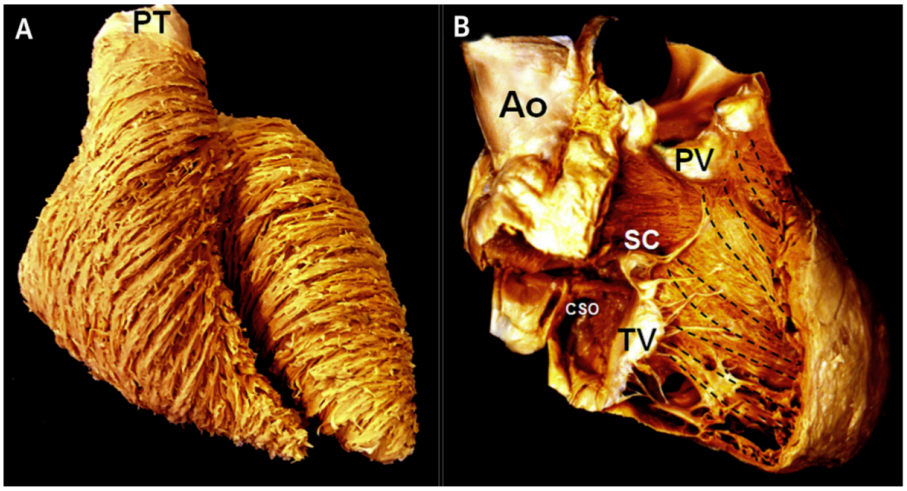

Adapted from Sanz et al. JACC imaging, 2019(8)

Figure 2 Right ventricle myoarchitecture. **A**: illustrates the circumferential arrangement of superficial RV and middle LV layers from a front view of the heart. **B**: shows the inner layer of the RV with longitudinally myocyte aggregates (black dashed lines). AO indicates aorta; CSO, Coronary sinus ostium; LV, Left ventricle; PT, pulmonary trunk. SC, supraventricular crest, TV, tricuspid valve and PT, pulmonary valve.

The **free wall** is composed predominantly of **transverse fibres**, whereas the **septum** contains **oblique helical fibres** without a transverse component. Interestingly, the RV outflow tract contains also oblique fibres but not the RV free wall explaining why the RV does not form a helix(9). This arrangement of muscle fibres within the RV wall contribute to the movement of the RV free wall towards the septum and to the base to apex movement of the free wall.

The RV contracts in a highly synchronized way that occurs 20 to 50 ms earlier in the inlet and apex than the outlet (infundibulum), resulting in a peristalsis-like motion facilitating blood flow into the pulmonary artery (10) (**Figure 3**).

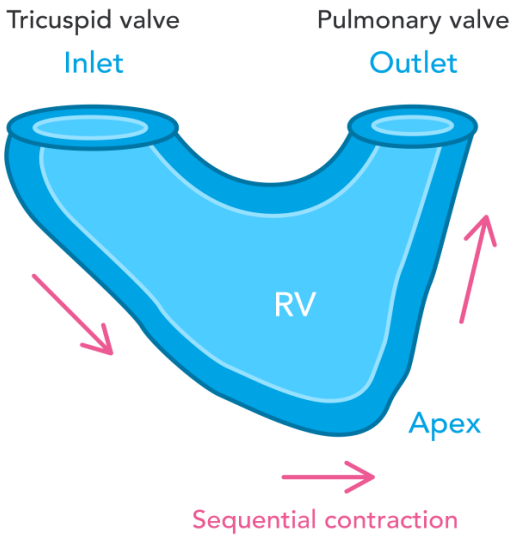

Figure 3 Schematic view of the right ventricle pointing out its sequential contraction. RV indicates Right ventricle.

1.3. CARDIAC FUNCTION

The accurate evaluation of cardiac function would imply the assessment of the true contractility of the myocardium, defined as the inherent capacity of the muscle to contract independently of changes in the preload or afterload, and reflecting the inotropic state of the myocardium.

Indeed, the functional properties of the cardiac muscle – how much tension it can develop, how rapidly it can contract – depend mainly on these two parameters: **preload** and **afterload**:

- The term **preload** indicates the load imposed on the cardiac muscle **before contraction** (by the end of diastole) and is proportional to the maximum elongation of myocardial fibers. The **end-diastolic volume** (EDV, the moment of maximal stretch of myocardial fibers before isovolumic contraction) is the equivalent of the initial sarcomere length and is a measure of preload.

- The **afterload** is defined as the additional load imposed on myocardial fibers by the ventricular pressure increase **during contraction**. In other words, it is the force that the contraction myocyte must overcome during ejection. RV afterload is determined by the filling pressures of the left ventricle and the resistance of the pulmonary circulation. In clinical practice, **pulmonary vascular resistance (PVR)** is the most frequently assessed index of RV afterload, although is far from being the perfect estimate of it. It can also be measured as **arterial elastance (Ea)** which is the change in pressure per unit change in volume (11).

1.3.1. Myocardial contractility and deformation

In an isolated myocyte under no load, contractility generates force and force development leads to shortening. However, in a loaded heart, there is a combination of **isometric contraction** (contraction with tension development without shortening) if the load is greater than the tension developed, and **isotonic contraction** (shortening without increasing tension) if the tension exceeds the load (**Figure 4**).

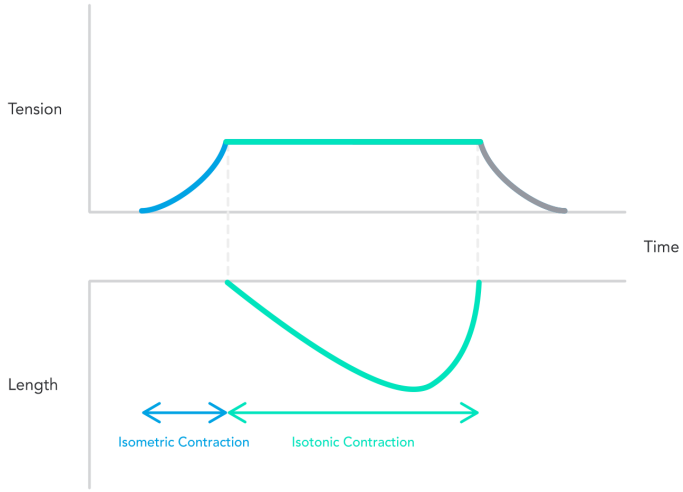

Figure 4 In a loaded heart, the muscle will increase tension with no shortening as long as the tension is below the load (isometric contraction). When tension exceeds the load imposed on the muscle fibers begins to shorten and the tension remains constant (isotonic contraction).

Adapted from Stoylen http://folk.ntnu.no/stoylen/strainrate/

The interaction between load and inotropy (i.e. contractility) is quite complex and is beyond this thesis. However, it is essential to understand that an increase in afterload or a decrease in contractility will result in less shortening, while both increased preload or increased contractility will result in more shortening. This point is well explained in **Figure 5, 6 and 7**.

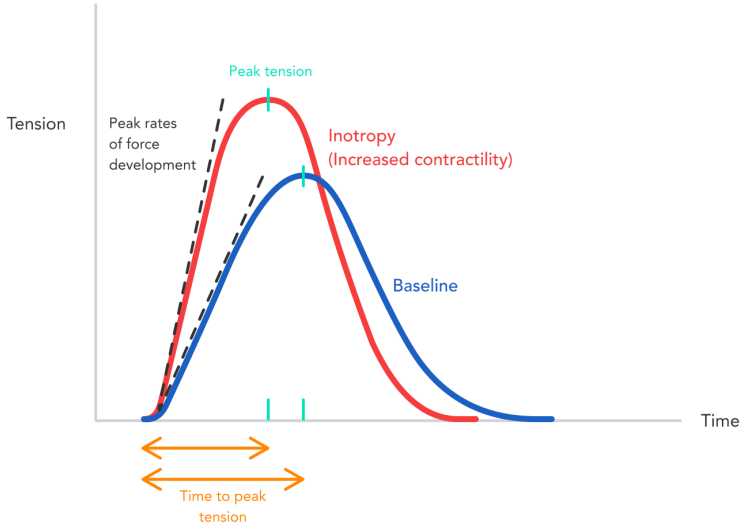

Figure 5 illustrates the effect of inotropy (for example noradrenaline), showing an increase in both peak tension, and rate of tension development and a shortening of time to peak tension.

Adapted from Stoylen http://folk.ntnu.no/stoylen/strainrate/ and Sonneblick, Am J Physiol 1962.

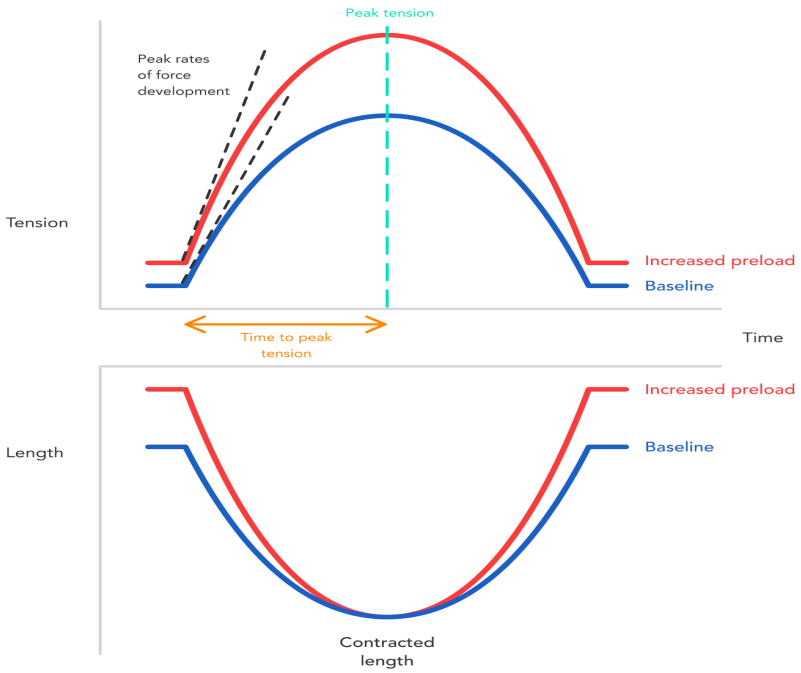

Figure 6 illustrates the effect of preload, showing an increase in both peak tension and the rate of tension development but the time to peak remains unchanged.

Adapted from Stoylen http://folk.ntnu.no/stoylen/strainrate/ and Sonneblick, Am J Physiol 1962.

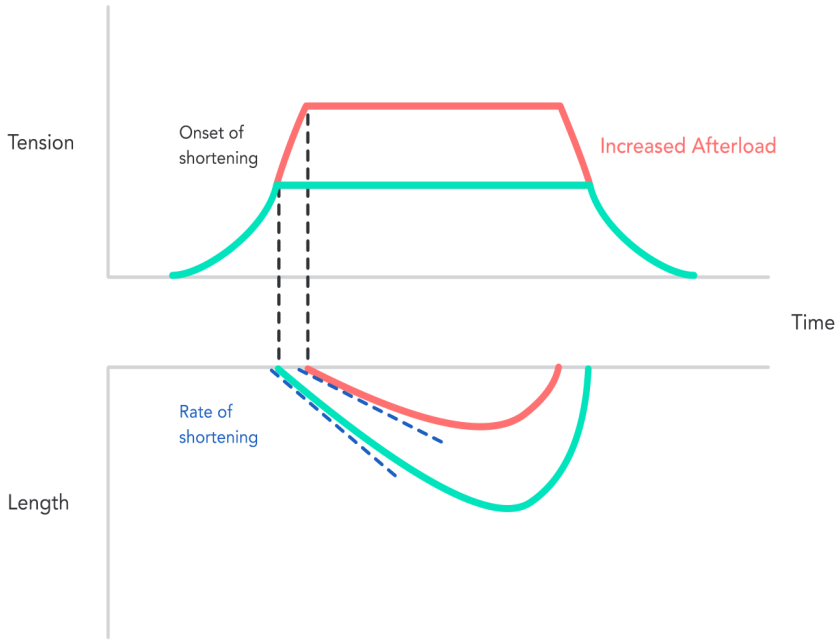

Figure 7 illustrates the effect of afterload, showing a decrease in the velocity of fibers shortening as well as less shortening.

Adapted from Stoylen http://folk.ntnu.no/stoylen/strainrate/ and Sonneblick, Am J Physiol 1962.

Additionally, there is clearly an intimate relationship between preload and afterload so that the two cannot be easily dissociated. Therefore, RV systolic function results from the complex interplay of RV contractility (12), RV preload and afterload. This concept is called "**ventricular-vascular coupling**" (or hemodynamic coupling) (5).

Finally, yet no less importantly, RV systolic function can also be influenced by ventricular interdependence, heart rhythm, and synchronicity of ventricular contraction (4).

1.4. OVERVIEW OF RIGHT VENTRICLE PHYSIOLOGY

The RV is a high-volume pressure pump(3). The end-systolic pressure in the RV is approximately six times lower than in the LV because it is coupled with low impedance and highly compliant vascular bed (4) Therefore, both of them pump the same stroke volume but the RV use only 25 % of the stroke work used by the LV.

1.4.1. Volume-pressure relationship

The length - tension relation in isolated muscle is equivalent to the pressure - volume relation in the intact heart. Therefore, contractility would represent the volume variation for a given pressure build-up.

Figure 8 illustrates the Pressure Volume (PV) loop relationship for a single cardiac cycle for the LV (represented in red) and the RV (represented in blue). The RV PV loops have a triangular shape because the isovolumic stages in the RV, and in particular the isovolumic relaxation, are not well defined. Consequently, it is harder to identify the end-systolic point, which results in a higher degree of uncertainty in the estimation of the slope of the PV relationship at end systole, as compared to the LV. Indeed, the main challenge is the assessment of RV contractility from elastance (ESPVR relationship).

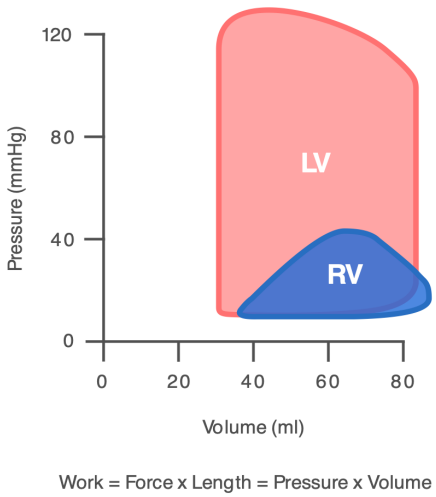

Figure 8 LV and RV Pressure volume loop diagram of a single cardiac cycle obtained by a catheterism where pressure is plotted against volume.

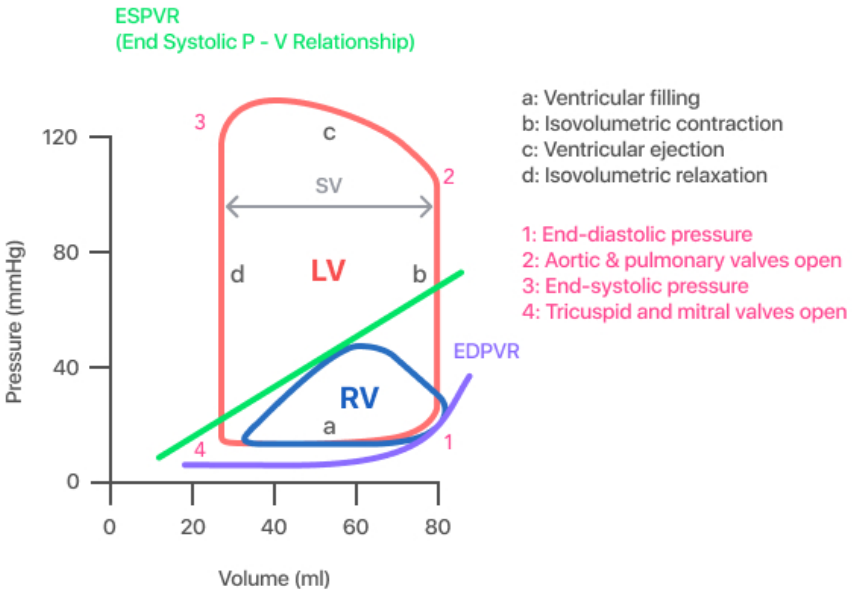

Time runs around the loop in a counterclockwise direction**.** The loop (or cycle) can be divided into four basic phases: ventricular filling (phase **a**; diastole), isovolumetric contraction (phase **b**; systole), ejection (phase **c**; systole), and isovolumetric relaxation (phase **d**; diastole). **Point 1**: Pressure and volume at the end of ventricular filling, and therefore represents the end-diastolic pressure and end-diastolic volume (EDV) for the ventricle.

At this time point, the mitral and tricuspid valves close. **Point 2**: Aortic and pulmonary valves will open. **Point 3**: the pressure and volume at the end of ventricular contraction, and therefore represent the end-systolic pressure and end systolic volume (ESV). **Point 4:** Tricuspid and mitral valves will open.

In the pressure-volume plane, the RV-PV loop is confined between two curves: the end-systolic pressure-volume relationship (**ESPVR**) and end-diastolic pressure-volume relationship **(EDPVR**). The green, dotted line touching the loop is the **ESPVR**, the maximal pressure that can be developed by the right ventricle at any given right ventricular volume and represents the **RV end-systolic elastance** which is a usually an acceptable approximation for **maximum elastance(3) .**The maximum elastance is the gold standard estimate of contractility and takes place just before end-systole in the normal RV and at end systole in the presence of pulmonary hypertension. The purple dotted line is the **EDPVR**, is the passive tension that the diastolic filling generates. The slope of the EDPVR at any point along the curves is the reciprocal of ventricular **compliance**. The area within the loop represents the ventricular stroke work. The width of the loop represents the difference between EDV and ESV, which is by definition the stroke volume (SV).

According to this diagram, it becomes obvious that myocardial contractility cannot be measured non-invasively, as it would require invasive volume and pressure recordings. Therefore, any kind of cardiac imaging, which is based on visualization of either wall deformation (strain) or cavity deformation (ejection fraction), can only be measure shortening never contractility. Moreover, only a fraction of myocardial work, the isotonic work, can be appreciated by imaging while the greatest part of the ventricle work, the isometric work, cannot be described by any imaging modality.

Finally, as shortening is secondary to force and load interaction, all deformation imaging methods are load dependent and should ideally be interpreted with knowledge of preload and afterload in the context on interdependence of inotropy and loading.

1.5. PATHOPHYSIOLOGY OF THE RIGHT VENTRICLE IN LEFT SIDED HEART FAILURE

First of all, let us introduce the definition of heart failure (HF) which is a clinical syndrome characterized by typical symptoms (e.g. breathlessness, ankle swelling and fatigue) that may be accompanied by signs (e.g. elevated jugular venous pressure, pulmonary crackles and peripheral oedema) caused by structural and/or functional cardiac abnormality, resulting in a reduced cardiac output and/or elevated intracardiac pressures at rest or during stress (13). HF includes a wide range of patients: from those with normal LVEF (≥50%) to those with reduced EF (<40%, HFrEF). Patients with a LVEF in the range of 40-49% is recently defined as heart failure mid-range ejection fraction (HFmrEF).

RV dysfunction is highly prevalent in HFrEF and it may be a sensitive indicator of poor prognosis in this type of population. Indeed, right ventricular status constitutes most of the time a “common final pathway “in the progression of congestive heart failure because the multiple influences affecting the right ventricular function due to left ventricular failure. RV dysfunction not only include changes in global RV systolic function but also abnormalities in the pattern of contraction and synchrony.

RV dysfunction may develop in association with LV dysfunction by several mechanisms:

1) An increase in afterload due to the increase of pulmonary venous and consequently pulmonary arterial pressure partly augments as a protective mechanism against pulmonary oedema (14)

2) A myocardial ischemia or a cardiomyopathic process affecting both ventricles.

3) A decrease in systolic driving pressure of right ventricular coronary perfusion caused by LV dysfunction, which may be a substantial determinant of right ventricular function(15)

4) A septal dysfunction via the interventricular dependence

5) A LV dilatation which may restrict right ventricular diastolic function in a limited pericardial compartment.

Nevertheless, RV dysfunction may also result from other conditions such as right-sided cardiomyopathies, valvular heart disease, congenital heart disease, RV infarction or from RV pressure overload in pulmonary hypertension.

1.6. IMAGING THE RIGHT HEART

The ideal imaging technique for assessment of right ventricular function would be widely available, non-invasive, providing a cheap, fast, accurate and reproducible assessment with no need for ionizing radiation or contrast administration. Unfortunately, no technique in cardiology meets all these requirements and its assessment continues to represent a challenge for the modern-day cardiology practice. Moreover, as previously mentioned, all parameters of RV systolic function are highly dependent on preload and afterload and its unique crescent shape adds even more complexity to the quantification of its size and function.

There are several modalities for the assessment of RV but in clinical practice, its initial evaluation usually starts with a two-dimensional transthoracic echocardiography (2D-TTE) and can be carried on, depending on initial findings, with complementary imaging technique such as three-dimensional (3D) -TTE, deformation imaging techniques, cardiac magnetic resonance (cMR), cardiac CT or scintigraphy.

To date, 2D-TTE and cMR are by far the most validated techniques, having references values for different parameters of RV function. Nowadays, the new flashlight of cardiac imaging is undoubtedly deformation imaging techniques such as speckle tracking echocardiography (STE) and feature tracking (FT). It is hoped that the RV assessment by deformation imaging techniques will soon gather enough evidence, from larger studies to potentially extend its application to clinical practice.

Another promising tool to assess indirectly right ventricular function is pulmonary transit time by cMR because it includes information not only from the right and left function but also the pulmonary congestion which influences the right ventricular systolic function. Importantly, it can be automated and easily made from routine clinical cMR.

In this chapter we will discuss about the most used non-invasive modalities for RV assessment and their measured parameters as well as their prognosis role in heart failure.

1.6.1 ECHOCARDIOGRAPHY

Two-dimensional echocardiography is still the first-line imaging technique used to assess the RV morphology and function and will probably remain so for the foreseeable future.
However, the assessment of RV function is challenging because of its retrosternal position and the complex geometry of the right ventricle with the inflow and outflow components not in the same plane. Furthermore, the poor acoustic windows often present in heart failure patients and the modest tissue characterization (especially the difficulty to differentiate the thin free wall from adjacent structures) limit even more the echocardiographic approach.

Nevertheless, echocardiographic assessment is fast, cheap and readily available and provides a relatively good general assessment of RV function, although frequently based on qualitative estimation.

For echocardiographic assessment, the right ventricle (RV) is usually divided into an **anterior, inferior, and lateral** (free) wall, as well as **basal, mid, and apical segments**.

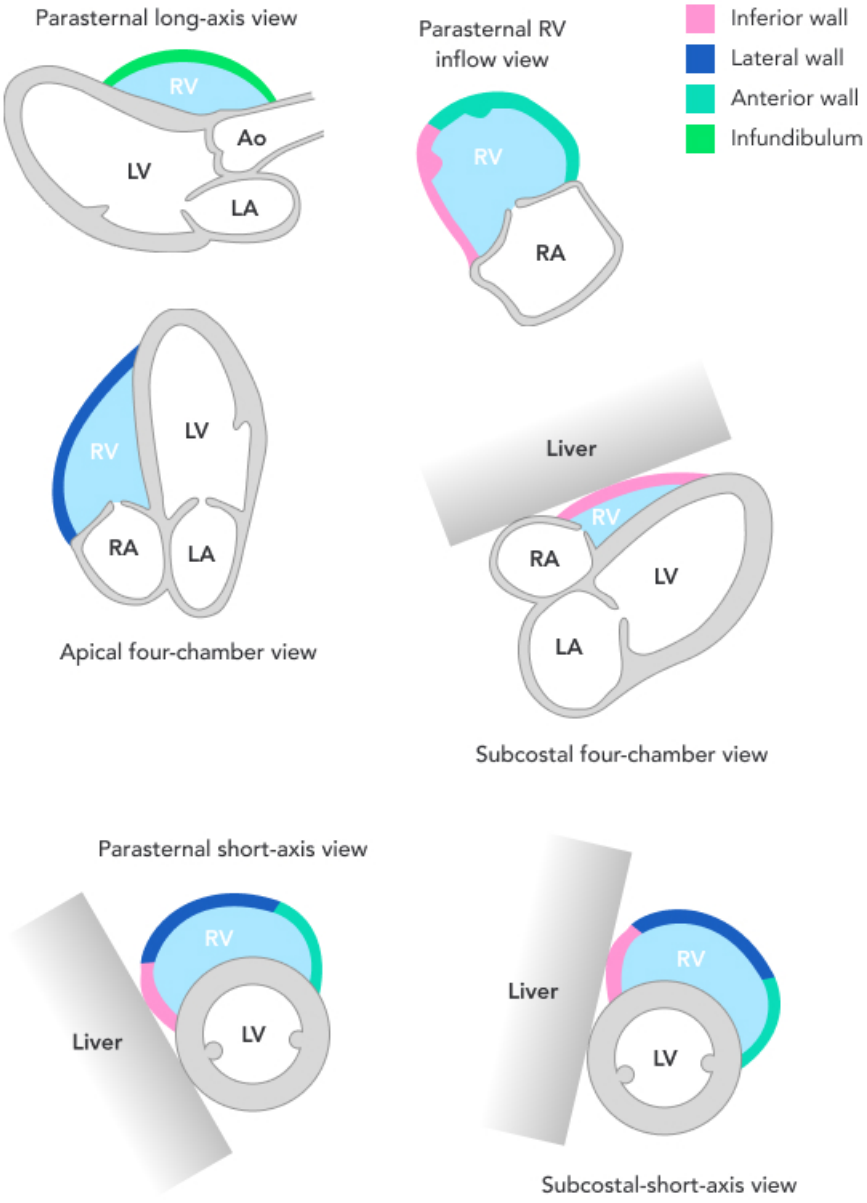

Figure 9 Right ventricle transthoracic echocardiographic views

Adapted From Venkatachalam et al. Echocardiography 2017.(16)

In an attempt to standardize the echocardiographic evaluation of the right heart, the American Society of Echocardiography published a guideline document, endorsed by the European Association of Cardiovascular Imaging, on measures and normal reference values of several echocardiographic parameters to identify RV pathology (17) highlighting three important points:

- The importance to obtain a **RV focused chamber view** with the LV apex at the center of the probe (to display the largest basal RV diameter and thus avoiding foreshortening). Indeed, the conventional apical four-chamber view focused on the left ventricle results in considerable variability in how the right heart is sectioned, and consequently, RV linear dimensions and areas may vary widely in the same patient with relatively minor rotations in transducer position (**Figure 10**).

- **The load dependency** of all echocardiographic parameters and the need to evaluate routinely the systolic pulmonary artery pressure with an estimation of peak tricuspid regurgitation (TRV) velocity and right atrial pressure derived from inferior vena cava size and collapse to complete the RV echocardiographic assessment.

- **The lack of a single echocardiographic parameter reliable enough to be universally accepted for assessing RV function** explaining why current guidelines recommend the use a combination of parameters to assess RV systolic function by echocardiography.

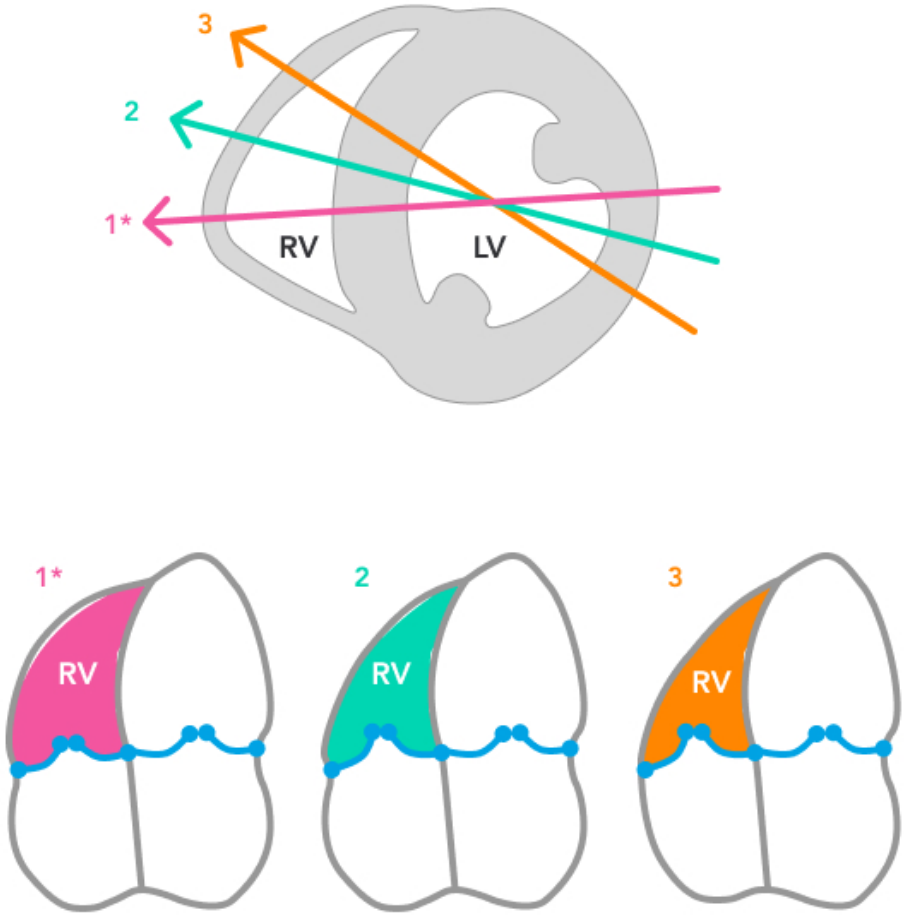

Figure 10 Variability of the right ventricular size with angular change despite similar size and appearance of the left ventricle. A, B and C lines on the mid short-axis view represent the lines of intersection of the 4 chamber view plane where A is a right ventricular focused showing the largest basal RV diameter.

Table 5 summarizes the most common RV echocardiography parameters used to assess RV geometry and systolic /diastolic function and their reference values. These reference values are based on published mean and SD data obtained from normal adult individuals without any histories of heart or pulmonary disease.

Variable	Unit	Cut off	how and where?	Requirements	Relevant comments
Chamber dimensions					
RV basal diameter	cm	**≤4.1**	4ch-RV focused view, end diastole	Optimal endocardial definition of the RV free wall and the apex.	RV dimensions are dependent on probe rotation and different RV views.
RV mid cavity diameter	cm	**≤3.5**	4ch-RV focused view, end diastole		
Longitudinal diameter	cm	**≤8.6**	4ch-RV focused view, end diastole		
RVOT diameter proximal in PLAX	cm	**≤3**	PLAX, From the anterior RV wall to the IV septal-aortic junction.	Optimal endocardial definition of the RV anterior wall.	Dependent on image plane position. Regional measure may not reflect global RV size.
RVOT diameter in SAX	cm	**<3.4**	SAX, end diastole		
RV wall thickness	cm	**≤0.5**	Subcostal view, end-diastole at the level of the tip of the anterior tricuspid leaflet.	Trabeculae, papullary muscles and epicardial fat should be excluded.	Challenging in case of thickening of visceral pericardium. There is no criterion for defining an abnormally thin RV wall .
Systolic function					
RV FAC (end-diastolic area—end-systolic area/end-diastolic area ×100)	%	**≥35**	4ch-RV focused view	Adequate image quality. Trabeculations, papillary muscles and moderator band should be include in the cavity area.	May not reflect global RV size RV size underestimation if RV cavity is foreshortened .
TAPSE The amount of longitudinal motion of the annulus at the systolic peak	mm	**≥17**	4ch- RV focused view, M Mode cursor aligned along the direction of trcuspid lateral annulus	The M-mode cursos need to be placed parallel to the plane of longitudinal motion (angle dependency).	TAPSE predominantly reflects RV longitudinal function so in patient with regional wall-motion abnormalities as in some cases of severe pulmonary arterial hypertension, the TAPSE can be misleading. Alternatively, the RV function may be globally preserved despite significantly reduced TAPSE, as often seen after cardiac surgery (24).
Pulsed doppler peak annular velocity (S')	cm/s	**≥9.5**	4ch- RV focused view; cursor at the level of the trcuspid lateral annulus using pulsed tissue Doppler and colour-code tissue Doppler.		Not fully representative of RV global function, particularly after thoracotomy, pulmonary thrombo-endarerectomy or heart transplantation.
TEI INDEX (isovolumetric relaxation time + isovolumetric contraction) / ejection time)	**-**	**Tei Index ≤ 0.43 by PW Doppler and ≤ 0.54 by DTI**		Oberserver expertise is crucial since the time intervals being measured are often difficult to delineate, and small variation can lead to substantial differences in the final calculated value(6).	Reflects both systolic and diastolic function of the RV (25) because it also takes into consideration the isovolumic relation period of the RV. Can be falsely in conditions associated with elevated RA pressures, which will shorten the IVRT.
3D-derived RVEF	%	**≥45**		Adequate image quality, patient cooperation and regular rhythm.	
Diastolic function					
E/A ratio	-	**0.8- to 2.1**	4ch- RV focused view		
E/E' ratio	-	**≤6**	4ch- RV focused view		
IVC diameter	cm	**≤2.1**	Subcostal view		
IVC collapse during inspiratory sniff	%	**≥50**	Subcostal view		
Hepatic vein velocity ratio	-	**Systolic >diastolic**	Subcostal view		

Adapted from five publications (18) (17) (18) (19) (20) 6)

Table 5 RV indicates right ventricle; 4ch, four chamber; RVOT, right ventricular outflow tract; PLAX, parasternal long axis; IV, interventricular; SAX, short axis view; FAC, fractional area change; TAPSE, tricuspid annular plane systolic excursion; PW, pulsed wave; DTI, tissue doppler echocardiographic; RA, right atrial; IVRT, isovolumetric relaxation time; RVEF, right ventricular ejection fraction and IVC, inferior vena cava.

1.6.1.1. Assessment of right ventricular size by echocardiography

The RV geometry evaluation is performed at **end-diastole** by measuring RV linear dimensions and the RV wall thickness.

RV linear dimensions include three different widths (basal, mid-cavity, and longitudinal diameter), which are assessed in a RV focused view, while the RV wall thickness is measured in a subcostal view. RV relative size should always be compared with the LV diameter to help in determination of RV dilatation.

1.6.1.2. Assessment of the right ventricular systolic function by echocardiography

In contrast to the LV assessment, it is not recommended to perform right ventricular ejection fraction derived from RV volumes in 2D echocardiography mainly because there is no geometric model that enables an estimate of its volumes on the basis of a 2-dimensional measurement.

Still, it is possible to assess some surrogate parameters such as RV fractional area (**RV FAC**), tricuspid annular plane systolic excursion (**TAPSE**), systolic excursion velocity of lateral tricuspid annulus by means of Tissue Doppler Imaging (**TDI S'**), RV index of myocardial performance (**TEI index)** and RVEF by 3D tridimensional echocardiography (3DE) **(Table 5)**.

All these parameters are also load-dependent so their appropriate clinical interpretation requires considering the load of the myocardial fibres, which may vary according to chamber geometry, wall thickness or cavity pressures

1.6.1.3 Correlation and reproducibility

The correlation of the RV 2D- echocardiographic parameters with cMR is sometimes discordant in the literature (**Table 6**), as well as the reproducibility of these parameters. Additionally, interstudy reproducibility is currently not known.

	Population	Sample size	TAPSE	TDI S'	RIMP	FAC
Anaverkar et al. Echocardiography 2007	Consecutive patients undergoing a cMR	36	0.17 P>0.05	NR	NR	0.8 p<0.001
Leong et al. Echocardiography 2012	Systolic HF	83	0.65 (p<0.001)	0.5 (p<0.001)	0.28 (p=0.03)	0.71 (p<0.001)
Vizzardi et al. J ulrasound med 2015	Chronic HF	31	0.54 (p<0.01)	0.81 (p<0.01)	NR	0.07 (p>0.05)
Focardi et al. Eur Heart J Cardiovasc Imaging 2015	Mixed population	63	0.45 (p=0.01)	0.52 (p=0.01)	NR	0.77 (p<0.001)
Li et al. Thromb Res 2015	Chronic thromboembolic PH	32	0.45 (p>0.05)	0.69 (p<0.01)	0.39 (p=0.04)	0.42 (p=0.02)
Lu et al. Echocardiography 2015	Mixed population	60	0.27 (p>0.05)	0.2 (P>0.05)	-0.36 (p>0.05)	0.33 (p=0.02)

Table 6 Correlation of RV echocardiographic parameters with cardiac magnetic resonance derived right ventricular ejection fraction. cMR indicates cardiac magnetic resonance; HF, heart failure; PH, pulmonary hypertension; TAPSE, tricuspid annular plane systolic excursion; TDI, tissue doppler imaging; RIMP or Tei Index, right ventricular index of myocardial performance and FAC, fractional area change.

Adapted from Longobardo et al. (22)

Nevertheless, RVEF by 3DE seems to be more reliable and have better reproducibility(21) (22) but the feasibility of this technique is still poor since it is extremely dependent on image quality, regular rhythm, and patient cooperation.

1.6.2. CARDIAC MAGNETIC RESONANCE

CMR is independent of geometric assumption (23) and has the extraordinary ability to image in any desired plane and with a nearly unrestricted field of view. In addition, its inherent 3-dimensional nature makes it particularly well suited to studying the RV.

Thus, despite continuous improvements in echocardiography, cMR is still considered to be the most accurate imaging technique. The main advantages of CMR over non-invasive cardiac imaging modalities are accuracy, reproducibility, unrestricted field of view, lack of ionizing radiation, and the ability to characterize myocardial tissue. Indeed, cMR is the reference to study the morphology, volume, function, and tissue determination of the RV with some limitation related to availability, costs, and presence of patient-related contraindications.

1.6.2.1. Assessment of RV systolic function by cardiac magnetic resonance

Typically, analysis of right ventricular systolic function consists of manual or semi-automatic contouring of the inner and outer boundaries (epicardial and endocardial) at end diastole and end-systole using a **short axis** or an **axial cine** stack without the need to make any geometrical assumptions, and therefore applies to ventricles of all sizes and shapes, even to those that have been extensively remodeled (**Figure 11)**.

Interstudy reproducibility of LV and RV measurements using a **short axis** orientation is relatively good (24) but the reproducibility is apparently better when measuring the RV using an axial stack (25) because it provides a better delineation of the mitral and tricuspid valves. However, the short axis view has the advantages that this orientation allows both ventricles to be measured simultaneously.

A number of analysis software packages are available for automated post-processing that provide a fast analysis of ventricular function, both systolic and diastolic, in most patient, and normal reference ranges have been reported for the RV (26).

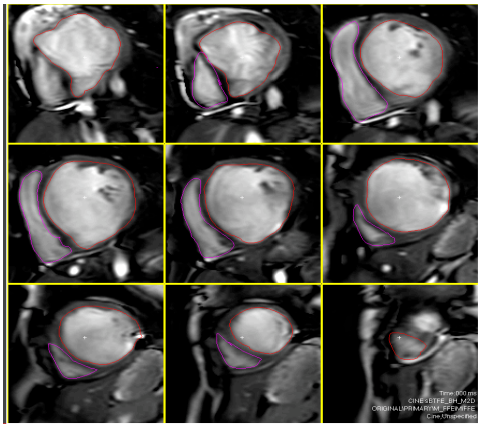

Figure 11 Short axis view allowing the measurement of LVEF and RVEF by contouring the inner and outer boundaries at end diastole and end-systole.

1.6.2.2. Reproducibility of the measurement

cMR is by far the most reproducible measurement to assess both LV and RV systolic functions (27,28). RV interstudy variability was reported as 6% for end-diastolic volume, 14% for end-systolic volume, 8% for ejection fraction, and 9% for RV mass(24)

Moreover, cMR has been shown to have considerable improvement in interstudy reproducibility compared with echocardiography, the sample size reduction through its use compared with echocardiography are considerable, ranging from 55% to 93%.(29)

1.6.2.3. Limitation

Although software programs are more automated and the contrast between flowing blood and the myocardium in SSFP images is most of the time excellent, the precise placement of the contours is reader-dependent and training is highly recommended due to the subjective nature of contour placement. Indeed, a study from seven cMR centers showed slight biases in the demarcation of inner and outer boundaries leading to integrated differences in overall mass and volume (30). Therefore, care should be taken when comparing patient results between centers.

The main sources of errors in mass and volumes are the demarcation of the base near the atrioventricular valves and outflow tracts, due to the difficulty of separating the ventricular from the atrial myocardium and the large motion of the base through the plane of the short

axis (slice thickness are typically 6-10mm) giving rise to significant partial voluming (mixture of different tissues within a voxel) at the base and apex. This is particularly problematic for RV analysis where demarcation of the basal extent of the ventricle is relatively difficult (31). Inclusion of long axis slices (typically two chamber, four chamber and three-chamber views) enables better delineation of the apex-base and this information is now included in several software packages.
Another limitation are the image related artifacts mainly due to poor breath-holds especially in heart failure patients, cardiac arrhythmias and metallic artifacts.

1.6.3. PULMONARY TRANSIT TIME

PTT defined as the time for a bolus of contrast to pass from the RV to the LV is a well-known measurement for evaluation of cardiopulmonary status containing information not only from right and left ventricle pump function but also pulmonary blood volume and congestion. Indeed, circulation time measurements are used since the mid-twentieth century for diagnosis of heart failure and PTT was first determined using radionuclide tracers by Blumgart et al in 1928(32).

It can be measured by a variety of techniques either invasively using indicator dilution methods with direct catheterization of the heart, or using different non-invasive imaging methods such as radionuclide imaging(33), computed tomography(34), and contrast enhanced transthoracic echocardiography (35,36). Recently PTT measurements were also proposed using cMR-first pass perfusion imaging with excellent reproducibility (37-41). Several investigators demonstrated that PTT is prolonged both in HFrEF, HFpEF(41) and in isolated pulmonary hypertension(40). According to the indicator dilution theory of Steward and Hamilton (42), formally validated by Meier and Zierler(42), PTT is directly proportional to pulmonary blood volume and indirectly related to the right ventricular cardiac output(43). Hemodynamic studies(36,40,41,44) confirmed that PTT correlates with RV stroke volume, RV cardiac output(35,41), LVEF and RVEF(37,45,46), but also importantly with parameters of increased pulmonary congestion(40,41). Indeed, in our previous work(47), we demonstrated a strong correlation between PTT assessed by CT scanner, mean pulmonary artery pressure (r=0.68) and pulmonary artery wedge pressure (r=0.74). PTT was also shown to correlate with N-terminal pro-B natriuretic peptide(35,47) which is an indicative for

volume and pressure overload in congestive HF. Overall, this suggests that prolonged PTT is a not only a measurement of low cardiac output, but mainly related to increased blood volume and thus, a parameter estimating pulmonary congestion in different types of HF.

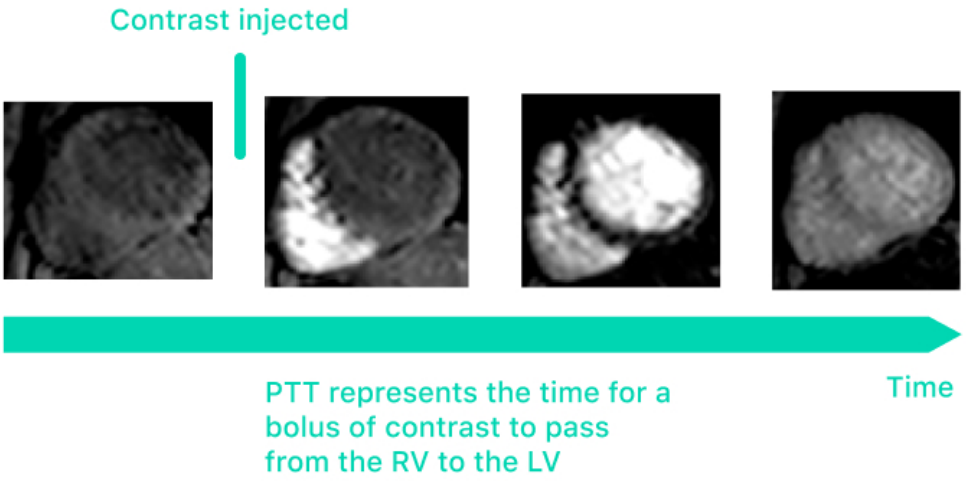

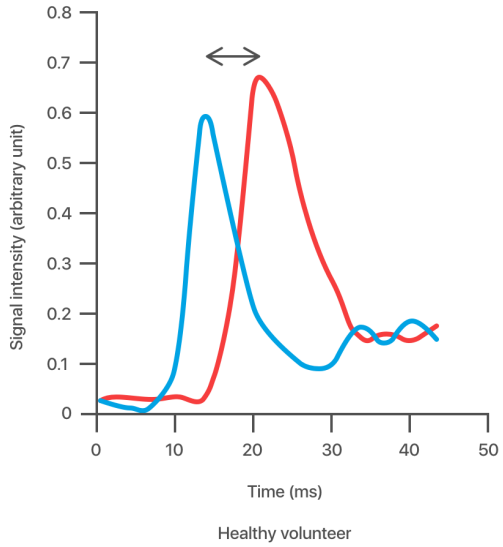

Figure 12
Dynamic contrast enhanced cardiac perfusion imaging. The signal intensity changes observed in first pass perfusion cMR data can be plotted over time for different regions of interest. The red curve represents the left ventricle, and the blue curve represents the right ventricle.

1.6.4. DEFORMATION IMAGING- STRAIN

With the advancement of cardiac imaging modalities, more sophisticated modalities have been developed in the attempt to characterize cardiac systolic function, from the cMR tissue tagging to the contemporary tissue tracking methods in two and three dimensions.
Myocardial tagging is the first non-invasive method by cMR used for strain evaluation (48) and remains the gold standard for strain quantification. However, this technique is time consuming and not well suited for the RV mainly because of its thin wall and increased trabeculations not allowing tags to be well-defined requiring significant operator expertise.

RV Strain is currently measured principally by 2D speckle tracking echocardiography (STE) but new promising tool are emerging such as three-dimensional echocardiography (3D) STE, myocardial work and cMR-Feature tracking approaches, but their validations still need larger studies and further insights into the algorithms used.

Definition of strain

Strain is about changes in myocardial dimension and is defined as the deformation of an object, normalized to its reference shape (49).

It is imperative to understand that strain imaging is explained by geometry not by material properties of the myocardium. Since it represents the relative amount of deformation, it is a dimensionless quantity and is expressed in percentage. Deformation and motion of the myocardium are cyclic processes with no natural beginning or end. Therefore, the position of the baseline is arbitrary.

There are two approaches to describe this length change: the **Langrangian** and **Eularian** strain, represented in **Figure 12.**

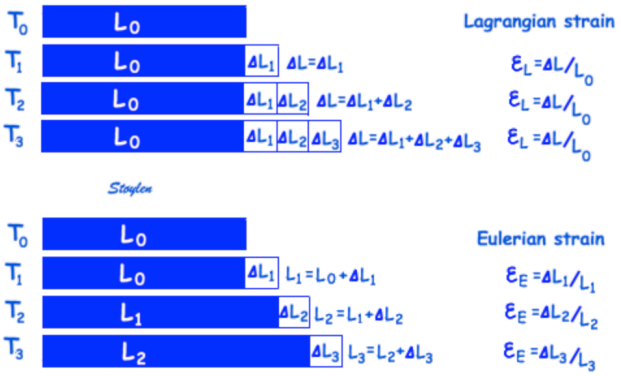

Figure 13 Lagrangian strain (top) and Eulerian strain (bottom). Lagrangian strain is the sum of all length increments up to that time divided by the baseline length, while Eulerian strain at any time is calculated as the sum of all ratios of length increments and the instantaneous length up to the actual time.

From Stoylen, htpp://folk.ntmu.n/ stoylen/strainrate/Basic_concepts.html

The **Lagrangian strain** is the fractional change in length of an element of the object, compared to its original length and can be written as:

$$\varepsilon = \frac{L - L_0}{L_0} = \frac{\Delta L}{L_0}$$

Where **DL** is the length change of the object after deformation and L0 is the original (baseline) length.

In a beating heart, the unstressed original length (L0) is difficult to measure, so end-diastolic length is most often used (50).

The deformation can also be expressed not only relative to the original length but also relative to the length at a previous moment in time. In this case, we talk about **instantaneous** or **Eularian strain**. In this definition the reference value is not constant over time, but changes during the deformation process and can be written as:

$$\varepsilon_E = \sum \frac{\Delta L}{L}$$

Where **DL** is the length change of the object during deformation and L is the instantaneous length.

Eulerian and Lagrangian strains can be converted into each-other using the formula:

$$\boldsymbol{\varepsilon_L = e^{\varepsilon_E} - 1}$$

By the above strain equations, positive strains occur if the object lengths exceed the original lengths (lengthening), and negative strain exists if the object length is shorter than the original length (shortening).

Strain components

All strain imaging techniques are based on a common principle: specific patterns or features are identified within an image and followed over time in the subsequent images of the sequence by searching the most probable pattern correspondence in successive image frames (51).

For practical use, myocardial deformation is expressed in terms of three physiologically relevant axes:

- **Radial strain** (perpendicular to the epicardium) shows the extent of RV myocardial thickening in a radial direction towards the center of the ventricle.

- **Circumferential strain** (tangential to the pericardium and orthogonal to the radial and longitudinal axis) describes myocardial shortening in an anticlockwise direction around the short axis of the right ventricle.

- **Longitudinal strain** (tangential to the pericardium) represents base to apex myocardial shortening of the oblique fibre of the septum.

These 3 strain components represent the deformation of a myocardial segment as defined by consensus of the imaging societies (17) in order to have a uniform reporting between deformation imaging techniques. However, in reality, the deformation of a myocardial segment during the cardiac cycle is far more complex than that because it is multidimensional. Indeed, in addition to the three deformation components described above, a myocardial segment will also show deformation occurring in planes between these predefined orthogonal heart coordinates, known as **shear strains**. Therefore, to completely determine the deformation of a myocardial segment, it would require the knowledge of not only the three normal strain components but also the three shear strain components.

Nevertheless, this is truer for the left ventricle but not for the RV. Indeed, studies showed that RV longitudinal shortening is a more important contributor to RV systolic function than circumferential shortening, while rotation and torsion are negligible (52). Accordingly, RV longitudinal strain is the only strain recommended by the Task Force (53).

1.6.4.1 Two-dimensional speckle tracking echocardiography

2D-STE is a user-friendly technique based on echocardiography image analysis and provides a non-doppler, angle-independent quantification of the RV myocardial deformation. STE has been used as a research tool since the 1990s to assess first the LV systolic function and now is breaching, partly, the clinical setting especially in cardio-oncology (51). It has the

advantage of being a semi-automated technique, which may more accurately reflect cardiac function than the others echocardiography parameters. The software packages were first designed for the evaluation of LV mechanics and recently been adjusted for the assessment of RV deformation. Indeed, dedicated software for RV strain have not yet been released.

How does it work?

After acquiring a RV focused view, the initial step in the analysis of a dataset is generally to recognize the key cardiac events: end-diastole (ED) and end-systole (ES). Secondly, the user will define semi-automatically the region of interest (ROI), by contouring the endocardial and epicardial boarders of the RV in ED and eventually in ES, with variation between software. The width of the ROI should be limited to the myocardium, excluding the pericardium, which may be sometimes difficult in particular in the thin RV free wall. Finally, the ROI is tracked throughout the cardiac cycle and after post processing, deformation curves are estimated, and strain values computed. Indeed, the software algorithm recognizes patterns in the image called speckles (a sort of ultrasound fingerprint that can be tracked) and measure their displacement frame by frame using a statistical approach based on the detection of the best matching area. The algorithm usually used is the **block-matching method**, which automatically identifies a pattern within a region or block of interest, compares it to all possible matching regions within the search region and finds the position of the best matching block compared with the original one.

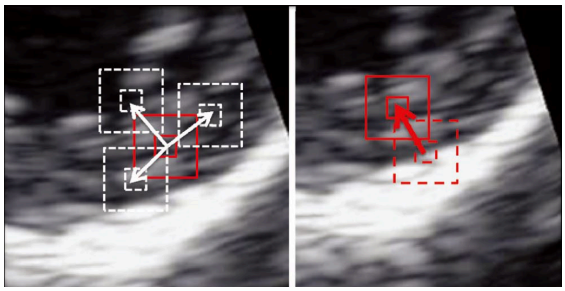

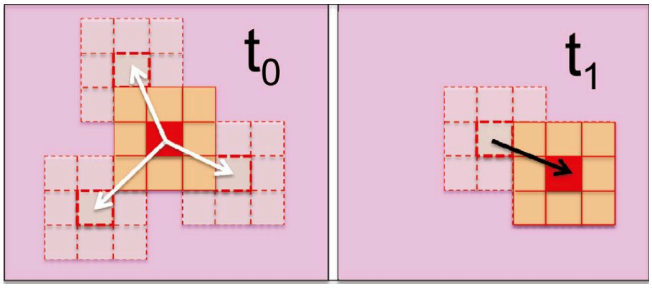

Figure 14 Block-matching method. tracking is performed by searching the most similar region (white arrows and red dashed line squares) in the next frame (t1) of the region of interest (solid red square) in the baseline frame (t0). Motion of the ROI between frames can be quantified as a vector (black arrow).

Adapted from From Yoshihiro Seo et al. Cir J 2014

The displacement of the speckled pattern is considered to follow myocardial movement, and a change between speckles is assumed to represent myocardial deformation. Since the frame rate of the echo loop is known (the velocity of the speckles), the regional deformation of the myocardium can be estimated. The obtained strain values are plotted over time to outline the myocardial deformation over the cardiac cycle.

The different steps of post processing are vendor-specific but usually include a semi-automated selection of the region to be interrogated, a short waiting time for processing by the tracking algorithm and to display the tracking result. The user should carefully check the tracking result by visually comparing the motion of the tracking point to the motion of the underlying grey-scale data. Complex algorithms are usually applied to derive velocity, displacement and deformation estimates from the initially very noisy tracking data. This part of the post-processing is vendor specific and cannot be controlled by the user.

Timing of measurement

Several time points can be measured in the attempt to describe RV myocardial deformation, the most used being the maximal deformation during right ventricular contraction (peak systolic strain) and not the deformation value at the end of right ventricular ejection (end-systolic strain) recommended for the LV since it is harder to identify the end-systolic time in the RV leading to more variability.

Regional strain and global strain

RV longitudinal strain (LS) is determined in six RV segments, visible in the four chamber apical view, as proposed by the guidelines (17). Indeed, when imaging the RV, it can be divided roughly into free and septal wall, as well as basal, mid and apical segments. The septal wall is a "shared" wall between the two ventricles so controversies remaining whether to consider it not part of the RV when assessing RV systolic function with STE. Indeed, in the literature, RV-LS is either perform using the 6 segments (global longitudinal strain, GLS) or only the 3 segments of the free wall (free wall longitudinal strain, FWLS).

In favor of using RV-FWLS, Cameli et al. (54) showed that RVFWLS had the highest diagnostic accuracy to predict a depress RV stroke work index in a simultaneous echocardiographic-catheterization study and therefore would reflect better the RV systolic function than the RVGLS. By the same token, RVFWLS has been shown to have the highest diagnostic accuracy for detecting severe myocardial fibrosis (55).

However, despite the facts that the ventricular septum is mainly a constituent part of the LV, it also true that the ventricular septum contributes importantly to RV systolic performance. That is why, others authors believe that global longitudinal strain is the most accurate since the LV contributes 20% to 40% to RV systolic pressure (56). Furthermore, canine studies demonstrated that the inactivation of the intraventricular septum leads to a significant decrease in RV function and the reduction of RVFWLS function does not affect RVEF in the presence of a preserved interventricular septum (57).

Correlation and Reproducibility

RVLS-STE has been shown to be significantly correlated with cMR (58,59). The feasibility of two-dimensional speckle tracking imaging is relatively good and ranged from 88% to 94% in large studies (60). RVGLS have been shown to be more feasible and more reproducible than RVFWLS in volunteers (61). The intraobserver and interobserver range of coefficients of variation for the RVGLS were 2-7% and 3-10%, respectively(58) (61). However, its interstudy reproducibility is still lacking in the literature.

Reference values of STE-RVLS in the literature

Reference values in the literature range between -21% to - 32 % (59,61-65). Additionally, it has been shown that women have significantly a better RVLS than men (60) (59). Since strain values differ among different software vendors, no definite reference ranges are currently recommended for either global or free wall RVLS because of the need for additional normative data from large studies involving multivendor software programs. Nevertheless, the reference limit for RV-GLS and RV-FWLS is more generally stated to be approximately -20% and -23% respectively (17) but most of the publication are partial to a single vendor from the general electric Healthcare (GE).

1.6.4.2. Cardiac magnetic resonance feature tracking

cMR-FT is a 2D imaging technique that can be applied to standard cMR cine SSFP sequences. This technique is gaining popularity by allowing measurement of myocardial deformation without the need for dedicated acquisition and complex post-processing (51).

How does it work?

It is mainly based on the **optical flow method** of recognizing the anatomic features in the cMR image that are different along the myocardial boundaries and tracked them in the following time frames by methods of maximum likelihood of regions of interest between time frames.

However, in contrast to STE, FT does not seem to distinguish speckles, as the grey level distribution in cine SSFP images is relatively homogenous. Indeed, cMR images do not have an equivalent of “speckle” because the apparent texture within the myocardium on cMR

images is due to random noise and does not provide information for tracking. The assessment of cMR-FT-RV is performed on 4 chamber cine-SSFP sequences which have excellent blood-tissue contrast and the delineation of endocardial features can be tracked through the cardiac cycle in a means similar to that used to analyze echocardiographic images. Regarding the timing of measurement, it is recommended to use also the peak systolic strain as STE.

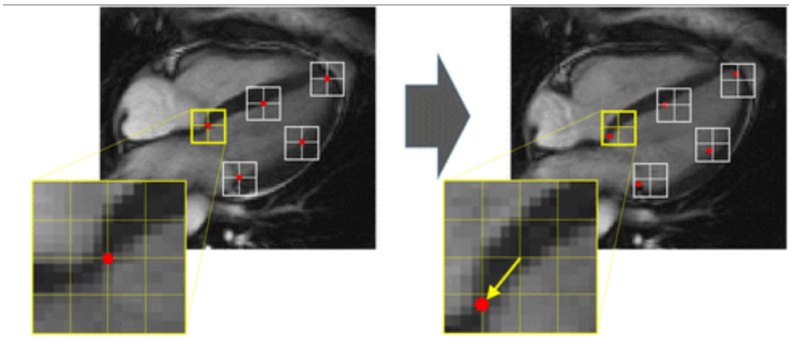

Figure 15 Principle of the feature tracking applied to cine-cMR image. Tracking the portion of tissues about a series of point (illustrated in red on the picture) is based on defining small square windows (or a patch of pixels) centered about such points on the first image (on the left) and searching the highest resemblance of the grey scale pattern on the following image. In this way, motion can be tracked through successive timeframes. Large windows allow to recognize large displacements of the tissue, while the reduction of the window search area about the previous estimated targets allows to improve the accuracy and the locality of the estimation.

Adapted from Pedrizeti et al. JCMR 2016.

Correlation and reproducibility

The reproducibility of FT is extremely good in the literature (66) for both cMR-FT-RVGLS (ICC 0.92 and 0.8 for the intravariability and intervariability respectively) and cMR-FT-RVFWLS (ICC 0.92 and 0.87 for the intravariability and intervariability respectively). In contrast to STE, It has been described no significant difference in cMR- FT between men and women(66). Also, a good agreement between the RV longitudinal global strain

measurements on FT and STE(67) has been shown. Moreover, the literature suggests that FT may be superior to STE in assessing RV longitudinal global strain due to its higher inter-observer reproducibility and the possibility to assess RV strain in a higher proportion of patients.

Reference value

Reference values of RV-cMR-FT are less extensive than 2D-RV- STE and range between -17% to -29% with no significant different between men and women(66-69). Importantly, As STE, no definite reference ranges are currently recommended since cMR-FT reference value are also software-dependent.

In summary, cMR-FT is a promising technique for evaluation of systolic and diastolic function, although there is still a long way to go before it becomes a routine standard of care essentially because of the lack of standardization of softwares and further insights into the algorithms used are needed to improve the quality of tracking in order to make more accurate judgments.

Limitations of deformation imaging

Overall, RVLS implementation in clinical settings has been hampered by the limited reference value, the need of high-quality image, the lack of uniformity in software's algorithm (including the vendor secrecy) and the lack of consensus whether to consider or not the septum wall part of the RV when assessing RV function with deformation imaging.

Limitation factors related to image, software and imaging modality are detailed below:

Image related factors

As deformation analysis methods are based on the analysis of specific image patterns throughout the cardiac cycle, **adequate spatial and temporal resolution are mandatory** to ensure the complete characterization of myocardial deformation in successive time frames (**Table 7**).

Resolution	2DE	3DE	cMR-FT
Spatial	0.2-0.3 mm	0.4-0.5 mm	1-2 mm in plane/ 6-10 mm through plane
Temporal	40-60 frame/sec	20-50 frame/sec	25-35 phases/ heart beat

Table 7 Spatial and temporal resolution across imaging modalities. 2DE, two-dimensional echocardiography; 3DE, three-dimensional echocardiography and cMR-FT, cardiac magnetic resonance- feature tracking.

Adapted from Schuster et al, Circ Cardiovascular imaging 2016.

If the temporal and spatial resolution are too low, the local patterns will become less comparable and displacements may become harder to identify (51). This effect is known as **image de-correlation**. cMR and 3DE have a lower temporal resolution than 2D echocardiography and therefore are more prone to image de-correlation. On the other hand, 2DE and 3 DE have a higher spatial resolution than cMR(70). The particularity of the spatial resolution of the ultrasound images is a lower lateral resolution than axial resolution and lower depth resolution (71)(71). In other words, the most reliable results in ultrasound images are obtained closer to the centerline of the image, at smaller depths. For that purpose, the Task Force (53) recommends to optimize the sector width and depth to allow high frame rates per cardiac cycle (or high temporal resolution) without significantly decreasing lateral resolution in order to allow good tracking across the speckles. Therefore, optimal frame rate is generally set between 60 and 80 frames per second. To increase reproducibility and decrease random noise, echocardiographic images should be obtained with at least three consecutive heart cycles. This is particularly important in patients with atrial fibrillation. However, in clinical practice, the analysis in patients with sinus rhythm is commonly performed using one beat (72) since most of the software programs use a single beat for analysis.

An adequate size of the tracking spatial unit is also needed in order to avoid either averaging the pattern over a large area in case of a large search window or become less feasible to recognize successive patterns if the search window is too small (51). Therefore, solving displacement between short distance regions is difficult and may explain why usually the radial strain (computed on the small distance between endocardium and epicardium) is less reliable than longitudinal and circumferential strain(73). To date, it is not recommended to perform RV circumferential strain due to its lower reproducibility.

Importantly, the region of interest should not include the pericardium, RV strain values will be underestimated otherwise(53) since the deformation of the endocardial layer is more important than in the mid and epicardial layers.

Software related factors: the software's black box

The inter-vendor-variability of strain values is certainly the major source of variability in strain measurements. Echocardiographic and cMR deformation imaging software programs propose different versions and employ different algorithms for the data pre- or post-processing in order to estimate the myocardial motion. Indeed, tracking methodologies differ by the way they establish image correspondence between the frame and the way these correspondences are regularized(74). Thus, the underlying algorithms of each software programs influence the measurement of strain values and may lead to an under-or overestimation of the interrogated parameter. As a result, the comparison between reported strain measurements from different software programs with different algorithms is impossible. That is why the types of software and their strain algorithms being used should be considered and always reported when measuring RV strain.

Furthermore, STE algorithms apply **spatial and temporal smoothing** to reduce the random noise, which can affect the measurement robustness by missing significant localized abnormalities in the case of spatial smoothing or by masking rapid event in case of temporal smoothing (51,75). The consequence is that local measures of deformation will show unavoidable estimation errors, which are smoothed-out when global measures are built by numerous spatial values. In view of this, parameters based on local results are less reliable than those based on a combination meaning that global strains are more reliable than segmental strains.

There are other software related factors that introduce variability such as:

- The computation of Lagrangian versus Eularian strain. These two type of strain are related - via a nonlinear relationship, so in small deformations the two strains are approximately equal, but in large deformations the difference becomes significant, with Langrangian strain having higher absolute value (76). It is recommended for the assessment of RV systolic function to report Lagrangian strain preferentially over Eularian strain.

- **The Calculation of global strain values** give slightly different result (77) if we use different formula (the average values computed at segmental level versus using the entire myocardial length)

- The Definition of ED and ES, which has been shown to have a major influence on the accuracy of strain measurements, up to the point that changing ED or ES by only 4 frame can impact strain values significantly(78). Thus, it is important to identify manually the end diastolic time since most analysis package define zero automatically as the value of the beginning of the QRS complex, which is not always accurate, especially with the presence of a bundle branch block. Importantly, as we mentioned before, the true end systolic time is hard to find for the right ventricle and is a major source of variability in the measurement. That is why it is recommended to report only the peak strain value.

A task Force has been set up for the LV strain by the European Association of cardiovascular Imaging (EACVI) and the American Society of Echocardiography (ASE) in order to reduce the variability of STE measurement in partnership with the manufacturer of echocardiographic equipment and software (77). Subsequent to the joint standardization task force initiative, several manufacturers have released improved software versions and the inter-vendor agreement for 2D-STE-LV has improved for GLS but not for regional strain measurements. A similar issue is also anticipated for FT, as inconsistencies between the commercially available software have been demonstrated, with acceptable differences for global longitudinal and circumferential strain. It is expected soon, a similar Task force initiative for STE and FT of the RV.

Imaging modality related factors

Since 2D imaging planes are usually not the same when acquires by echocardiography and cMR due to different scanning angle, complete correspondence between myocardial segments is extremely difficult preventing an accurate intermodality comparison of 2D regional deformation. Additionally, the foreshortening (not depicting the true apex in long and short axis views) and the through-plane motion represent a limitation of 2D analysis, which are overcome by 3D techniques.

1.7. CLINICAL APPLICATION

1.7.1. Contribution of RV systolic function to prognosis in heart failure reduced ejection fraction

RV systolic function has been shown in numerous studies to be a strong prognostic factor in HFrEF population, in contrast to LVEF, which loses strength, when applied to this kind of population because of the tight range of LVEF values. This was true for all means of assessment of RV systolic function such as measured by echocardiography with RV-FAC (45,79), TAPSE(80) (81-83) or Tei index (81,82); by cMR (83,84) or RVEF based on radionuclide ventriculography (86-89) the conclusion is still concordant with a worse outcome in patient with RV dysfunction (RVD). Therefore, RV function could better define the prognosis of HFrEF patients. The prevalence of RV dysfunction in HF-rEF is not known but Puwanant and Damy described a 1.5- to 2-fold higher prevalence of RVD in HFrEF compared with HFpEF (85,86).

This association of RVD and worse outcome could be explained by the fact that RV function reflects not only the intrinsic myocardial contractility of the RV, but also the afterload effect imposed by increases in LV filling pressures and pulmonary vascular pathology. Hence, the RV function could be compared as an extremely sensitive barometer of any "downstream" factors since it is more profoundly affected by increases in afterload(87) than the LV.
Most of the RV prognosis literature is based on radionuclide ventriculography since the RV assessment has historically been difficult in echocardiography but recent developments in echocardiographic technology, in particular the development of STE and FT are changing this situation. **Table 8 and 9** illustrate the largest studies of the prognostic value of RV systolic function in HF assessed by cMR and STE respectively.

cMR-FT- RV is still poorly investigated in advanced heart failure. So far, most of the studies, regarding feature tracking in heart failure have assess only the left ventricle and have included patients with different degrees of alteration of EF. Romano et al. showed an incremental prognostic information of cMR-FT-LV to cMR-LVEF in predicting mortality in a large population of more than 1000 patients with a LVEF < 50%(88). Unfortunately, the results of the prognostic information of cMR-FT- RV were not published.

Importantly, both RVGLS and RVFWLS assessed either by STE or FT have a prognostic value in HF and thus we may conclude that quibbling over which is the best measure should not obscure the importance of measuring the RV in heart failure with something. **Table 8** and **Table 9** show the largest studies regarding the prognostic value in HF-rEF of cMR-RVEF and RVLS (RVGLS or RVFWL) respectively.

Authors	Endpoints	Sample size	Population	LVEF %	RVEF Cut off	Key message	FUP time
Marwa et al. 2016 (84)	Overall mortality	588	ICM	24±10	3 groups*	RVSD is associated with increased mortality in ischemic patients.	5.7 year (median)
Gulati et al. 2013 (83)	1.All-cause mortality or CT 2. CV mortality or CT 3. HF death, HF hospitalization or CT	250	DCM	<50	45%	RVSD is an independent predictor of transplant-free survival and adverse HF outcomes in DCM.	6.8 years (median)
Bourantas et al. 2010 (89)	Overall mortality	380	CHC mixed population ICM&DCM	<45	-	Greater RV dimension predicts mortality in patients in CHC. RVESVI was not an independent predictor of mortality when clinical markers of fluid overload were included.	45 months (median)
Pouleur et al. 2016 (90)	CV death	107	ICM after CABG	<35	35%	RVSD independently predicts CV in patients with CAD and low EF undergoing CABG	4.7 years (median)
Mikami et al.(91)	Sudden cardiac arrest or appropriate ICD therapy	314	Mixed: ICM & DCM	< 54	45%	RVSD is a strong, independent predictor of arrhythmic event	773 days

Table 8 Prognostic value of cMR-RVEF in heart failure in the literature.

LVEF, left ventricular ejection fraction; RVEF, right ventricular ejection fraction; FUP, follow-up; ICM, ischemic cardiopathy; RVSD, right ventricular systolic dysfunction; CT, cardiac transplantation; CV, cardiovascular; RV, right ventricle; HF, heart failure; DCM, dilated cardiomyopathy; CHC, chronic heart disease; RVESVI, right ventricular end-systolic volume index; CABG, coronary bypass grafting; CAD, coronary artery disease and ICD, Implantable Cardioverter Defibrillator.
*Patients were categorized in three groups: RVEF< 35%; RVEF: 35%-50% and RVEF > 50%.

Authors	RVLS	Endpoints	Sample size	LVEF	Population	Cut-off	Key message	FUP	Software
Vizzardi et al. 2014(92)	RVGLS & RVFWLS	1: CV death and HF hospitalization 2: HF hospitalization only	n=60	< 40%	CHF: DCM and ICM	-	RVFWLS strain is a powerful prognostic variable for the prediction of major cardiac events in patients with CHF.	32+/- 13 months	GE Healthcare (Vivid)
Guendouz et al. 2012 (93)	RVGLS	Death, Emergency, CT, emergency LVAD or acute HF	n= 118	< 40%	CHF: ICM and DCM	>-21%	RVLS is an independent predictor of severe adverse events in CHC.	37+/- 14 months	GE Healthcare (Vivid)
Cameli et al. 2013 (94)	RVGLS & RVFWLS	CV death, HF hospitalization, CT, IABP and LVAD	n= 98	< 35%	CHF: ICM and DCM	-11.4%	FW and RV-GLS are stronger predictor of outcome than LV-LS.	1.5+/- 0.9 years	GE Healthcare (Vivid)
Motoki et al. 2014 (103)	RVGLS	Death, CT, and HF hospitalization	n= 171	< 35%	CHF: ICM and DCM	-14.8%	RVGLS provides incremental prognostic value of LVFE in HFrEF	5 years	GE Healthcare Vivid
Iacoviello et al. 2016 (104)	RVGLS	1: Overall mortality 2: CV death, CT or death due to WHF.	n=332	<45%	CHF: ICM and DCM	-	RVGLS predicts mortality in CHC.	36+/- 26 months	GE Healthcare Vivid
Carluccio et al. 2018 (105)	RVFWLS	Overall death and HF hospitalization.	n=200	<40%	CHF: ICM and DCM	-15.3%	RVFWLS provides incremental prognostic information over a preserved TAPSE in HFrEF.	28 months	GE healthcare Vivid

Table 9 Prognostic value of RVLS in HF-rEF in the literature

RVLS, right ventricular longitudinal strain; LVEF, left ventricular ejection fraction; FUP, follow-up; RVGLS, right ventricular global longitudinal strain; RVFWLS, right ventricular free wall longitudinal strain;; CV, cardiovascular; CHF, chronic heart disease; HF, heart failure; CT, cardiac transplantation; LVAD, Left Ventricular Assist Device); IABP; intra-aortic balloon pump; LVLS, left ventricular longitudinal strain; HF-rEF, heart failure and reduced ejection fraction WHF, worsening of heart failure and TAPSE, tricuspid annular plane systolic excursion.

II: AIM OF THIS THESIS

In the current setting of highlighting the clinical importance of the right ventricle (RV) in innumerous diseases, we sought to contribute to the current state-of-the-art by addressing part of the gaps in evidence of validation and clinical application of deformation imaging modalities and the pulmonary transit time in predicting outcome in heart failure and reduced ejection fraction (HFrEF). Therefore, our work was aimed to first evaluate the variability day-to-day of these widely used deformation imaging techniques and, secondly, to investigate the additional prognostic value of these technique in HFrEF in direct comparison with cardiac magnetic resonance, the gold standard of RV systolic function.

The strength of a technique relies on its reproducibility.

The quantification of left and right heart function in a reproducible and repeatable manner is decisive for risk stratification and clinical decision making in several cardiac diseases conditions such as ischemic cardiomyopathy (95,96), heart failure(97) (98), valve disease(99-101), pulmonary hypertension, tricuspid regurgitation, arrhythmogenic cardiomyopathy (102) and several grown up congenital cardiac diseases. Therefore, in these clinical situations, and especially in cardio-oncology(103) it is crucial to serially and accurately follow changes of cardiac systolic function over time to monitor for potential deleterious cardiotoxic effects of drugs or medications.

Cardiac magnetic resonance (cMR) is currently considered the reference standard for reproducible evaluation of left ventricular ejection fraction (LVEF) and RVEF(104) with a relatively good interstudy reproducibility which is defined as the standard deviation of the mean difference between 2 repeated studies of the cMR-RVEF.

Additionally, cMR interstudy reproducibility has been shown to have considerable improvement compared with echocardiography. cMR- RV interstudy reproducibility was reported as 6% for end-diastolic volume, 14% for end-systolic volume, 8% for ejection fraction, and 9% for RV mass(24). Additionally, the sample size reduction through its use compared with echocardiography is considerable, ranging from 55% to 93%.(29)

The scientific literature of deformation imaging techniques is recently overflowing (105) with the promise of higher accuracy and reproducibility in the assessment of the LV and RV

function. Notwithstanding the enthusiastic scientific interest, myocardial deformation assessment has only partly breached the clinical setting, as several concerns have been raised regarding its robustness in the real-life scenario. Yet, most studies evaluated only their inter-observer or intra-observer variability, and only limited data exist on the test–retest reliability than on their observer variability. The interstudy reproducibility is the pivotal factor for determining the ability of a technique to perform consecutive follow-up examinations to detect a change in volume. High reproducibility or in other words, low standard deviation, leads not only to greater reliability of observed changes in parameters under measure but also smaller sample size in clinical trials.

Therefore, the first aim of this thesis was to contribute to the advancement in the filed by filling the gap in the literature evaluating whether speckle tracking echocardiography (STE) and cMR feature tracking (FT) global longitudinal (GLS) and circumferential (GCS) strains allow better test-retest reproducibility of LV and RV systolic function than conventional cMR and echocardiographic parameters. Further, to allow decision which parameter would be most conclusive in design of prospective drug trials, we also sought to compute the sample sizes needed to demonstrate significant changes in LV and RV function by different methods. Hence, we performed head to head comparison of test–retest reliability of these methods in a prospective trial of 50 subjects with a wide range of left ventricular function undergoing both echocardiography and cMR simultaneously on two separate days.

Additional prognostic value of deformation imaging techniques in advanced heart failure

It is certainly true that RV-STE has already been intensively studied by a tremendous number of publications in HF. However, these publications only showed an additional prognostic value of RV-STE over simple echocardiographic parameters such as RV-FAC or TAPSE and inter-technique comparison can only demonstrate their relative performance. Also, most of the clinical validation studies published so far have a short follow-up, softer composite primary endpoints (i.e. including heart failure), and include a very small number of subject, which can only hardly represent the diverse pathological phenotypes encountered in clinical

practice. Moreover, as these are all echocardiographic studies, the contribution of evaluating the function by cMR was not integrated in the clinical prediction models

There is recently also a growing interest in the literature for cMR-FT strain derived parameters, motivated by the easily and possible retrospective application on regular cine SSFP images and higher signal to noise ratio compared to echocardiography. Nevertheless, clinical validation of FT-RV in HF-rEF is still extremely scarce. Importantly, so far, no study has evaluated whether the prognostic value of these new approaches equals cMR-RVEF to identify HF patients at higher risk of mortality.

Therefore, the second aim of this thesis was to estimate the prognostic significance of 2D STE-RVGLS and FWLS, in patients with HF with reduced EF (HFrEF) in direct comparison with CMR-RVEF and feature tracking (FT) and to conventional
echocardiographic parameters. We focus on patients with heart failure and reduced ejection fraction because we believe they deserve further attention since they have not been completely characterized in term of prognosis despite their well know increased risk of morbidity and mortality.
Accordingly, we prospectively studied 266 patients with HFrEF to assess the independent additional prognostic value of 2D-STE versus CMR-RVEF to predict overall and cardiovascular (CV) survival over baseline clinical and echocardiographic data.

Additional prognostic value of pulmonary transit time in advanced heart failure

Pulmonary transit time (PTT) assessed by cMR has been shown to be increased both in heart failure (HF) with reduced and preserved ejection fraction (EF)(41). This is easy explained by the fact that PTT is a well-known parameter to evaluate global cardiopulmonary function containing information not only from right and left ventricle pump function but also pulmonary blood volume and hemodynamic congestion. However, its prognostic value is so far clearly insufficiently investigated and has not yet been compared to other known clinical and imaging parameters. To date, only one study (100) has assessed the prognostic value of PTT by cMR in a HF population with a mild LV dysfunction (LVEF< 50%) using a softer

primary composite endpoint including cardiovascular death, HF hospitalization, sustained ventricular arrhythmia or appropriate implantable cardioverter defibrillator.

Therefore, we sought to evaluate the prognostic significance of PTT by first pass perfusion cMR in patients with HFrEF because PTT will reflect mostly RV function and pulmonary congestion in this population since LV function is overall decreased. Hence, a high PTT will reflect a combination of raised pulmonary pressures and RV dysfunction suggesting that the contractile reserve is struggled to maintain output against the heightened afterload and portends a particularly ominous prognosis (117,118).

Thus, the third and last aim of this thesis was to compare the ability of PTT to predict both overall mortality and a combined endpoint of cardiovascular survival and HF hospitalization over and above other well-validated parameters in the prognosis of heart failure and in direct comparison with LV and RV feature tracking.

III. ARTICLE 1

Test–retest reliability of left and right ventricular systolic function by new and conventional echocardiographic and cardiac magnetic resonance parameters

Laura Houard MD[1,2], MD, Sebastian Militaru MD PhD[1], Kaoru Tanaka[2] MD,
Agnès Pasquet MD PhD[1] David Vancraeynest MD PhD[1],
Jean-Louis Vanoverschelde MD PhD[1,]
Anne-Catherine Pouleur MD PhD[1], Bernhard L. Gerber MD PhD[1]

(1) Division of Cardiology, Department of Cardiovascular Diseases,
Cliniques Universitaires St. Luc
Pôle de Recherche Cardiovasculaire (CARD)
Institut de Recherche Expérimentale et Clinique (IREC)
Université Catholique de Louvain (UCLouvain)
Brussels, Belgium

(2) Afdeling Hart en Vaatziekten, Universitair Ziekenhuis Brussel,
Vrije Universiteit Brussel (VUB)
Brussels, Belgium

Eur. Heart J. Cardiovascular Imaging: 2020 Aug 13;jeaa206. doi: 10.1093/ehjci/jeaa206.

ABSTRACT

Aims:

Reproducible evaluation of left (LV) and right (RV) ventricular function is crucial for clinical decision-making and risk stratification. We evaluated whether speckle tracking echocardiography (STE) and cardiac magnetic resonance feature tracking (cMR-FT) global longitudinal (GLS) and circumferential (GCS) strains allow better test-retest reproducibility of LV and RV systolic function than conventional cMR and echocardiographic parameters.

Methods and Results:

30 healthy volunteers and 20 chronic heart failure patients underwent cMR and STE twice on separate days to evaluate test-retest coefficient of variation (CV), intraclass correlation coefficient (ICC) and estimated sample sizes for significant changes in LV and RV function. Among LV parameters, cMR-LV ejection fraction (EF) had the highest reproducibility (CV=6.7%, ICC=0.98), significantly better than cMR-FT-GLS (CV=15.1%, ICC 0.84) and GCS (CV=11.5%, ICC=0.94) and echocardiographic LVEF (CV=11.3%, ICC=0.93). STE-LV-GLS (CV=8.9%, ICC=0.94) had significantly better reproducibility than cMR-FT-LV-GLS. Among RV parameters, STE-RV-GLS (CV=7.3%, ICC=0.93) had significantly better CV than cMR-RVEF (CV=13%, ICC=0.82). cMR-FT-RVGLS (CV=43%, ICC=0.39) performed poorly with significantly lower reproducibility than all other RV parameters. Owing to their superior interstudy reproducibility, MR LVEF (n=12), RVEF (n=41) and STE-LV and RV-GLS (both n=14) were the parameters allowing the lowest calculated sample sizes to detect 10% change in LV or RV systolic function.

Conclusion:

STE-LV-GLS and STE-RV-GLS showed higher test–retest reliability than other echocardiographic measurements of LV and RV function. They also allowed smaller calculated sample sizes, supporting the use of STE-LV and RV-GLS for longitudinal follow-up of LV and RV function.

INTRODUCTION

Evaluation of systolic left ventricular (LV) and right ventricular (RV) function is decisive for risk stratification and clinical decision making in many cardiac conditions such as myocardial infarction(95,96) heart failure(97) valve disease(99-101), heart failure and reduced ejection fraction (HFrEF) (98), pulmonary hypertension, tricuspid regurgitation, arrhythmogenic cardiomyopathy (102) and several grown up congenital cardiac diseases. In many of these clinical situations, and particularly in cardio-oncology(103) it is crucial to serially and accurately follow changes of cardiac systolic function over time to monitor for potential deleterious cardiotoxic effects of drugs or medications.

Echocardiography is the most commonly used imaging technique to assess the systolic function of both ventricles. However, it has well-recognized limitations in evaluating chamber volumes and ejection fraction (EF) due to its two-dimensional (2D) characteristics. This is particularly true for the RV, where there is no geometric model that enables an estimate of its volumes based on 2D measurements. Therefore, right ventricular ejection fraction (RVEF) derived from RV volumes by 2D-echocardiography is not recommended. Indeed, current guidelines propose the use of a combination of surrogate parameters to assess RV systolic function by echocardiography(17). Cardiac magnetic resonance (cMR) is currently considered the reference standard for reproducible evaluation of left ventricular ejection fraction (LVEF) and RVEF(104). It has this huge advantage to offer a full three-dimensional (3D) coverage of the entire LV irrespectively of the cardiac or body shape with high contrast and sharpness between blood pool and endocardial borders of the myocardium. More recently, deformation imaging techniques have become popular(105) promising higher accuracy and reproducibility of LV and RV function assessment. Yet, most studies evaluated only their inter-observer or intra-observer variability, and only limited data exist on their test–retest reliability.

Therefore, the aim of this study was to investigate test–retest reliability and minimal detectable changes of speckle-tracking-derived strain echocardiography (STE) and cMR feature tracking (FT) in comparison to conventional echocardiographic and cMR parameters of systolic LV and RV function. Further, we also sought to compute the sample sizes needed to demonstrate significant changes of prespecified differences in LV and RV function by different methods in order to identify which parameter would be most conclusive in design

of prospective drug trials, Hence, we performed head to head comparison of test–retest reliability of these methods in a prospective trial of 50 subjects with a wide range of left ventricular function undergoing both echocardiography and CMR simultaneously on two separate days.

METHODS

Study population and protocol

The study protocol was approved by the ethics committee of our institution (Comité Ethique Hospitalo-Facultaire de l'Université Catholique de Louvain, Brussels, Belgium: 19MAR2019 CARDIO-EVAL-ECHO-IRM) and informed written consent was obtained from each subject before participation in the study. We prospectively included 50 subjects including 30 healthy volunteers with no history of cardiovascular disease and 20 patients with stable chronic heart failure (CHF) who had left ventricular systolic dysfunction (LVEF< 50%). Stable chronic heart failure was defined as the absence of increase in severity of symptoms or signs of heart failure within 30 days. Exclusion criteria were non-sinus rhythm (atrial fibrillation or flutter), severe chronic kidney disease defined as a Glomerular Filtration Rate (GFR) <30 ml/min/1.73m2 or others generally accepted contraindications of cMR (cardiac devices, cerebral aneurysm clips and claustrophobia).

Each subject underwent respectively 2 CMR and 2 echocardiography exams in random order within a maximal delay of 5 days for healthy volunteers and 1 day for CHF patients to avoid changes in hemodynamic conditions, and within approximately 20 minutes between each technique. The same acquisition protocols with the same cMR and echocardiographic systems were used for all the patients. Importantly the same operator (LH) performed both acquisitions. Both studies (study 1 and 2) were anonymized and analyzed off-line by the same operator (LH). For intraobserver and interobserver variability the same experienced reader (LH) re-analyzed 20 random cMR and echocardiography studies 6 weeks later blinded to prior measurements. A second reader (SM) performed the analysis on the same 20 cMR and echocardiography studies also blinded to prior measurements. For all participants, age, sex, body mass index, body surface area, medical history was collected at baseline. Additionally, blood pressure and heart rate were measured at each visit.

2D transthoracic echocardiography

Standardized comprehensive transthoracic echocardiography (TTE) exams were acquired using Philips EPIQ 7 ultrasound system (Philips Medical Systems, Andover, MA, United States) equipped with a X5-1 probe in harmonic imaging (2.6/1.3 Mhz), stored on a PACS server (Intellispace CV, Philips Medical Systems, Andover, MA, United States). Two-dimensional grayscale harmonic images were acquired in the 3 standard apical views (2-, 3- and 4-chamber) and the 3 standard short axis views (at the basal, mid- and apical ventricular level) during breath-hold (3 heartbeats each). The average frame rate of the clips was 59±9 frames per second. Care was taken to avoid foreshortening and to image the true apex in apical views. Data was anonymized and analyzed off-line by one single experienced observer (LH).

LV volumes were calculated according to the biplane modified Simpson's rule after semi-automatically tracing end-diastolic and end-systolic endocardial boundaries in the apical 2 and 4 chamber views. LVEF, TAPSE, FAC were also performed according to the latest guidelines(17). LV and RV-STE were assessed using Tomtec software (4.6 Version; Tomtec Imaging Systems, Germany) as previously reported(98). Endocardial borders of the RV and LV were automatically tracked throughout the cardiac cycle by the software, with manual corrections if necessary. STE-LV- end-systolic- global longitudinal strain (GLS) was computed by averaging 2, 3 and 4 chamber views. For the RV- we evaluated both peak systolic GLS and RV Free Wall longitudinal strain (FWLS). LVEF and GLS were both performed automatically with manual correction if necessary.

Cardiac magnetic resonance

All subjects underwent a standardized cMR myocardial function study on a 3T scanner (Achieva, Philips Medical Systems, Best, the Netherlands). 10-12 consecutive short axis images covering the entire LV, and respectively one 2- 3- and 4 chambers long-axis cine SSFP images were acquired for assessment of myocardial function. Imaging parameters were as follow: field of view: 320 mm, imaging matrix 160x154 resulting in spatial resolution of 2x2.1 mm, slice thickness 8 mm with 2 mm gap, flip angle 60 degrees, repetition time (TR) 3.6 ms, echo time (TE) 1.7 ms using SENSE acceleration factor 2.The frame rate was 25

cycles / heart beat. Acquisitions were performed with retrospective gating and 3 slices were acquired per breathhold. CMR RV and LV volumes and EF were computed using the freely available software Segment version 2.2 (*http://segment.heiberg.se*) (106) from short-axis cine images by tracing the endo- and epicardial contours in the end-diastolic (ED) and end-systolic (ES) phases. LV and RV endocardial and epicardial contours were detected automatically with manual corrections if needed. Values were indexed to the body surface area. FT-LV and RV GLS was computed using CVI-42 software (Circle CV, Montreal, Canada). Mid-ventricular global circumferential strain (GCS) was obtained from consecutive short axis views, FT-LV-GLS by averaging measurements of 2, 3 and 4 longitudinal views and FT-RV-GLS on a 4-chamber view.

Statistical analysis

Statistical analyses were performed using SPSS 21 and R software (version 3.3.2). The power of our study was computed using R package *ICC power* indicating a power of 0.8 to distinguish difference of intraclass correlation (ICC) of 0.79 from null hypothesis 0.9 with alpha 0.05.

Continuous variables were expressed as mean ± one standard deviation (SD), categorical variables as counts and percentages. All cMR and echocardiographic measurements were normally distributed as determined by the Kolmogorov-Smirnov test.

To investigate test–retest reliability we performed Bland-Altman analysis with computation of within-subject coefficient of variation (CV) and single measures two-way mixed ICC with interaction for the absolute agreement. Differences in CV were compared using an asymptotic test according to Felz and Miller using the routine *cvequality* (Version 0.1.3; Marwick and Krishnamoorthy 2019). Differences in ICC were compared using F test according to the method described by Feldt, and p values were adjusted for multiple comparison by Hochman's method. Standard error of measurement (SEM) was assessed as $\sigma_i\sqrt{1-ICC}$ where σ is standard deviation. The smallest detectable change (SDC) representing the minimal difference between the measurements that mu6.7st overcome to ascertain a true change or difference with a less than 5% chance of error was computed as $1.96 * \sqrt{2} * SEM$. We also estimated sample sizes to demonstrate clinical change for the different parameters studied using typical cutoff values used in the literature (i.e. >5% LVEF,

>2% strain), but also 5% and 10% of relative normal values in healthy volunteers. These sample size computations were made assuming a power of 90% and an α error of 0.05. These computations were performed using the *pwr.t.test* function in R.

Finally, intraobserver and interobserver reproducibility of the measurement studied was evaluated in 20 randomly selected patients using respectively single measures two-way mixed-effect ICC and two-way random effect ICC with absolute agreement. All tests were 2 sided and p value <0.05 was considered statistically significant.

RESULTS

Baseline characteristics of the study population

Table 1 illustrates the baseline characteristics of the study population. The mean age was 46±19 years with 69% of men. The population had a wide range of LV and RV ejection fraction.

	All (n=50)	HV (n=30)	Heart-failure pts (n=20)
Age (years)	46±19	35±11	63±17
Female Sex (n, %)	15 (31%)	10 (33%)	2 (26%)
BMI (kg/m2)	23±3	22±2	25±4
BSA (m2)	1.8±0.2	1.8±0.2	1.9±0.2
ATH (n, %)	9 (18)	0 (0)	6 (24)
Diabetes (n, %)	6 (12)	0 (0)	6 (30)
History of CAD (n, %)	6 (12)	0 (0)	6 (30)
Echocardiography			
LVEDVi (ml/m2)	91±38	80±18	108±53
LVESVi (ml/m2)	39±5	30±7	74±40
LVEF (%)	51±16	63±4	33±8
STE-LV-GLS (%)	-19±6	-24±3	-12±3
STE-RV-FWLS (%)	-25±7	-28±6	-21±6
STE-RV-GLS (%)	-24±5	-27±3	-19±4
TAPSE (mm)	22±5	24±4	19±5
FAC (%)	45±10	48±5	40±14
cMR			
LVEDVi (ml/m2)	110±65	85±15	146±90
LVESVi (ml/m2)	61±58	32±7	103±92
LVEF (%)	50±17	62±54	31±10
FT-LV-GLS	-11±4	-14±2	-7±3
FT-LV-GCS	-13±5	-17±2	-8±3
RVEDVi (ml/m2)	85±22	87±18	81±26
RVESVi (ml/m2)	41±19	38±11	45±25
RVEF (%)	51±11	55±6	43±13
FT-RV-GLS (%)	-14±6	-16±6	-11±6

Table 1 Clinical characteristics of the study population.

BMI indicates Body mass index; BSA: body surface area; ATH: arterial hypertension; CAD:coronary artery disease; HV: healthy volunteers; LVEDVI: left ventricular end diastolic volume indexed; LVESVI: left ventricular end systolic volume indexed; LVEF: left ventricular ejection fraction; STE-LV-GLS: speckle tracking echocardiography - left ventricular - global longitudinal strain; RV-FWLS: right ventricular -free wall longitudinal strain; RV-GLS: right ventricular - global longitudinal strain; TAPSE: tricuspid annular systolic excursion; FAC: fractional area change; cMR: cardiac magnetic resonance; FT: feature tracking; LV-GCS: left ventricular global circumferential strain; RVEDVI: right ventricular end diastolic volume indexed; RVESVI: right ventricular end systolic volume indexed and RVEF: right ventricular ejection fraction.

Table 2 shows hemodynamic measurements between the two acquisitions. There was no statistical difference in blood pressure or heart rate between study 1 and 2 neither between echocardiography and cMR studies on the same day.

		Day1	Day2	P value
cMR	HR (bpm)	67±11	66±12	0.79
	SBP (mmHg)	118±17	120±13	0.28
	DBP (mmHg)	75±11	75±8	1
	MAP (mmHg)	89±12	90±9	0.63
Echo	HR (bpm)	64±10	64±10	0.87
	SBP (mmHg)	118±17	120±13	0.28
	DBP (mmHg)	75±11	75±8	1
	MAP (mmHg)	89±12	90±9	0.63

Table 2 Hemodynamics measurements.
cMR indicates cardiac magnetic resonance; Echo, echocardiography; HR, heart rate; SBP, systolic blood pressure; DBP, diastolic blood pressure; MAP, mean arterial pressure.

Example of STE and FT measurement from a healthy volunteer and a patient are shown in **Figure 1a and 1b.** For the LV, STE-LV-GLS (r=-0.94, p<0.001), cMR-FT-LVGLS (r=-0.91, p<0.001), cMR FT-LVGCS (r=-0.93, p<0.001) were highly correlated to cMR-LVEF. Also, STE-LVGLS was highly correlated to FT-LVGLS (r=0.90, p<0.001) and Echocardiography-LVEF to cMR-LVEF (r=0.96, p<0.001). However, STE-LV-GLS provided significantly greater values than FT-GLS (-19±6 vs -11±4, p<0.001). There were no significant differences in LVEF between cMR and Echo (p=0.23). For the RV, FAC (r=0.60, p<0.001), TAPSE (0.54, p<0.001), STE-RVGLS (r=-0.66, p<0.001), FT-RVGLS (r=-0.58, p<0.001) and FT-RVGLS (r=-0.56, p<0.001) were moderately correlated with RVEF. STE-RVGLS was moderately correlated to FT-RV-GLS (r=0.67, p<0.001), but STE-RV-GLS values were significantly greater than FT-RVGLS (-24±5 vs -14±4%, p<0.001).

Figure 1a: Example of Speckle Tracking Echocardiography assessment

Healthy Volunteer

LV-GLS: -25.00%

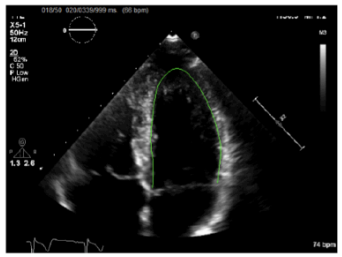

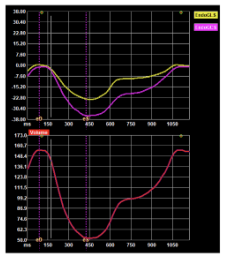

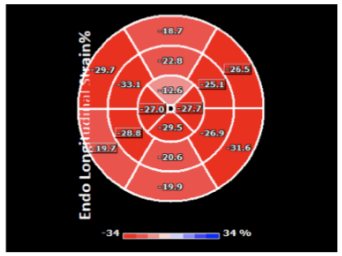

RV-GLS: -23.77%

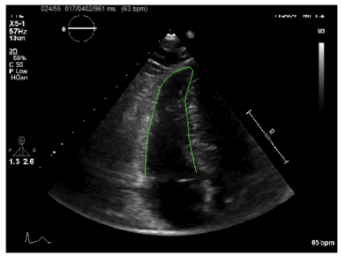

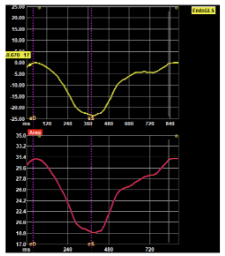

Heart Failure Patient

LV-GLS: -7.57%

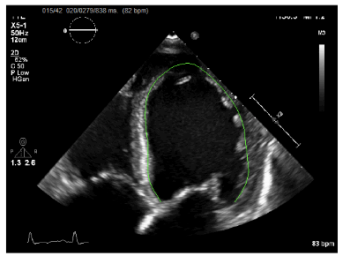

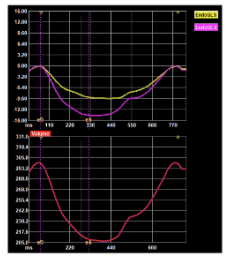

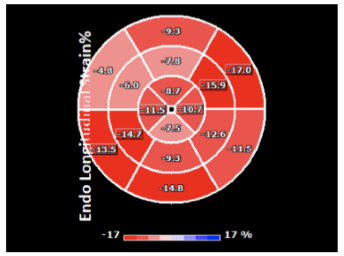

RV-GLS: -8.66%

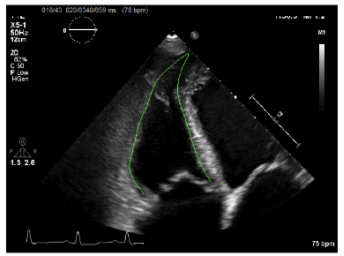

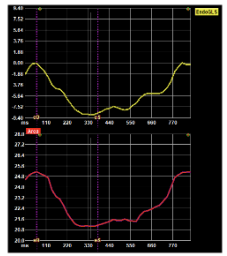

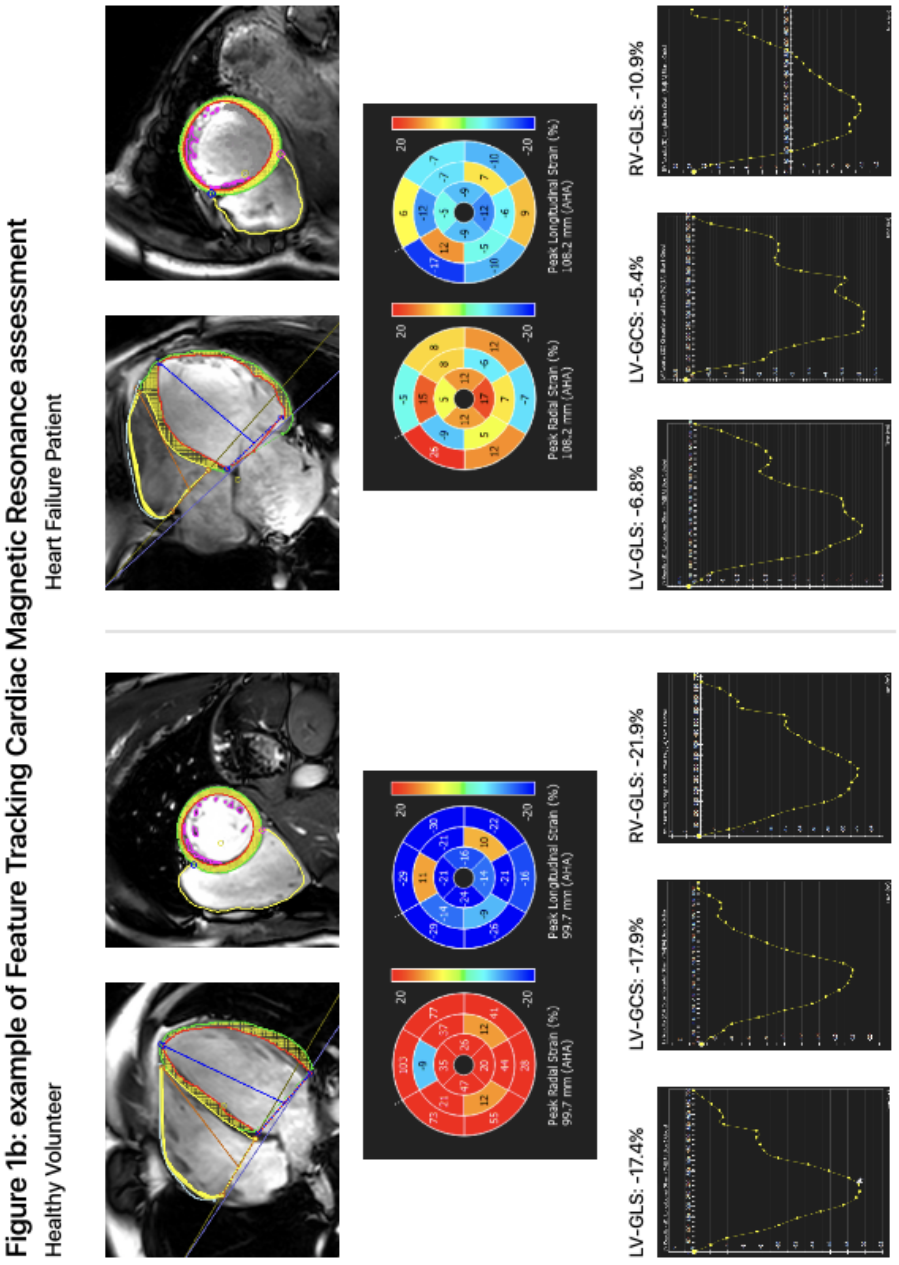

Figure 1 Example of speckle tracking echocardiography and cardiac magnetic feature tracking assessment. Graphs are not scaled to same data range.

	LV parameters	Measurement Day 1	Measurement day 2	Mean Difference +- SD	P value	CV	ICC	SDC95 abs. (%)	SCD95 rel. (%)
cMR	LVEF (%)	49.2±17.3	49.0±16.8	0.23±3.65	.66	6.7#	0.98 [0.96;0.99]#	1.5	3.1
	FT-LVGLS (%)	-11.1±3.8	-11.1±3.9	0.08±2.22	.ξ	15.1*	0.84 [0.73;0.90]*	2.5	22.2
	FT-LVGCS (%)	-13.1±4.7	-13.1±4.8	0.00±1.64	.99	11.5*	0.94 [0.90;0.97]*#	1.1	8.5
Echo	LVEF (%)	48.9±15.5	50.9±16.1	-1.89±5.88	<0.03	11.3*	0.93 [0.87;0.96]*#	4.4	8.7
	STE-LVGLS (%)	-19.4±6.1	-19.1±6.6	-0.21±2.14	.47	8.9#	0.94 [0.91;0.97]*#	1.4	7.2
RV parameters									
cMR	RVEF (%)	50.7±11.3	50.2±13.1	0.46±7.55	.66	13.0¶†	0.82 [0.69;0.89]¶	9.1	18
	FT-RV-GLS (%)	-13.6±5.2	-14.8±4.8	1.14±5.77	.17	42.9†	0.39 [0.13;0.59]†	12.5	88
Echo	STE-RV-GLS (%)	-24.1±4.9	-24.3±5.2	0.20±2.14	.51	7.3¶	0.91 [0.85;0.95]¶	1.7	7.2
	STE-RV-FWS (%)	-26.0±5.8	-25.6±6.5	0.72±3.81	.19	12.8¶†	0.81 [0.69;0.88]¶	5.8	22.6
	TAPSE (mm)	22.3±5.6	22.2±5.1	0.13±3.61	.62	16.5¶†	0.78 [0.63;0.87]†	4.7	21.2
	FAC (%)	44.4±9	45±11	-0.64±9.06	.79	12.1¶†	0.60 [0.39;0.75]†	15.8	35.5

Table 3 Test-Retest reproducibility and smallest detectable difference

cMR: cardiac magnetic resonance; CV: coefficient of variation; Echo: echocardiography; ICC: intraclass correlation, LV left ventricular; RV: right ventricular; SD: standard deviation; SDC: small detectable change; abs: absolute and rel: relative. The SDC represents the minimal difference between the measurements that must overcome to ascertain a true change or difference with a less than 5% chance of error.

LV parameter comparisons: *): p<0.05 vs cMR-LVEF, #) p<0.05 vs cMR-FT-LVGLS.
RV parameter comparisons: ¶): p<0.05 cMR-FT-RVGLS †): p<0.05 vs STE-RVGLS

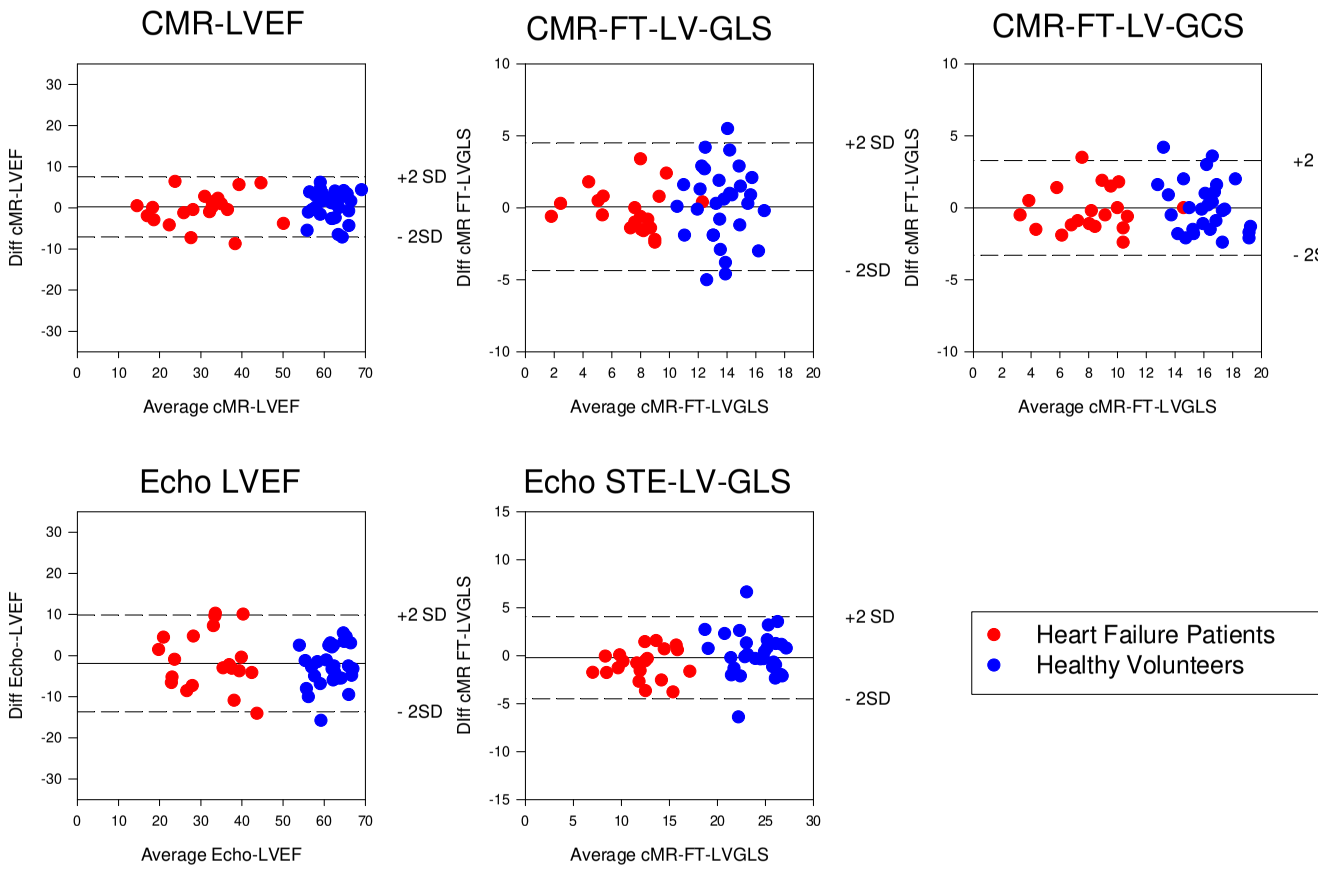

Figure 2 Bland Altmann analysis with mean differences and limits of agreement of paired measurements of the studied parameters to assess left ventricular systolic function. The blue dots represent asymptomatic volunteers and the red dots heart failure patients. To allow comparisons all graphs are scaled to same data range.

Interstudy reproducibility data

Average values of LV measurements on day 1 and day 2, their difference, CV, limits of agreement, ICC and smallest detectable difference are shown in **Table 3** while Bland-Altmann graphs are shown in **Figure 2**.

Overall there were no significant difference in LV measurements between day 1 and day 2, except for a small difference of LVEF by echocardiography Simpson's method, which was slightly ($p<0.03$) higher on day 2. For all LV parameters, the coefficient of variability was good, and all ICC were high (>0.75) indicating good reproducibility. cMR-LVEF had the highest reproducibility of all LV parameters, with a significantly ($p<0.05$) higher ICC than the other modalities and a significantly lower CV ($P<0.005$) than cMR-FT-LVGLS, cMR-FT-LVGCS and echocardiography-LVEF. STE-LVGLS was the second most reproducible parameter. Interestingly, the CV of STE-LV-GLS was significantly ($p<0.005$) better than the CV of cMR-FT-LVGLS. Also, the ICC of cMR-FT-LV-GCS, echocardiography-LVEF and STE-LVGLS were significantly ($p<0.05$) better than cMR-FT-GLS. **Figure 3** illustrates the temporal variability of the LV parameters studied.

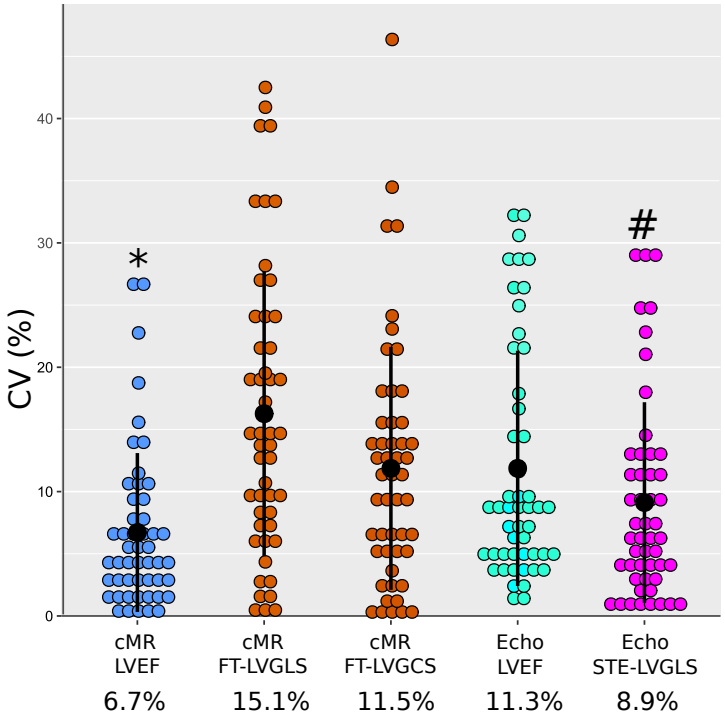

Figure 3
Temporal Variability of left ventricular parameters. *): p<0.05 CV vs cMR-LV-GLS, cMR-LVGCS and LV-Echo EF, #) p<0.05 CV vs cMR-FT-LVGLS

Table 3 shows the average values of RV measurements on day 1 and day 2, their difference, CV, limits of agreement, ICC and their smallest detectable difference, while Bland-Altmann graphs are illustrated in **Figure 4**.

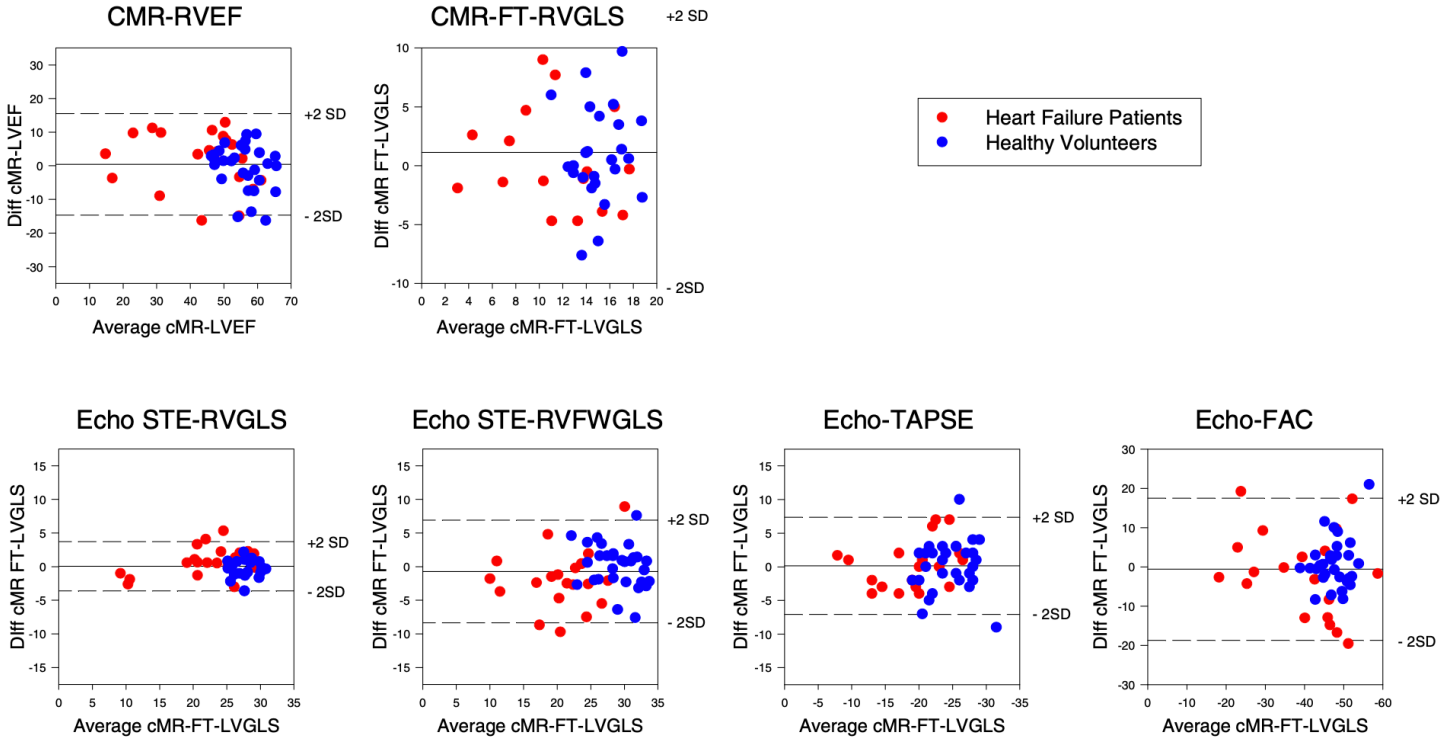

Figure 4 Bland Altmann analysis with mean differences and limits of agreement of paired measurements of the studied parameters to assess right ventricular systolic function. The blue dots represent the asymptomatic volunteers and the red dots the heart failure patients. To allow comparisons all graphs are scaled to same data range.

All parameters had acceptable reproducibility with CVs <20% and ICCs>0.75, except FAC who had an ICC of 0.60 and cMR-FT-RVGLS which had poor day-to- day reproducibility (CV 43% and ICC 0.39). Among RV parameters STE-RV-GLS was the most reproducible parameter with a significantly ($p<0.005$) lower CV than all other parameters and a significantly ($p<0.005$) higher ICC than cMR-FT-RVGLS, TAPSE and FAC. On the other hand, cMR-FT-RVGLS was the least reproducible parameter with significantly ($p<0.001$) worse CV than all other parameters and significantly ($p<0.001$) lower ICC than cMR-RVEF, STE-RV-GLS and FW-RV-GLS. **Figure 5** illustrates the temporal variability of the RV parameters studied.

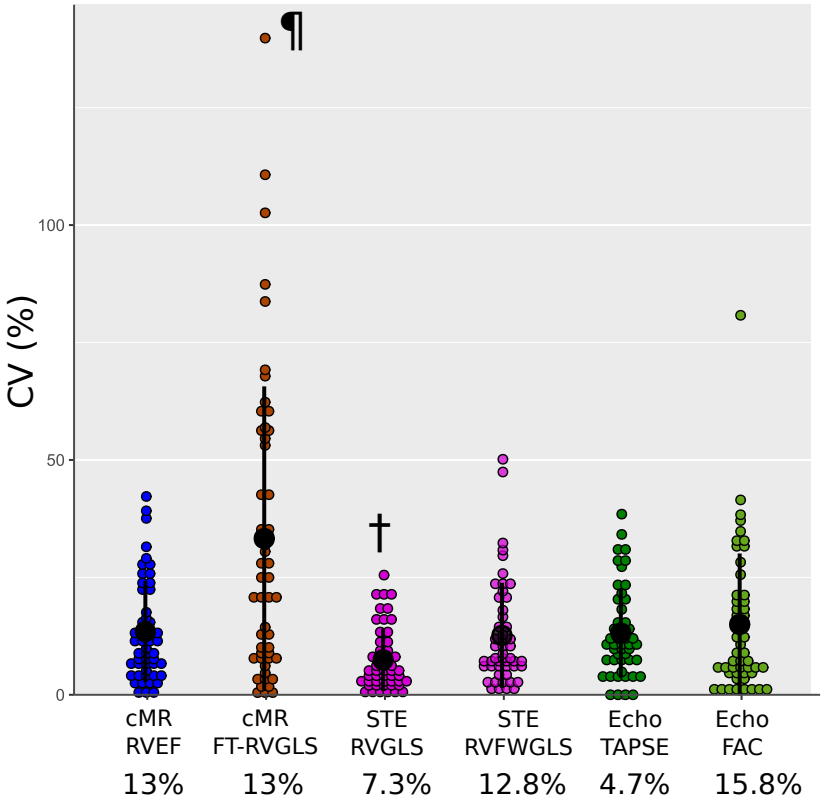

Figure 5 Temporal Variability of right ventricular parameters. ¶): $p<0.05$ CV cMR-FT-RVGLS vs all other groups †): $p<0.05$ CV STE-RVGLS vs all other groups.

Sample size computation

Table 4 and **Figure 6** reveal the sample size computations for different changes in LV and RV functional parameters.

		Absolute changes		Relative changes			
				Change in >5% normal value in HV		Change in >10% normal value of HV	
LV parameters		Cutoff value	Sample size	Cutoff value	Sample size	Cutoff value	Sample size
cMR	LVEF	>5%	12	>3.1%	30	>6.1%	12
	LV-GLS	>2%	27	>0.7%	227	>1.4%	56
	LV-GCS	>2%	15	>0.8%	86	>1.6%	22
Echo	LVEF	>5%	30	>3.1%	76	>6.2%	19
	LV-GLS	>2%	25	>1.4%	54	>2.7%	14
RV parameters							
cMR	RVEF	>5%	48	>2.75%	160	>5.5%	41
	RV-GLS	>2%	148	>0.7	1348	>1.5%	399
Echo	RV-GLS	>2%	25	>1.4%	53	>2.7%	14
	RV-FWS	>2%	77	>1.4%	146	>2.9%	37
	TAPSE	>2mm	70	>1.25 mm	184	>2.5 mm	47
	FAC	>7%	36	>2.5%	276	>5%	70

Table 4 Sample Sizes Required to Detect a Clinically Significant Change in Left and Right Ventricular function (with 90% power and an α error of 0.05) using two tailed t test.
cMR: cardiac magnetic resonance; Echo: echocardiography; HV: healthy volunteer. LV left ventricular; RV: right ventricular.

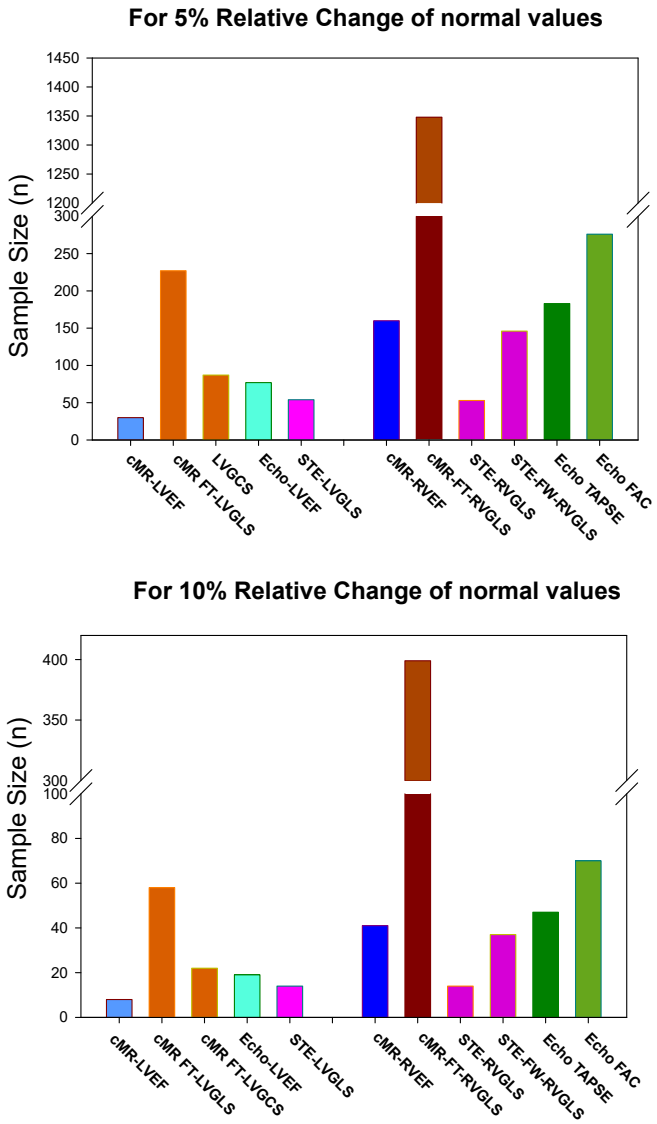

Figure 6 Estimated sample sizes to demonstrate 5% and 10% relative change of normal values in healthy volunteers for different LV and RV parameters.

Among LV parameters, given its highest interstudy reproducibility, cMR-LVEF required the smallest sample size to demonstrate a clinical change in 5% and 10% of relative normal value (i.e. n=30 and n=12). To demonstrate a similar change using Echocardiography-LVEF, a sample size of n=76 and n=19 would have been required. cMR-FT-LV-GLS and FT-LV-GCS did not allow to reduce sample sizes relative to cMR-LVEF. STE-LV-GLS, however, allowed smaller sample sizes to demonstrate >5% and >10% normal values (i.e. >1.4% and >2.7% absolute strain changes and n-54 and 14) than echocardiographic LVEF. Interestingly, projected sample sizes for STE-LV-GLS were also smaller than those for cMR-FT-LV-GLS and FT- LV-GCS.

For the RV, demonstration of absolute and relative changes of cMR-RVEF by 5 and 10%xx required larger sample sizes than absolute and relative changes of cMR-LVEF. Among all RV parameters, STE-RV-GLS allowed the smallest sample size to demonstrate a change in 5% and 10% of relative normal values. The sample sizes needed to demonstrate changes in RV function by STE-RV-FWLS, TAPSE and FAC were larger. Given the observed low reproducibility, cMR-FT-RVGLS would have required the largest sample size to evaluate significant statistical relative changes in normal RV function.

Inter and intra-observer variability data

The reproducibility of the studied measurements is shown in **Table 5.** All measurements had good intra-observer and inter-observer reproducibilities except cMR-FT-RV-GLS.

	Intraobserver reproducibility		Interobserver reproducibility	
	Coefficient of variation % (95%CI)	ICC	Coefficient of variation % (95%CI)	ICC
LVEF Simpson	7.9	0.97	4.7	0.96
FAC	9.5	0.98	13.9	0.79
TAPSE	7.9	0.97	8.5	0.88
STE-LV-GLS	10.2	0.86	11.8	0.9
STE-RV-GLS	9.2	0.92	10.3	0.83
STE-RV-FWLS	13.3	0.93	10.8	0.85
cMR-LVEF	5.2	0.99	8.1	0.98
cMR-RVEF	7.3	0.98	13.9	0.92
FT-cMR-LV-GCS	11.1	0.99	10.9	0.97
FT-cMR-LV-GLS	12.9	0.94	21.5	0.90
FT-cMR-RV-GLS	39.6	0.63	38.6	0.24

Table 5 Intra-inter observer reproducibility data

CI: confidence interval; ICC: Intra-class correlation coefficient; LVEF simpson: left ventricular ejection fraction calculated according to the biplane modified Simpson's rule; FAC: fractional area change; TAPSE: tricuspid annular systolic excursion; STE-LV-GLS: speckle tracking echocardiography - left ventricular - global longitudinal strain; RV-GLS: right ventricular - global longitudinal strain; RV-FWLS: right ventricular -free wall longitudinal strain; cMR-LVEF: cardiac magnetic resonance - left ventricular ejection fraction; cMR-RVEF: cardiac magnetic resonance – right ventricular ejection fraction; FT-cMR-LV-GCS: Feature tracking- cardiac magnetic resonance- left ventricular- global circumferential strain; FT-cMR-LV-GLS: Feature tracking- cardiac magnetic resonance- left ventricular- global longitudinal strain; FT-cMR-RV-GLS: Feature tracking- cardiac magnetic resonance- right ventricular- global longitudinal strain

DISCUSSION

Our study is to our knowledge the first head-to-head comparison of test-to-test reproducibility of not only LV and RV STE but also cMR-FT techniques vs conventional echocardiography and cMR. The salient findings of our study were: a) Among LV parameters, LVEF by cMR had the highest reproducibility followed by STE-LV-GLS. Both had better test–retest reliability than LVEF by 2D echocardiography. cMR-FT-GLS was less reproducible than cMR-LVEF and STE-GLS. b) Among parameters of RV function, STE-RV-GLS had the highest test-retest reliability to assess RV systolic function. By contrast cMR-FT-RV-GLS performed poorly. c) Due to their better reproducibility, cMR-LVEF, RVEF and STE-LV-GLS and STE-RV-GLS were the parameters allowing the lowest calculated sample sizes to detect significant change in LV or RV systolic function when planning research studies.

The observation that cMR-LVEF is the most reproducible parameter for evaluation of LV systolic function was expected in accordance with earlier works(107-110). cMR-LVEF was also confirmed to be more reproducible than LVEF by 2D biplane echocardiography Simpson's method, which may be restricted by echocardiographic windows, geometrical assumptions, difficult endocardial definition and foreshortening. Nevertheless, the reproducibility of 2D-LVEF in our study was satisfactory and somewhat better than in prior studies(107,111-113), possibly reflecting improvements in imaging technology. In agreement with earlier reports for 2D(114) and 3D STE(115) but in contrast to the study by Baron et al.(113), we showed that STE strain is a highly reproducible method for assessment of systolic function by echocardiography with better test-retest reproducibility than echocardiography-LVEF. This probably reflects that strain analysis is more automated and thus less user dependent(105) than LVEF analysis. Surprisingly, however, this was not the case for cMR deformation techniques, since both cMR-FT-GLS or FT-GCS were less reproducible than cMR-LVEF. Also, cMR-FT-GLS had lower reproducibility than STE-LV-GLS. While other studies reported comparable measurements of cMR-FT and STE strains(116,117), no such comparison of test-retest reproducibility between STE and cMR-FT has been performed until now. cMR-FT reproducibility in our study was consistent with other reports(118-120), ruling out methodological issues. Therefore in our opinion, the most likely explanation of why STE allows more accurate estimates of strain than cMR-FT, is

mainly due to the presence of physical markers (speckles) and much higher spatial and temporal resolution(105). Indeed, STE evaluates speckle motion, while cMR-FT doesn't distinguish intramyocardial features, as the grey level distribution in cine SSFP images is relatively homogenous. Finally, cMR-FT showed significantly lower strain value than STE. This fact is in accordance with our previous works comparing STE to tagging(121) The most likely explanation for this is that STE software provide more endocardial strain estimates than cMR-FT software which provide mid-ventricular strain. Also, the lower frame rate of FT-cMR could also explain lower strain values than STE(105).

The comparison of test-retest reproducibility of RV functional parameters is also novel. To the best of our knowledge, our study is the first to directly compare test-retest variability of RV echocardiographic and cMR parameters. Reproducibility of cMR-RVEF was similar to earlier works(107). The main source of errors in evaluation of volumes by cMR Simpson's method are the demarcation of the basal slice near the atrioventricular valves and outflow tracts, and the large motion of the base through the plane of the short axis (slice thickness are typically 8-10 mm), giving rise to significant partial volume effects at the base and apex. Because of its smaller wall thickness demarcation of the basal extent of the RV is more challenging than for the LV(122), probably explaining the larger test-retest variability of cMR-RVEF than cMR-LVEF. For echocardiographic assessment of RV systolic function, current guidelines(17) recommend mainly the use of FAC and TAPSE. In our study these parameters had excellent inter and intra-observer variability, but poor test-retest variability compared to the other parameters studied. This is probably related to the fact that they are not only strongly geometry dependent with difficulties reproducing similar views in repeat studies, but also operator dependent. By contrast, in line with our observations for STE LV analysis, STE-RV-GLS presented much more robust reproducibility. This is probably again explained by automated analysis of STE benefitting from physical markers, but also translates the fact that RV function is mainly dependent on longitudinal shortening. Unexpectedly, however, cMR-FT-RV-GLS performed very poorly in terms of reproducibility. This was probably because the FT tracking algorithm used track less well the RV than the LV., Indeed, cMR-FT-RVGLS often failed to adequately track the base of the RV especially in subjects with relatively vigorous annular motion or in presence of flow artifacts.

CLINICAL IMPLICATIONS

We have demonstrated that STE deformation techniques were the most accurate echocardiographic approach for detecting small changes in LV and RV function. For the LV, they performed nearly as well as cMR, and for the RV they even surpassed the reproducibility of cMR-RVEF. This suggests that these STE techniques could be used clinically to reliably follow patients for development of subclinical dysfunction in different conditions, for example to monitor cardiotoxic effects of cancer therapy(123,124) or to detect afterload mismatch in aortic stenosis(125). Obvious advantages of using STE over cMR are wider availability and lower costs. Nevertheless, STE has potential limitations such as the need of high quality image and the lack of uniformity in software algorithms(105) and intervendor differences, despite efforts to standardize STE measurements(77).

The second clinical implication of our study applies to the design of clinical studies. Given the high reproducibility and low variability, cMR is often used to reduce sample size(104) of prospective studies evaluating changes in LV or RV function. Our study suggests that sample sizes for studies may be nearly as low when using STE. This suggests that, when taking precautions for uniformity of acquisitions and analysis, STE could also be useful for evaluation of LV and RV systolic function in longitudinal studies with a potentially lower costs than cMR. By contrast, we did not observe advantages of FT over conventional cMR, for reproducibility of LV or RV function assessment. Therefore, we cannot currently recommend these techniques to limit sample sizes in research studies. The reproducibility of FT-cMR strains could be theoretically improved by higher temporal and spatial resolution, either through parallel imaging or iterative reconstruction techniques. Nevertheless, with the compromise of decreasing signal-to-noise ratio leading to more artefacts and consequently to a less good tracking.

LIMITATIONS

Our study was limited by being single-center observational study of limited sample size. Nevertheless, we had enough statistical power to detect small differences between different cardiac techniques. Atrial fibrillation/flutter, acute heart failure and poor image quality were exclusion criteria and therefore our study findings may not apply to these populations.

Systolic cardiac function is load dependent, and all evaluations of cardiac deformations are preload and afterload dependent, whether they are based on visualization of either wall deformation (strain) or cavity deformation (ejection fraction). Importantly, systolic cardiac function evaluates shortening and not contractility. In our study, we wanted to include the physiological effects of variable loading conditions and evaluated true day-to-day variability of the different cardiac imaging techniques rather than test-retest on the same day. Hemodynamic conditions were stable with no significant difference in the heart rate and the blood pressure between the 2 days since we included only stable euvolemic patients and we performed the 2 acquisitions with a short delay. However, the evaluation of cardiac function over a longer delay or in different population might result in larger physiological variations of loading conditions and, consequently larger variability of ejection fraction. Additionally, 2D echocardiography may suffer from incomplete reproducibility of imaging planes, foreshortening and through-plane motion. Indeed, 3D echocardiography may have better reproducibility(21,126) and test-retest variability(112) by allowing more reproducible views and less geometric assumptions. Nonetheless, this technique was not tested in our study since its feasibility is still extremely dependent on high image quality, regular rhythm and patient cooperation. Finally, STE and FT strain analysis were performed with one single vendor so they may not apply to other software.

CONCLUSION

In head-to-head comparison with cMR, STE-LV and RV-GLS measurement showed high test–retest reliability, perfuming more accurately with smaller detectable changes than other echocardiographic measurements of LV and RV function. This suggests that these techniques might be useful for longitudinal follow-up of LV and RV function. Furthermore, computed sample sizes to demonstrate clinically significant changes of LV and RV function by these approaches were low, permitting potential use for longitudinal follow-up in research studies.

III. ARTICLE 2

Additional prognostic value of 2D Right ventricular speckle tracking strain for prediction of survival in heart failure and reduced ejection fraction: A comparative study with cardiac Magnetic Resonance.

Laura Houard, MD, Marie-Bénédicte Benaets MD, Christophe de Meester de Ravenstein PhD, Michel F. Rousseau MD PhD FACC, Sylvie A. Ahn AS, Mihaela-Silvia Amzulescu MD, Clotilde Roy MD, Alisson Slimani MD, David Vancraeynest MD PhD, Agnès Pasquet MD PhD FACC, Jean-Louis J. Vanoverschelde MD PhD FACC, Anne-Catherine Pouleur MD PhD, Bernhard L. Gerber MD PhD FACC

Division of Cardiology, Department of Cardiovascular Diseases,
Cliniques Universitaires St. Luc
Pôle de Recherche Cardiovasculaire (CARD)
Institut de Recherche Expérimentale et Clinique (IREC)
Université Catholique de Louvain (UCLouvain)
Brussels, Belgium

JACC Cardiovasc Imaging 2019 Dec;12(12):2373-2385.

STRUCTURED ABSTRACT

Objectives

To compare the prognostic value of 2-dimensional (2D) right ventricular (RV) speckle tracking (STE) against Cardiac Magnetic Resonance (cMR) RV ejection fraction (EF) and feature tracking (FT) and conventional echocardiographic parameters on overall and cardiovascular survival in patients with heart failure and reduced ejection fraction (HF-rEF).

Background

Prior works showed that RV systolic function predicts prognosis in HFrEF. 2D-RVSTE had recently been proposed as new echocardiographic method to evaluate RV dysfunction.

Methods

266 patients with HF-rEF (mean LVEF 23±7%, age 60±14 years; 29% female) underwent RV function assessment using cMR and 2D echocardiography and were followed for a primary endpoint of overall death and secondary endpoint of CV death.

Results

Average cMR-RVEF was 42%±15%, average STE-RVGLS was -18.0% ±4.9% average cMR-FT-RVGLS was -11.8±4.3%). After a median follow-up of 4.7 years, 102 patients died, 84 of CV cause. RVEF, FT-RVGLS, TAPSE, FAC and STE-RVGLS were significant univariate predictors of overall and cardiac death. In multivariate cox regression, age, ischemic etiology, diabetes, NYHA class III-IV, and beta blocker treatment were independent clinical predictors of overall mortality. cMR-RVEF ($\chi 2$ to enter=3.9, $p<0.05$), FT-RVGLS ($\chi 2$ to enter 3.7, $p=0.05$), FAC ($\chi 2$ to enter 6.2, $p=0.02$), and TAPSE ($\chi 2$ to enter=4.9, $p=0.04$) provided additional prognostic value over these baseline parameters, but the additional predictive value of STE-RVGLS ($\chi 2$ to enter=10.8, $p<0.001$) was significantly ($p<0.05$) higher than the other tests. Additional Hazard ratio [95% confidence interval] to predict overall mortality was 2.5 [1.6;3.9] for STE-RVGLS<-19%, 2.15 [1.34-3.43] for TAPSE>15 mm. 1.6 [1.02-2.49] for FAC>39% and 1.93 [1.25-2.99] for RVEF>41% and 1.87 [1.10-3.19] for cMR-FT-RVGLS<-15%

Conclusion

2D RVGLS provides strong additional prognostic value to predict overall and cardiovascular mortality in HF-rEF, with higher predictive value than cMR-RVEF, cMR-FT-RVGLS, TAPSE or FAC. This supports use of STE-RVGLS to identify higher risk HFrEF patients.

INTRODUCTION

Right ventricular (RV) systolic dysfunction has been recognized as an important predictor of outcome in heart failure (HF) (79,83,90,127,128). While cardiac magnetic resonance (cMR) derived RV ejection fraction (EF) is currently considered the gold standard technique for RV evaluation, echocardiography is more readily available in daily practice. Yet, accurate echocardiographic assessment of RV function remains challenging. Indeed, because of the complex shape of the RV there is actually no single RV echocardiographic parameter universally accepted for assessment of global right ventricular systolic function. Due to less angle dependency than conventional RV parameters(129), two-dimensional Speckle tracking echocardiography (2D STE) derived-RV myocardial global (RVLS) and free wall longitudinal strain (RVFWLS) have recently been proposed to evaluate RV dysfunction(62). However, so far no study has evaluated whether the prognostic value of these new approaches equals cMR derived RVEF to identify HF patients at higher risk of mortality.

Therefore, the aim of this study was to estimate the prognostic significance of 2DSTE-RVGLS and FWLS, in patients with heart failure and reduced ejection fraction (HF-rEF) in direct comparison to cMR RVEF and Feature tracking (FT) and to conventional echocardiographic parameters such as TAPSE and FAC. Accordingly, we prospectively studied 266 patients with HFrEF using Cox survival analysis to assess the independent additional prognostic value of 2DSTE vs RVEF-cMR to predict overall and cardiovascular survival over baseline clinical and echocardiographic data.

METHODS

Study population

From a prospective registry, we identified consecutive patients with LVEF < 35% who underwent cMR between 2002 and 2015 in our institution. Inclusion criteria were stable chronic heart failure patients in sinus rhythm and available transthoracic echocardiography (TTE) within 40 days of cMR. Exclusion criteria were image quality precluding RV strain analysis, hemodynamic instability, atrial fibrillation or flutter, moderate and severe primary valve disease. Secondary cardiomyopathies and cardiotoxic chemotherapy, severe chronic kidney disease defined as a Modification of Diet in Renal Disease formula (MDRD) <30 ml/min/1.73 m2 and patients with life expectancy <1 year due to other comorbidities were also excluded. 266 patients satisfied the inclusion criteria (**Figure 1**) and constituted the final study population. The study protocol was approved by the IRB of the institution.

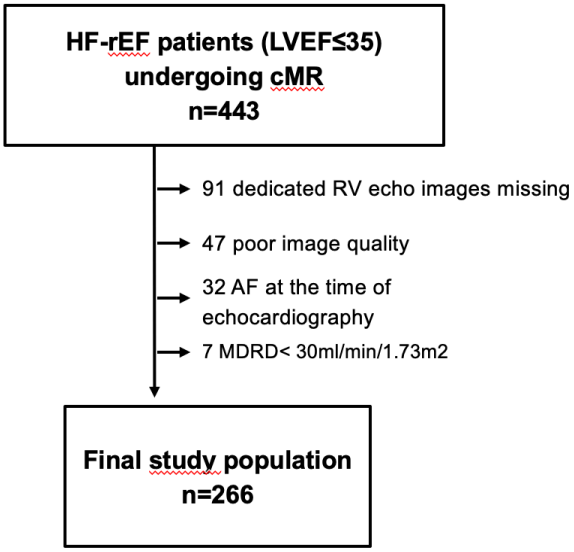

Figure 1 Flowchart of patient inclusion. Flowchart of patient inclusion and exclusion criteria. HF-rEF indicates Heart failure reduced ejection fraction; AF, atrial fibrillation; MDRD, Modification of Diet in Renal Disease

Clinical Data

Patient's medical history and treatment were prospectively recorded. Other information was retrieved from medical files and from review of hospital records. The etiology of heart failure was considered ischemic or non-ischemic on the basis of documented prior myocardial infarction or angiographically proven coronary artery disease according to Felker et al(130).

Transthoracic Echocardiography

Standardized complete TTE exams acquired according to established guidelines using Sonus 7500 or iE33 ultrasound systems (Philips Medical Systems, Andover, MA, United States) equipped with a 3.5/1.75-MHz phased-array transducer and stored on a XCELERA 2.1 PACS server were analyzed off-line by a single observer (LH) blinded to follow-up clinical and cMR data. TAPSE and FAC were measured according to established guidelines on 4 chamber views oriented to the RV. Estimated pulmonary systolic artery pressure (eSPAP) was calculated based on the Bernouilli simplified equation on continuous wave Doppler imaging of tricuspid regurgitation maximum jet velocity. Pulmonary hypertension was considered when eSPAP was >40 mmHg. LV and RV strains were computed using 2D-STE Tomtec software (4.6 version, Tomtec Unterschleissheim, Germany). Endocardial borders of the RV and LV were automatically tracked throughout the cardiac cycle by the software, with manual corrections if necessary. Images with poor quality tracking were excluded. LV peak global longitudinal strain (GLS) was computed by averaging four and two chambers view. For the RV we evaluated both peak systolic global RV longitudinal strain (RVGLS) and peak systolic free wall longitudinal strain (RV FWLS). The average frame rate of the clips for RV and LV strain analysis was 47±11 frame rates per second.

Cardiac Magnetic Resonance

cMR studies were acquired using a 1.5T or 3T systems (Intera CV and Achieva, Philips Medical Systems, Best, the Netherlands) as described before (131). Briefly, 10-12 consecutive short axis images covering the entire left ventricle, and respectively one 2- 3- and 4 chambers long-axis cine SSFP images were acquired for assessment of myocardial

function. 10-15 minutes after injection of 0.2 mmol/kg gadolinium based contrast, identical prescriptions of short- and long-axis slices were acquired using a 2D- or 3D inversion recovery sequence allowing for the assessment of myocardial viability.

CMR studies were analyzed using the freely available software Segment version 2.2 (*http://segment.heiberg.se*) (106) by one experienced observer (BG). Right and left ventricular volumes and EF were computed from the short-axis cine images by semi-automatically tracing the endo- and epicardial contours in the end-diastolic (ED) and end-systolic (ES) phases. Values were indexed to the body surface area. Presence and extent of late gadolinium enhancement (LGE) was evaluated visually and quantified with a semi-automated algorithm, as previously reported(131). FT-RVGLS was performed using the same Segment software in 4 chamber cine view,

Follow-up

Patients were prospectively followed until April 2017 by phone contact with the patients, their relatives, or their physician. All deaths were recorded and categorized as cardiac or noncardiac. Cardiac death was defined as death attributable to congestive heart failure (i.e. death preceded by acute worsening or exacerbation of heart failure) myocardial infarction, sudden death (i.e. unexpected, unwitnessed, or witnessed death in absence of other apparent causes) or occurring after cardiac revascularization. **The primary endpoint** was overall death. The **secondary endpoint** was cardiovascular (CV) death. Since time to heart transplantation is not only determined by the patient status, but also by organ availability, heart transplantation was not considered an event, but patients were censored at the date of the procedure.

Statistical analysis.

Statistical analyses were performed using R software (version 3.3.2). All tests were 2 sided and p value <0.05 was considered statistically significant. Continuous variables were expressed as mean ± one standard deviation (SD), categorical variables as counts and percentages. Hazard Ratios (HR) were expressed as mean and 95% confidence intervals (CI).

Interobserver and intraobserver reproducibility of measurement of RV function was evaluated in 15 randomly selected patients using intraclass correlation coefficient (ICC) and Bland-Altman analysis with computation within-subject coefficient of variation. Our study had 90% power with α=0.05 to detect a twofold increase of hazard of death (ie 60% vs 78% survival at 5 years) in low vs high median of RV function. Continuous and categorical variables of baseline characteristics of patients were compared among tertiles of RVGLS using ANOVA or $\chi 2$ test respectively. The correlation between CMR-derived RVEF vs echocardiographic measures of RV function was examined using Pearson's correlation coefficient. To determine independent predictor of the primary endpoint, uni and multivariate Cox proportional hazard models were used. For the secondary endpoint we used a proportional subdistribution hazards' regression model accounting for competing risk (crr function in cmprsk package).All clinical, echocardiographic and MR parameters were proposed for inclusion in the univariate model. Then a stepwise backward model including all significant ($p<0.10$) univariate clinical correlates of survival was used to construct a clinical baseline model predicting either overall or cardiovascular survival. To assess the potential additive prognostic value of RVGLS and the others RV parameters we evaluated the ability of all the RV parameters to improve the prediction of death from this baseline model by comparing the additional increase of chi square of the combined model over the baseline model. Finally we determined the cutoff values of RVEF, RVGLS, FAC and TAPSE by the highest hazard ratios to predict survival, and computed Kaplan-Meyer survival graphs adjusted for baseline covariates as well as incremental $\chi 2$ values over baseline model. Models were compared using likelihood tests.

RESULTS

Baseline characteristics of patients

Median delay between cMR and echo was 7 (IQR 1-15) days. FT-cMR was not feasible in 16 patients because of poor tracking. The mean age of HF patients were 60±14 years and 71% were male. Etiology of heart failure was ischemic in 51% of patients and 56% were in New York Heart association (NYHA) class III or IV. Mean LV-EF was 23±7%. **Table 1** shows characteristics of the study population according to tertiles of STE-RVGLS.

	Total population (n=266)	Tertile 1 RV GLS(n=89)	Tertile 2 RV GLS (n=88)	Tertile 3 RV GLS (n=89)	P-value
Clinical Characteristics					
Age (years)	60 ± 14	60± 15	62 ± 14	59 ± 13	0.37
Women (n. %)	78 (29%)	28 (31%)	24 (27%)	26 (29%)	0.85
ICM (n, %)	135 (51%)	53(60%)	43 (49%)	39(44%)	0.088
BMI (kg/m²)	26 ± 5	25 ± 4	26 ± 5	26 ± 5	0.55
BSA (m²)	1.84 ± 0.21	1.82 ± 0.2	1.85 ± 0.2	1.85 ± 0.2	0.79
MAP (mmHg)	86± 13	87± 13	85± 13	85± 13	0.52
Heart rate(bpm)	80± 19	73± 19	80 ± 16	87± 19	<0.001
NYHAIII-IV (n. %)	146 (55%)	23(27%)	54(61%)	68(76%)	<0.001
Comorbidities					
HTA (n. %)	121(46%)	45 (51%)	42 (48%)	34(38%)	0.24
Diabetes Mellitus (n. %)	63 (24%)	14 (16%)	19 (22%)	28 (33%)	0.12
Ever smoker (n. %)	164(62%)	48 (54%)	52(59%)	64(72%)	0.09
HistMI (n. %)	105 (39%)	39(44%)	346(41%)	30(33%)	0.37
HistPCI (n. %)	39 (15%)	15 (17%)	16 (18%)	8 (9%)	0.19
HistCABG (n. %)	13 (5%)	3 (3%)	7 (8%)	3(3%)	0.56
Blood results					
MDRD (ml/min/1.73m²)	71 ± 22	76 ± 26	68 ± 20	68 ± 18	0.033
Sodium (mg/dl)	138 ± 4	138 ± 3	138 ± 4	137 ± 5	0.007
Hemoglobin(g/dl)	12.24±1.8	13.3± 1.4	13.3± 1.8	13.6± 2.12	0.27
Medication. n (%)					
Aspirine	182(68%)	62(70%)	61(69%)	59(66%)	0.8
ACE/ARB	262 (98%)	88 (99%)	88 (100%)	86 (97%)	.17
Beta blockers	238(89%)	78(88%)	78(89%)	82(92%)	0.62
Digitale	7(3%)	2 (2%)	3 (4%)	2(2%)	0.86
Aldosterone blockers	192 (72%)	52(58%)	66 (75%)	74(83%)	<0.001
Diuretics	182 (68%)	44(49%)	66(75%)	72(81%)	<0.001
Statin	139(52%)	47(53%)	52(59%)	40(45%)	0.24
Antiarrythmic drugs	41(15%)	13(15%)	11(13%)	17(19%)	0.34
Echocardiographic measurements					
STE-RV-GLS(%)	-18.0 ± 4.9	-23.± 2	-18 ± 2	-12 ± 2	By design
STE-RV-FWLS(%)	-18.7 ± 6.6	-25 ± 5	-18 ± 4	-13 ± 4	<0.001
TAPSE(mm)	18 ± 5	21 ± 4	18 ± 4	16 ± 4	<0.001
RV-FAC(%)	37 ± 12	46 ± 9	36 ± 9	28 ± 10	<0.001
eSPAP(mmHg)	34 ± 11	28± 9	36 ± 11	36± 12	<0.001
eSPAPS>40mm Hg	62(23%)	10(11%)	20 (23%)	32 (36%)	<0.001
E/A ratio	1.5 ± 1.0	1.2 ± 1.25	1.6 ± 0.9	1.95 ± 0.85	<0.001
E/e' ratio	19 ± 14	14 ± 8	19 ± 9	22 ± 14	<0.001
Moderate/severe TR (n.%)	26(10%)	1(1%)	8(9%)	17(19%)	<0.001

LV GLS(%)	-10.5 ± 3.3	-12± 3	-11 ± 3	-9± 3	<0.001
cMR measurements					
LV-EDVi (ml/m²)	155 ± 49	143± 37	159 ± 57	164± 49	0.009
LV-ESVi (ml/m²)	121 ± 47	106 ± 34	125 ±52	134 ± 48	0.0001
LV-EF (%)	23 ± 7	27 ± 6	23 ± 7	19 ± 7	<0.001
RV-EDVi (ml/m²)	86 ± 33	69 ± 18	89 ± 32	100 ± 38	<0.001
RV-ESVi (ml/m²)	53 ± 33	33 ± 15	57± 30	710± 37	<0.001
RV-EF (%)	42 ± 15	54 ± 11	38 ± 12	32 ± 13	<0.001
RV-EF>45% (n. %)	110(41%)	72 (81%)	25 (28%)	13(15%)	<0.001
FT-RVGLS	-11.8±4.3	-14.1±4.3	-11.8±4.2	-9.7±3.3	<0.001
LV Scar (n. %)	156(59%)	52(58%)	56(64%)	48(54%)	0.43
Scar burden (%)	8± 9	10± 10	9± 10	6± 7	0.57

Table 1 Clinical characteristics of HF-rEF patients according to tertiles of RV GLS Across-group P value is for the difference across the tertiles of RVGLS(lower, middle and upper tertiles) by the Anova test.

ACEI/ARB: angiotensin converting enzyme inhibitor/angiotensin receptor blocker; BMI: body mass index; BSA: body surface area; CABG: coronary artery bypass graft; EDVi: indexed end-diastolic ventricular volume; ESVi: indexed end-systolic ventricular volume; EF: ejection fraction; eSPAP: estimated systolic pulmonary artery pressure; FAC: fractional area change; FWLSL: free-wall longitudinal strain; GLS: global longitudinal strain; Hist: History of; HTA: arterial hypertension; ICM: ischemic cardiomyopathy; LV: left ventricular; MI: myocardial infarction; MAP: mean arterial pressure; MDRD: Modification of Diet in Renal Disease formula; MR: mitral regurgitation; PCI: percutaneous coronary intervention; RV: right ventricular; TASPE: Tricuspid annular plane systolic excursion; TR: tricuspid regurgitation;

There were no significant differences in age or sex between the tertiles. By contrast, patients with a more impaired RV strain had a higher resting heart rate, more advanced NYHA class, higher diuretic and aldosterone blocking drug use, lower LVEF, higher indexed LV ventricular volumes, estimated systolic pulmonary artery pressure (eSPAP), E/a ratio and more severe tricuspid regurgitation than those with less altered systolic RV strain. Also, CMR-derived RV volumes and FT-RVGLS were higher, while RVEF, TAPSE and FAC were significantly lower in patients with the most depressed STE-RVGLS.

Correlation of RV function by echocardiography vs cMR

Table 2 shows correlation of RV functional parameters by echocardiography vs cMR RVEF. All RV echocardiographic parameters correlated significantly (r between 0.60 and 0.65) with CMR-derived RVEF. Surprisingly, cMR FT-RVGLS correlated however only moderately with cMR-RVEF (r=0.45, p<0.001) and with STE-RVGLS (r=0.47, p<0.001). A moderate correlation between CMR-derived RVEF and LVEF was also observed (r=0.55 p<0,001) whereas the correlation with LV-GLS (r=-0.34; p<0.001) was weak. Finally, STE-RVFWLS and STE-RVGLS were highly correlated among each other (0.85, p<0.001), but average STE-RVFWLS was significantly greater than STE-RVGLS.

	Pearson's correlation (R)	p value
RV-FAC	0.65	<0.001
TAPSE	0.62	<0.001
STE-RV-GLS	-0.62	<0.001
STE-RV-FWLS	-0.57	<0.001
cMR-LVEF	0.55	<0.001
LV-GLS	0.34	<0.001

Table 2 Pearson's linear correlations of parameters with CMR derived RVEF. Abbreviations as in table 1.

Events at Follow-up

Follow-up was 100% complete for a median duration of 4.7 years. During follow-up 102 patients died, 84 of cardiovascular causes: 3 postoperatively, 38 suddenly, 3 of stroke, 7 of cardiogenic shock, and 33 of heart failure. 18 patients died of non-cardiac causes (10 cancers, 2 Alzheimer, 5 sepsis, 1 COPD). 21 patients underwent heart transplantations and were censored. Accordingly, 102 patients reached the primary endpoint of all-cause death and 84 the secondary endpoint of CV death.

Predictors of overall and CV survival

Table 3 shows the univariate cox regression analysis for the primary endpoint of overall survival. Age, ischemic etiology, diabetes, NYHA functional class III or IV, estimated systolic pulmonary artery pressure (eSPAP)> 40mmHg, STE and FT-RVGLS, RVFW, RV-FAC, TAPSE, E/A and E/é ratio, MDRD, beta blocker treatment and cMR-derived RV indexed volumes and RVEF were associated with overall mortality. LV-GLS and cMR-LGE presence or scar burden >2% were associated with mortality. However LV-EF was not predictive of either overall or cardiovascular mortality in univariate analysis.

	Alive N=164	Dead N=102	HR (95% CI)	P-value
Clinical characteristics				
Age(years)	56 ± 10	66 ± 11	1.52[1.03;1,07]	<0.001
Women (n,%)	54 (33%)	24 (24%)	0.66[0.41;1.04]	0.07
ICM (n,%)	60 (36%)	73 (73%)	2.2[1.42;3.46]	<0.001
HTA (n,%)	66 (40%)	55 (54%)	1.39[0.95;2.06]	0.09
Diabetes Mellitus (n,%)	25 (15%)	38 (37%)	2.19[1.46;3.28]	<0.001
NYHA III-IV (n,%)	84 (51%)	62 (61%)	1.56[1.05;2.33]	0.03
Medications (n,%)				
Aspirin	98 (60%)	83 (82%)	1.87[1.12;3.118]	0.02
Beta-blockers	153 (93%)	85 (83%)	0.48[0.29;0.82]	0.006
Diuretics	107 (65%)	75 (74%)	1.71[1.10;2.67]	0.02
Laboratory test				
MDRD (ml/kg/1.73m²)	74 ± 23	66 ± 19	0.98[0.97;0.99]	<0.001
Echocardiographic measurements				
LV-GLS (%)	-11 ± 3	-10 ± 3	1.06[0.99;1.13]	0.05
STE-RV-GLS (%)	-18 ± 5	-17 ± 5	1.06[1.1;1.11]	0.002
STE-RV-FWLS (%)	-19 ± 7	-18 ± 6	1.06[1.02;1.09]	0.001
TAPSE (mm)	19 ± 4	18 ± 5	0.95[0.91;0.99]	0.011
RV-FAC (%)	37 ± 12	36 ± 11	0.985[0.96;0.99]	0.021
eSPAP>40mmHg	32 (18%)	30 (36%)	1.81[1.19;2.04]	0.005
E/a ratio	1.5 ± 1.1	1.6 ± 0.8	1.36[1.12;1.67]	0.002
E/e'	18±8	20±10	1.03 [1.01;1.06]	0.012
cMR measurements				
RV-EVDi (ml/m²)	84 ± 3	89 ± 33	1.007[1.001;1.014]	0.01
RV-ESVi (ml/m²)	52 ± 33	56 ± 32	1.008[1.002;1.015]	0.005
RV-EF (%)	42 ± 15	41 ± 16	0.98[0.97;0.99]	0.03
FT-RVGLS (%)	-12.0±4.1	11.7±4.5	1.06 [1.01;1.11]	0.015
LV-EF (%)	23 ± 7	23 ± 7	0.98[0.9;1.01]	0.16
Presence of LV scar (n. %)	83 (51%)	73 (72%)	1.578[1.02;2.4]	0.04
Scar burden > 2%	71 (43%)	71 (70%)	1.84 [1.2; 2.8]	0.004

Table 3 Univariate predictors of overall death. All parameters were tested, but only parameters with p<0.10 were reported. CI: Confidence Interval; HR: Hazard Ratio. All other abbreviations as in table.

Multivariate models for overall and cardiovascular survival are shown in **Tables 4 and 5,** respectively. Age, ischemic cardiomyopathy, diabetes, NYHA class > II and betablocker treatment were independent predictors of overall death. CV death was predicted by the same parameters and, in addition, eSPAP>40 mmHg and MRDR. Baseline models using these parameters were constructed to predict overall and CV death. cMR-RVEF, FT-RVGLS,

STE-RVGLS, RV-FWLS andRV-FAC were found to have significant additional prognostic value for overall and cardiovascular mortality over these baseline models.

Parameter	**Partial HR**	**X^2**	**P value**
Age	1.05 [1.03;1.07]	24.2	<.0001
Ischemic Etiology	1.85 [1.17;2.93]	6.9	.008
Diabetes	1.95 [1.29;2.96]	9.9	.002
NYHA class III-IV	1.75 [1.16;2.64]	7.0	.008
Betablocker R/	0.51[0.30;0.86]	6.4	.011
Combined Baseline model		58.2	<0.001

Parameter	X2 to improve	Partial HR	p
cMR-RVEF	3.9	0.98[0.97;1.00]	0.05
cMR-FT-RVGLS	3.7	1.05 [0.99;1.10]	0.05
STE-RVGLS*	10.8	1.08[1.03;1.13]	<0.001
STE-RVFWLS¶	9.3	1.06[1.02;1.10]	0.002
RV-FAC	6.2	0.97[0.96;0.99]	0.02
TAPSE	4.1	0.95[0.91;0.99]	0.04

Table 4 Multivariate Cox analysis for prediction of overall death
*p<0.05 vs FAC, TAPSE and cMR-RVEF, ¶ p<0.05 vs TAPSE and cMR-RVEF
Abbreviations as in Table1.

Parameter	Partial HR	X^2	P value
Age	1.03 [1.01;1.06]	10.5	<0.007
Ischemic Etiology	2.52 [1.53;4.18]	10.1	<0.001
Diabetes	1.52 [0.97;2.41]	4.8	.07
NYHA class II-IV	1.62 [1.01;2.61]	4.5	.05
Betablocker R/	0.41 [0.23;0.73]	8.2	.002
eSPAPs>40 mmHg	1.80 [1.14;2.82]	5.4	.01
MDRD	0.99 [1.01;1.00]	3.1	.05
Combined Baseline model		56.9	<0.001

Parameter	X2 to improve	Partial HR	p
cMR-RVEF	4.2	0.98[0.97 ;0.99]	0.0394
cMR-FT-RVGLS	7.5	1.09 [1.04 ;1.14]	<0.001
STE-RVGLS*	10.6	1.09[1.03 ;1.15]	0.001
STE RVFWLS¶	8.4	1.06[1.02 ;1.10]	0.001
RV-FAC	6.9	0.97[0.95 ;0.99]	0.001
TAPSE	1.3	0.97[0.93 ;1.01]	0.18

Table 5 Multivariate subdistribribution hazard model for prediction of cardiovascular death corrected for subdivision
*p<0.05 vs FAC, TAPSE and cMR-RVEF, ¶ p<0.05 vs TAPSE and cMR-RVEF
Abbreviations as in Table 1.

TAPSE was found to only provide additional value for overall, but not for cardiovascular mortality. The predictive value of RV-GLS and RV-FWLS was similarly good (p=NS), and significantly (p<0.001) higher than of cMR RVEF and FT-RVGLS. By contrast, cMR-LVEF did not have additional prognostic value for overall (X2 to improve=1.78, p=0.18) or cardiovascular mortality (X2 to improve 1.6, p=0.19). LVGLS had incremental value for cardiovascular (X2 to improve 6.3, HR 1.10[1.03 ;1.19], p=0.008) but not overall mortality (X2 to improve 0.4, p=0.51). Also, since LGE presence or scar burden >2% was highly correlated with ischemic etiology (kappa=0.64, p<0.001), they did not have additional prognostic value over baseline models for either endpoints. Optimal cutoff values of RV parameters yielding the highest additional HR for overall survival were 41% for RVEF 41%, 39% for RV-FAC 39%, 15 mm for RV-TAPSE 15 mm, -15% for FT-RVGLS and -19% for RV-GLS and RVFWLS. **Figure 2** shows Kaplan Meier survival graphs for adjusted overall and CV mortality stratified by these cutoff values. It clearly demonstrates that both overall and cardiovascular survival significantly declined with worsening RV function irrespective of the method used.

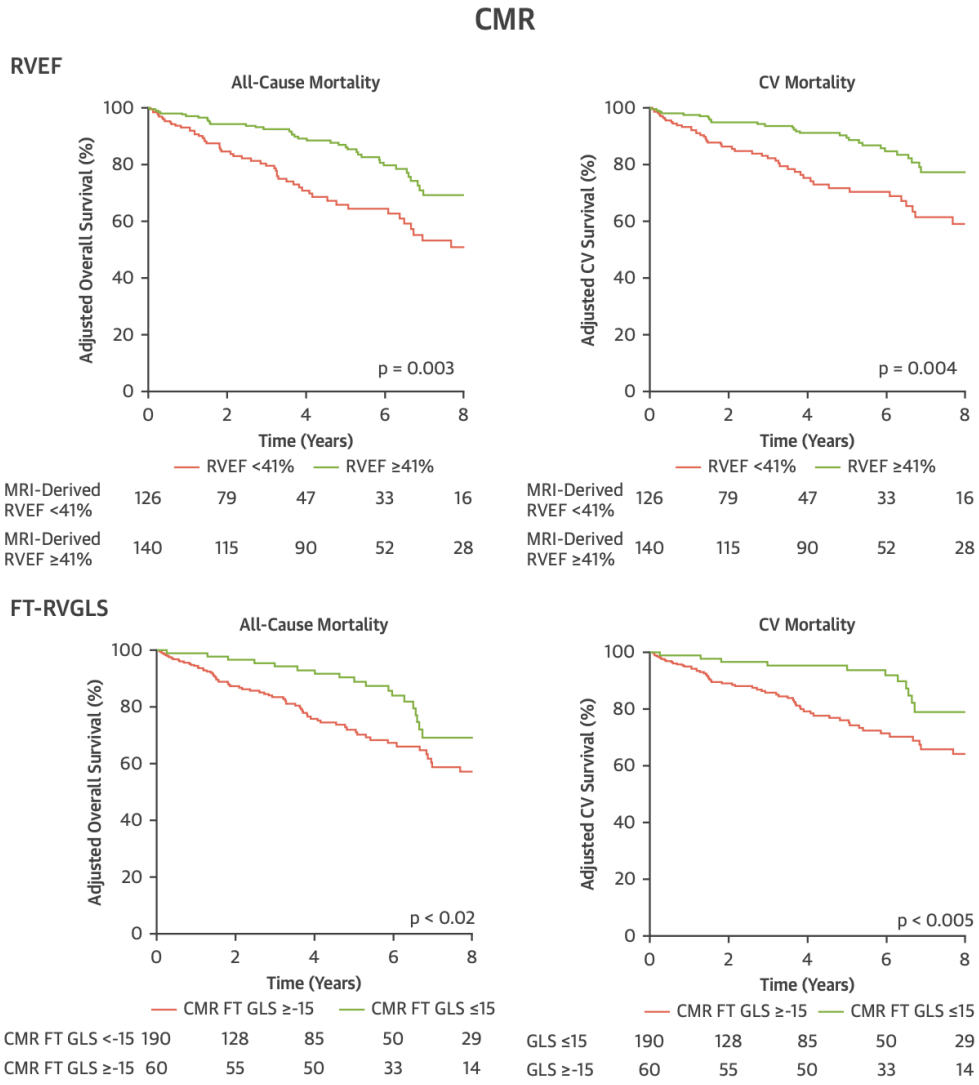

Figure 2 Kaplan-Meyer Event-Free Survival curves for cardiac magnetic resonance (cMR) parameters.
Kaplan-Meyer event-free Kaplan Meyer adjusted overall and cardiovascular survival stratified by optimized cutoff value of RVEF<41% and cMR-FT RVGLS<15%.. Adjustments were made for age, ischemic etiology, NYHA class, Diabetes, betablocker treatment, pulmonary hypertension and MDRD

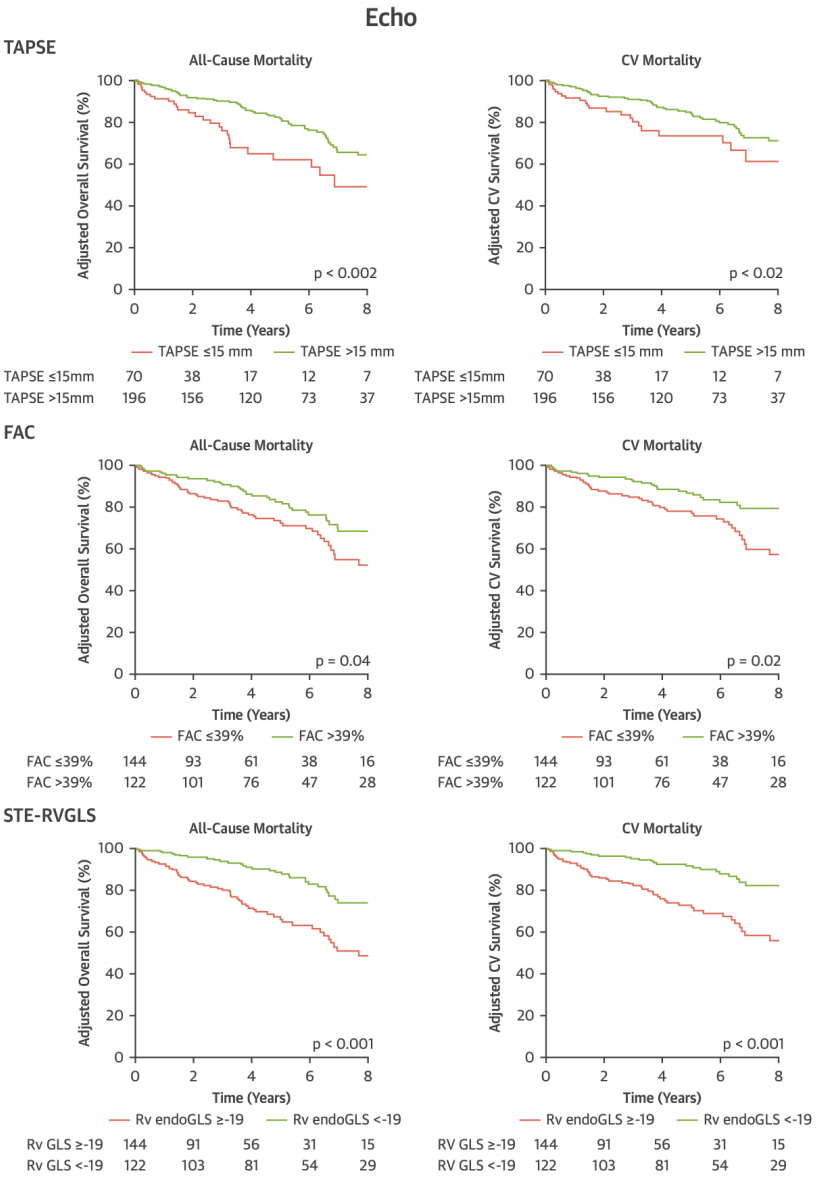

Figure 2 Kaplan-Meyer Event-Free Survival curves for echocardiography parameters. Kaplan-Meyer event-free Kaplan Meyer adjusted overall and cardiovascular survival stratified by optimized cutoff value of TAPSE<15 mm , FAC<39% and RV-GLS<19% . Adjustments were made for age, ischemic etiology, NYHA class, Diabetes, betablocker treatment, pulmonary hypertension and MDRD

Figure 3 compares the additional χ2 statistic value of different RV parameters by cMR and echocardiography to increase predictive value for overall and cardiovascular survival while **Figure 4** shows the additional hazard ratio of these tests.

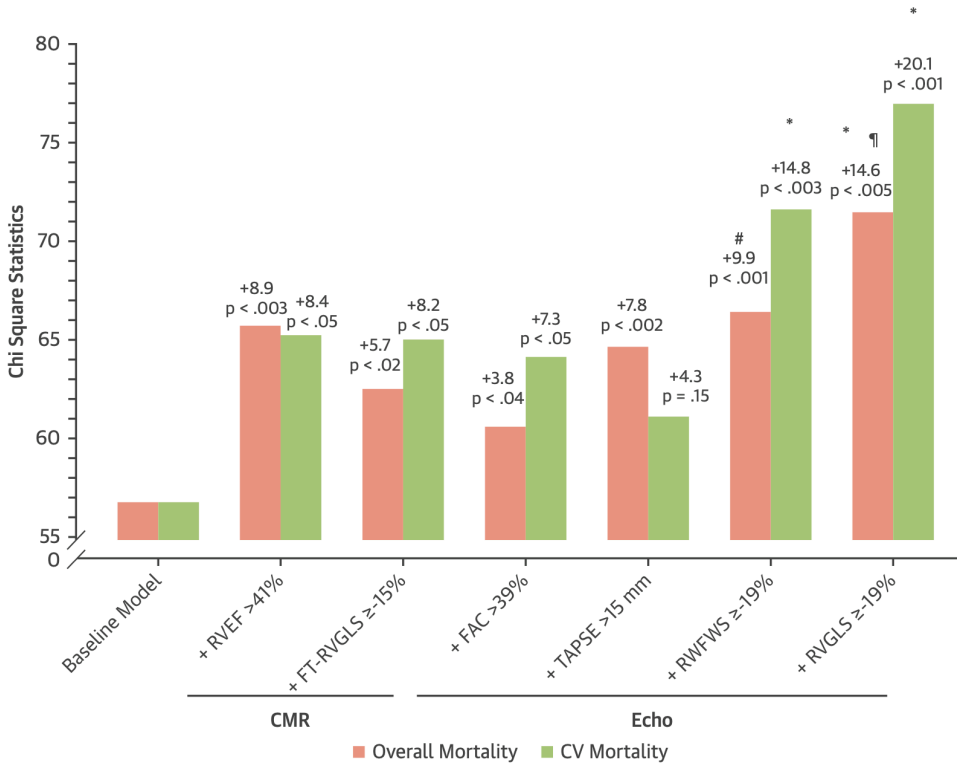

Figure 3 Chi square statistic of Models.
Chi square statistic of baseline model for overall (white) and cardiovascular (grey) mortality andof different RV functional tests stratified by optimized cutoff value to predict overall and cardiovascular mortality over baseline parameters**.** Values indicate the additional Chi square of the different models. * indicates p<0.05 vs other tests # indicates p<0.05 vs FAC, ¶ indicates p<0.05 vs RVGLS vs RVWFS. Statistical comparisons by likelihood ratio tests.

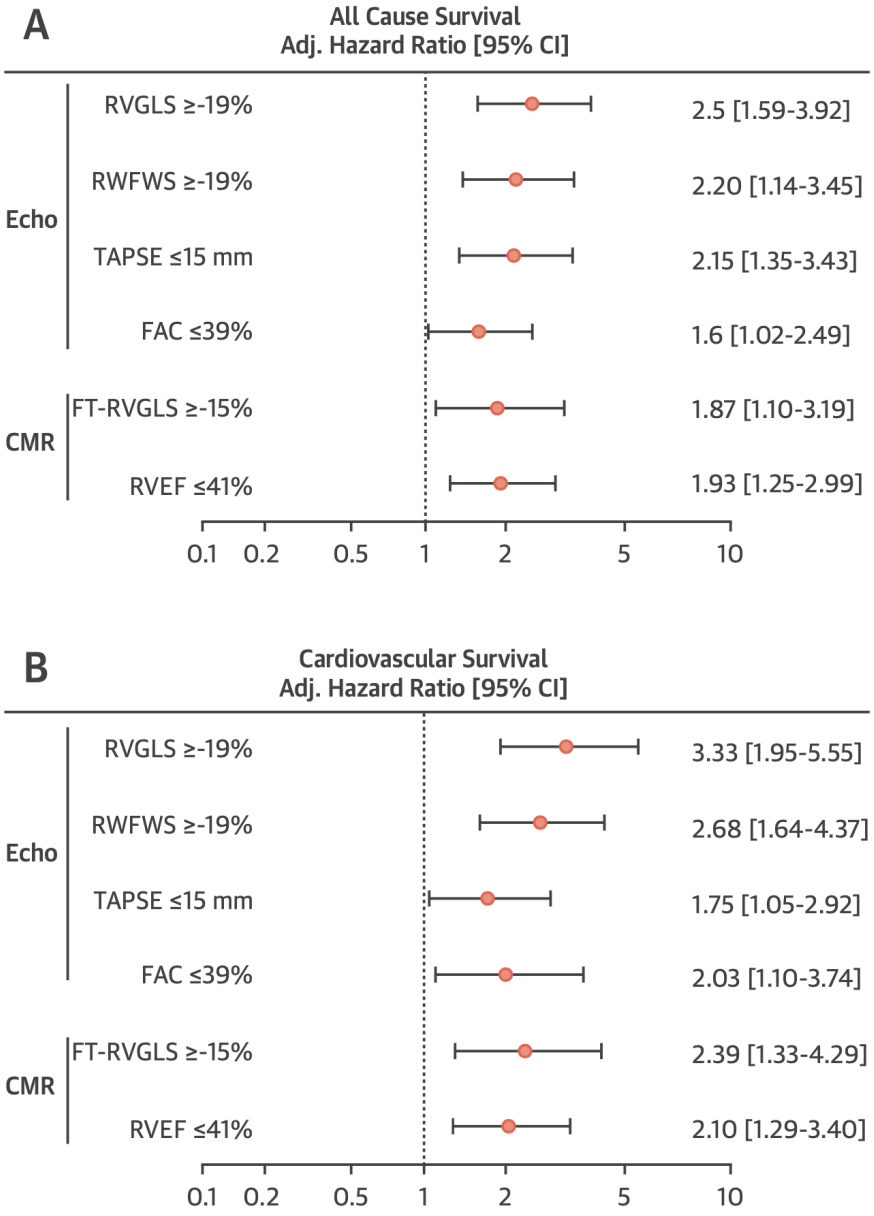

Figure 4 Additional Hazard ratios
Adjusted additional Hazard ratios of different right ventricular parameters to predict a) overall b) cardiovascular survival over baseline clinical parameters.

RVEF>41%, FT-RVGLS<-15 %, TAPSE>15 mm and FAC>39% significantly improved prediction of overall and cardiovascular mortality over baseline clinical variables to similar amounts. However RVGLS<-19% had the highest incremental predictive value and provided the highest increase in hazard ratio for both overall and CV mortality. Notably, the incremental value of RVGLS was significantly higher than that of RVFWLS for overall mortality.

Reproducibility of RVLS measurements

Reproducibility of RV measurements is shown in **Table 6**. All measurements had good intra- and interobserver reproducibility.

	Intra-observer Reproducibility		Inter-observer Reproducibility	
	CV [95% CI]	ICC	CV [95% CI]	ICC
cMR RV-EF	13.1% [3.4;18.3]	0.96	11.3% [6.5;14.7]	0.94
TAPSE	4.7% [3.3;5.8]	0.98	18.3% [5.7;25.3]	0.82
RV-FAC	7.3% [2.7;10]	0.91	13.8% [9.8;16.9]	0.76
STE-RVGLS	3.6% [2.0;4.8]	0.98	9.6% [6.3;12.0]	0.86
STE-RVFWLS	13.9% [10.4;16.8]	0.80	15.6% [9.0;20.1]	0.82

Table 6 Reproducibility of measurements

CI: confidence interval; CV: coefficient of variation; ICC: Intra-class correlation coefficient. Other Abbreviations as table 1.

DISCUSSION

The principal findings of our study were:
1) RV dysfunction assessed either by cMR or echocardiography, predicts overall and cardiovascular survival with significant additional value over baseline clinical parameters such as age, NYHA class, ischemic etiology, betablocker treatment, renal function and eSPAP.
2) RVGLS and RVFWLS were strongly correlated, but RVGLS had slightly better predictive value than RVFWLS.
3) Most importantly, the predictive value of echocardiography derived 2DSTE-RV GLS was superior to CMR-derived RVEF, FT-RVGLS, TAPSE and FAC for both overall and CV mortality.

Prognosis of HFrEF and the importance of RV function

Heart failure (HF) is associated with significant morbidity and mortality. However individual patients may have highly variable prognosis. Therefore, it is important to identify patients at higher risk for mortality who might benefit from more intensive monitoring and therapy. Several prognostic markers of death and/or HF hospitalization have been identified and various clinical risk scores have been proposed in patients with HF-rEF(132,133). Our present study not only confirmed the role of several of these previously described risk factors, in particular age, NYHA class, renal function and pulmonary hypertension, but also demonstrated significant additional prognostic value of RV dysfunction over and above these well-known clinical parameters both in ischemic or non-ischemic HFrEF patients. Importantly, the additional prognostic value of all the RV parameters was significantly higher and independent of LV systolic functional parameters, which lose their prognostic value in these HF-rEF patients with severely depressed LV function because of the tight range of LVEF and LVGLS values in these patients.
This is consistent with several recent studies demonstrating that RV dysfunction assessed using different techniques such as echocardiography (79,85,134), radionuclide ventriculography(127,128,135,136), right heart catheterization (137) and CMR (83,84) is a key determinant of outcome in HFrEF patients. Indeed, in HFrEF, RV dysfunction can be

caused from several mechanisms such as postcapillary pulmonary hypertension, RV myocardial ischemia, ventricular interdependence due to septal dysfunction. It may also represent a common disease process affecting cardiomyocytes in both ventricles(137,138). RV dysfunction is thus likely not only a marker of more severe LV disease and higher pulmonary pressures, but also directly contributes to less efficient cardiac performance, more severe exercise intolerance and heart failure.

Assessment of RV function by echocardiography

Despite its importance, the complex geometrical anatomy of the RV makes the assessment of RV systolic function by cardiac imaging techniques difficult. Initial works to evaluate RV function relied on radionuclear angiography, but CMR has emerged as the gold standard for RV function. Indeed, CMR is ideally suited for the assessment of the RV because it allows high-resolution time-resolved visualization of the complex anatomical shape of the right ventricle in different directions. However, it has limited availability and high costs. Echocardiography is more widely used for clinical assessment of patients with heart failure, and would be better suited for HFrEF risk stratification. Yet, echocardiography has certain limitations for the assessment of RV systolic function in particular due to the to the complex RV shape, and restricted RV echo-windows. Hence no optimal parameter for RV functional measurements by echocardiography has been identified. Indeed, 2D-echo-derived RV ejection fraction and volumes were found to be poorly reliable and are currently not recommended for clinical use or standard reference in research. TAPSE has been proposed as a simple measurement of longitudinal function but may not accurately reflect global RV function. Nevertheless, it has the important advantage of being easily measurable even when image quality is poor. RV FAC may better reflect RV function but dependents on image plane, requiring complete visualization of the entire RV structure. Also, it was found to have high inter- and intraobserver variability and poor performance when endocardial definition is suboptimal. In prior works, the evidence for both FAC and TAPSE as predictive parameter was conflicting(134). In our study, however, both TAPSE and FAC were significantly correlated to cMR-derived RVEF. While FAC was talented to predict overall and cardiovascular outcome, TAPSE was not found to predict cardiovascular mortality over baseline parameters.

More recently 2D-STE has been proposed as better method for evaluation of RV function by echocardiography(139). It has the advantage of being an automated user-independent parameter, which may more accurately reflect RV function than FAC or TAPSE. Indeed, several studies demonstrated that 2D RV strain has prognostic value in HF (64,140-142). However, most of these studies did not evaluate the additional prognostic value over clinical and echocardiographic parameters(64,140-143) or against cMR RVEF. Importantly, we demonstrated that both 2D RVGLS and FWLS were the most reliable echocardiographic measures of RV function, surpassing FAC and TAPSE for predicting overall and cardiovascular mortality. Surprisingly, STE-RVGLS was also superior to cMR-FT-RVGLS. This might be explained by differences in software, less temporal resolution for FT-cMR than for STE and the fact that FT does not rely on anatomical speckles to track. An important debate in RV strain methodology is whether GLS or FW should be evaluated. The majority of studies evaluated the prognostic value of RVFWLS, based on the fact that the intraventricular septum (IVS) is a constituent part of the LV, and that RVFWLS would thus more closely evaluate RV function than RVGLS. In favor of this, Cameli and al. (144) showed that RVFWLS had the highest diagnostic accuracy to predict a depressed RV stroke work index in a simultaneous echocardiographic-catheterization study. Conversely, through the IVS, the LV contributes 20-40% to RV systolic pressure(145), and canine studies demonstrated that the inactivation of the IVS leads to a significant decrease in right ventricular function and that the reduction of RVFWLS function does not affect RVEF in the presence of a preserved IVS(146). In our study RVGLS and FW were strongly correlated, but RVGLS had a slightly better reproducibility and higher predictive value for overall mortality than RVFWLS. This contrasts with findings in isolated pulmonary hypertension(147) and probably reflects the more important role of LV-RV interaction in HFrEF than in isolated pulmonary hypertension.

Importantly both 2D RVGLS and RVFWLS were found to have even higher prognostic value for overall and cardiovascular mortality than CMR-derived RVEF and FT-RVGLS.

CLINICAL IMPLICATIONS

Our study suggests that RV assessment should be part of the comprehensive evaluation and stratification of HFrEF patients in order to identify patients at higher risk for bad outcome. More importantly our study strengthens and expands previous studies by showing that RV-GLS by echocardiography may provide similarly or even better risk prognostic value than cMR derived RVEF with high intra and interobserver reproducibility. This simple echocardiographic measurement, which can easily be performed at bed site, could thus avoid less accessible and more costly cMR exams for risk stratification. Although RV-GLS was the best echocardiography method for prognosis, the fact that other RV parameters had also good predictive value, suggests that in clinical practice, simpler parameters such as TAPSE could be suitable alternatives when the image is too poor for RV strain analysis.

LIMITATIONS

Although our study was a large cohort of homogenous and consecutive patients with short interval between echocardiography and cMR, it is limited by being a single center retrospective observational study of patients referred to cMR for evaluation of cardiac function, with a potential referral reference bias and by the fact that both tests were not performed simultaneously. We excluded 13% of patients due to poor image quality precluding strain analysis. Indeed, a significant limitation of RV strain remains the need for high quality images and frame rate dependency as well as limited standardization and intervendor variability with wide range of normal value. In prospective design higher frame rate and better image quality would certainly be obtained. We also excluded subjects with comorbidities such as atrial fibrillation and severe chronic kidney disease (CKD) at the time of examination, which are strongly associated with mortality in these patients and therefore our study findings may not apply to this populations. Also, FT and STE Strain analysis were performed with two different vendor- software and specific cut off values reported in this study may not apply to other software or other populations. Also, we assessed only the longitudinal function of the RV by 2D strain, since longitudinal shortening, rather than circumferential deformation, determines RVEF. Despite the fact that RV radial shortening plays also a role to the overall RVEF, radial strain is difficult to measure especially in the

thin-walled RV and the reproducibility is extremely low (148). Finally, brain natriuretic peptide, right-sided index of myocardial performance (RIMP) and peak tissue Doppler systolic velocity (S'wave) were not available for the entire study and could not be evaluated in models of outcome prediction.

CONCLUSION

Our study clearly establishes that 2STE-RV strain is a strong independent predictor of overall and cardiovascular mortality, providing additional prognostic value over clinical parameters in patients with HFrEF. Importantly, both 2STE-RV GLS and FWS were found to have higher predictive value than cMR RV-EF, RV-FTRVGLS, FAC and TAPSE. This supports systematic evaluation of right ventricular function by 2DST for risk stratification in HFrEF patients.

CLINICAL PERSPECTIVES

Competency in Medical Knowledge

In this retrospective study, comparing cMR and echocardiography, right ventricular dysfunction was found to be a strong independent predictor of overall and cardiovascular mortality in patients with HFrEF. The use of echocardiographic derived right ventricular global longitudinal strain was the most powerful echocardiographic parameter and had higher prognostic value than cMR derived RV- EF, suggesting that systematic evaluation of RV function by 2D STE could be important for risk stratification in HFrEF patients.

Translational Outlook

The retrospective design in a single center, as well as the use of a single vendor software for right ventricular strain analysis remain a limitation. Additional clinical studies should confirm the value of 2D-STE in such populations in prospective, multicenter design and using different softwares to allow more general recognition of this method for risk stratification of HFrEF patients.

III : ARTICLE 3

Prognostic value of pulmonary transit time by cardiac magnetic resonance on mortality and heart failure hospitalization in patients with advanced heart failure and reduced ejection fraction.

Laura Houard, MD[1,2], Mihaela-Silvia Amzulescu MD, PhD[1,2], Geoffrey Colin MD[1], Helene Langet PhD[3], Sebastian Militaru MD PhD[1,2], Michel F. Rousseau MD PhD[1,2], Sylvie A. Ahn AS[1,2], Jean-Louis J. Vanoverschelde MD PhD[1,2], Anne-Catherine Pouleur MD PhD[1,2], Bernhard L. Gerber MD PhD[1,2]

(1) Division of Cardiology, Department of Cardiovascular Diseases, Cliniques Universitaires St. Luc

2) Pôle de Recherche Cardiovasculaire (CARD) Institut de Recherche Expérimentale et Clinique (IREC) Université Catholique de Louvain, Brussels, Belgium

3) Philips Clinical Research Board, Suresnes, France

Circ Cardiovascular Imaging. 2021 Jan;14(1):e011680.doi: 10.1161/CIRCIMAGING.120.011680

STRUCTURED ABSTRACT

Background

Pulmonary transit time (PTT) from first-pass perfusion imaging is a novel parameter to evaluate hemodynamic congestion by cardiac magnetic resonance (cMR). We sought to evaluate the additional prognostic value of PTT in heart failure with reduced ejection fraction (HFrEF) over other well-validated predictors of risk including the MAGGIC risk score and ischemic etiology.

Methods

We prospectively followed 410 chronic HFrEF patients (61±13 years, LVEF 24±7%) who underwent a clinical cMR to assess the prognostic value of PTT for a primary endpoint of overall mortality and secondary composite endpoint of cardiovascular death and heart failure hospitalization. Normal reference values of PTT were evaluated in a population of 40 asymptomatic volunteers free of cardiovascular disease.

Results

PTT was significantly increased in patients with HFrEF as compared to controls (9±6 beats and 7±2 beats respectively, $p<0.001$), and correlated not only with NYHA class, cMR-left ventricular (LV) and -right ventricular (RV) volumes, cMR-RV and -LV ejection fraction (EF) and feature tracking global longitudinal strain (FT-GLS), but also with cardiac output. Over 6-years median follow-up, 182 patients died and 200 reached the secondary endpoint. By multivariate Cox analysis, PTT was an independent and significant predictor of both endpoints after adjustment for MAGGIC risk score and ischemic etiology. Importantly in multivariable analysis, PTT in beats had significantly higher additional prognostic value to predict not only overall mortality (χ^2 to improve=12.3, HR:1.35; 95%CI:[1.16;1.58];$p<0.001$) but also the secondary composite endpoints (χ^2 to improve=20.1, HR:1.23; 95%CI:[1.21;1.60]; $p<0.001$) than cMR LVEF, cMR-RVEF, LV-FT-GLS or RV-FT-GLS. Importantly, PTT was independent and complementary to both pulmonary artery pressure and reduced RVEF<42% to predict overall mortality and secondary combined endpoints.

Conclusion

Despite limitations in temporal resolution, PTT derived from first pass-perfusion imaging provides higher and independent prognostic information in HFrEF than clinical and other cMR parameters including LV and RV-EF or FT-GLS.

CLINICAL IMPACT AND PERSPECTIVE

In this retrospective study, evaluating 410 patients with heart failure and reduced ejection fraction undergoing cardiac magnetic resonance, pulmonary transit time from first-pass perfusion imaging was found to be a strong independent predictor of overall and cardiovascular mortality over median follow up of 6 years. Pulmonary transit time an integrative marker of hemodynamic congestion, was found to have high intra and interobserver reproducibility. More importantly it had independent predictive value above clinical parameters such as MAGGIC score and ischemic etiology and was the most powerful imaging parameter with higher prognostic value than cMR derived left and right ventricular ejection fraction and strain. This suggest that systematic evaluation of pulmonary transit time by cMR should be integrated in the risk stratification process of HFrEF patients. Nevertheless, the retrospective design in a single center of our study remains a limitation. Additional clinical studies should confirm the value of pulmonary transit time in prospective, multicenter design, to allow more general recognition of this method for risk stratification of HFrEF patients

INTRODUCTION

Pulmonary transit time (PTT) is a well-known parameter to evaluate global cardiopulmonary function containing information not only from right and left ventricle pump function but also pulmonary blood volume and hemodynamic congestion. It can be measured either invasively using indicator dilution methods with direct heart catheterization, or using different non-invasive imaging methods such as radionuclide imaging(149), computed tomography(47) and contrast enhanced transthoracic echocardiography (TTE)(35,36). Recently, it was proposed that PTT measurements could be derived from first pass perfusion by measuring the time for a bolus of contrast to pass from the right ventricle (RV) to the left ventricle (LV)(37-41). Furthermore, cMR-derived PTT was shown to be increased both in heart failure (HF) with reduced and preserved ejection fraction (EF)(41). However, the prognostic value of this parameter has not yet been compared to other known clinical and imaging parameters.

Therefore, we sought to evaluate the prognostic significance of PTT by first pass perfusion cMR in patients with HF with reduced EF (HFrEF). We thus compared the ability of PTT to predict both overall mortality and a combined endpoint of cardiovascular survival and HF hospitalization over and above other well-validated parameters in the prognosis of heart failure and in direct comparison with LV and RV feature tracking.

METHODS

Study population

We retrospectively identified consecutive patients in optimal medical therapy with stable chronic HF and LVEF < 35% who underwent cMR between 2002 and 2018 in our institution. All patients included in the study were either outpatients or stable inpatients hospitalized for pre-transplant evaluation. Inclusion criteria were patients in sinus rhythm who had TTE within 30 days of cMR. Exclusion criteria were non-sinus rhythm, right to left shunts, cardiac devices, moderate and severe primary valve disease, severe chronic kidney disease defined as a Glomerular Filtration Rate (GFR) <30 ml/min/1.73m2, severe chronic obstructive

pulmonary disease (stage III-IV), pulmonary fibrosis or life expectancy <1 year due to other comorbidities.

The study protocol was approved by the IRB (2011/11AVR/144, 2017/02MAR/117 and 2014/19NOV/599) and subject gave informed consent. Patient's history and treatment was retrieved from medical files and from review of visit or hospital records. The HF etiology was considered ischemic when patients had previous history of myocardial infarction or > 70% narrowing in at least one major epicardial artery on angiography by visual inspection.

Normal reference values of PTT and other cMR parameters were evaluated in a previously published population of 40 asymptomatic volunteers (AV) free of cardiovascular disease(150).

Transthoracic Echocardiography

Standardized comprehensive TTE exams acquired according to established guidelines using commercial ultrasound systems, were analyzed off-line retrospectively by a single experienced observer (LH) blinded to follow-up clinical and cMR data. Estimated pulmonary systolic artery pressure (eSPAP) was calculated from tricuspid regurgitation maximum jet velocity and pulmonary hypertension was considered when eSPAP was calculated above 40 mmHg. LV filling pressure markers and RV systolic function parameters such as tricuspid annular plane systolic excursion (TAPSE) and fractional area change (FAC) were measured as stated by the established guidelines on 4 chamber view.

Cardiac magnetic resonance

Details in expanded data supplements. All patients and volunteers underwent a standardized cMR myocardial viability study on a 1.5 T or 3T scanner as described previously(131). After short and long long-axis cine SSFP images for assessment of myocardial function, a first Gadolinium contrast bolus was injected at a speed of 3 ml/s followed by a saline chaser of 20 cc. During contrast injection, a dynamic first pass perfusion scan of 40 phases was acquired using an ECG-gated saturation recovery interleaved spoiled gradient echo pulse sequence with parallel imaging (SENSE), allowing 8 short-axes images to be acquired every

other heartbeat (temporal resolution 2 RR intervals). Additional Gadolinium contrast (total dose of 0.2 mmol/kg) was injected and 10-15 minutes thereafter, late gadolinium enhancement (LGE) images were acquired using a 2D- inversion recovery sequence allowing for the assessment of myocardial viability in identical prescriptions of short- and long-axis slices as cine images.

cMR studies were analyzed using the freely available software Segment version 2.2 (106) by one experienced observer level III European Association of Cardiovascular Imaging (EACVI) certified observer (BG) and PTT data was evaluated by LH. End-diastolic (ED) and end-systolic (ES) RV and LV volumes and EF were computed from the short-axis cine images and indexed to the body surface area. Presence and extent of LGE was evaluated visually and quantified with a semi-automated algorithm using 4.7 SD of remote region to define LGE, as previously reported(131). RVFT-GLS was computed in apical 4 chamber view and LVFT-GLS cMR was calculated from the average of 3 long-axis-cine-views. For PTT computation, circular regions of interests (ROI) were placed in the center of the RV and the LV on a basal slice of the first pass perfusion study ascertaining that the ROI remained in the respective cavity and time attenuation curves were generated. PTT was calculated automatically as the lag time between the RV and LV bolus peaks, relying on a peak-detection algorithm implemented in Python **(appendix 1).** The PTT was expressed both in seconds and number of heart beats. Indexed pulmonary blood volume (PBVi) was computed by the product of PTT beats and the anterograde phase contrast stroke volume indexed to body surface area(151). Example of PTT measurements in a healthy volunteer and a HFrEF patient is shown in **Figure 1**.

Follow-up

Two independent researchers (MR and SA blinded for clinical data) prospectively followed the study population until November 2018 by phone contact with the patients, their relatives, or their physician. All deaths were recorded and categorized as cardiac or noncardiac. Cause of death was adjudicated by the 2 researchers previously mentioned. Cardiac death was defined as death attributable to congestive HF (i.e. death preceded by acute worsening or exacerbation of heart failure), myocardial infarction, sudden death (i.e. unexpected, unwitnessed, or witnessed death in absence of other apparent causes) or occurring after

cardiac revascularization. The primary endpoint was overall mortality, and the secondary endpoints were cardiovascular (CV) death and HF hospitalization. Heart transplantations were censored at the date of the procedure since the waiting time for that kind of surgery is more determined by the organ availability rather by the patient status.

Statistical analysis

Detailed statistical methods in data supplements. Statistical analyses were performed using R software (version 3.3.2). All tests were 2 sided and p value <0.05 was considered statistically significant. Continuous variables were summarized as mean ± one standard deviation (SD) as median and interquartile range, categorical variables as counts and percentages and compared using paired t test, Wilcoxon U and $\chi 2$ test respectively. Hazard Ratios (HR) were expressed with 95% confidence intervals (CI). The correlation between PTT vs cMR and echocardiographic measures was assessed using Pearson's or Spearman correlation coefficient. Uni- and multi-variable Cox proportional hazard models were used to assess predictors of primary and secondary endpoints. Secondary endpoint was evaluated using competing risk analysis. Weibull distribution was used in case of violation of proportional hazard (RVEF). Multivariable analysis included all MR parameters except those with evident collinearity together with the Meta-Analysis Global Group in Chronic Heart Failure (MAGGIC) Risk score(152) and ischemic etiology.

For the full assessment of the incremental benefit of PTT, we compared the potential additive prognostic value of PTT and other cMR parameters to improve the prediction of death over the baseline model including MAGGIC score and ischemic etiology using multiple discrimination measures including likelihood ratio and the additional increase of $\chi 2$ of the combined model over the baseline model, net reclassification improvement (NRI) and the integrated discrimination improvement index (IDI)

Survival graphs were used to compare patients with normal and abnormal PTT and RVEF. Interobserver and intraobserver reproducibility of measurement of PTT was evaluated in 30 randomly selected patient population using intraclass correlation coefficient (ICC) and

Bland-Altman analysis with computation within-subject coefficient of variation (CV). Test-retest reproducibility of PTT was assessed using CV and ICC in 12 subjects from prior studies: ie 8 healthy volunteers (3 male, mean age 30±1 years)(150) and 4 patients (3 male, mean age 66±7 years) with myocardial infarcts (153) in whom we had performed contrast-enhanced cMR using the same protocol on 2 consecutive days.

RESULTS

Patient's population

410 patients satisfied the inclusion criteria and constituted the final study population (**Figure 2**). **Table 1** shows the characteristics of the HFrEF patients. The mean age was 61±13 years and 75% were male. Etiology of HF was ischemic in 59% of patients and 48% were in New York Heart association (NYHA) class III or IV. Average LVEF was 24±7%, average LV-FT-GLS was -6.6%. Average RVEF was 42% and RV-FT-GLS was -11.7%. After cMR, 79 patients underwent Implantable Cardioverter Defibrillator (ICD) implantation (of which 10 for secondary prevention after arrhythmic event), 33 patients had a Cardiac Resynchronization Therapy- Defibrillator (CRT- D) and 29 a CRT- Pacemaker (P) implantation.

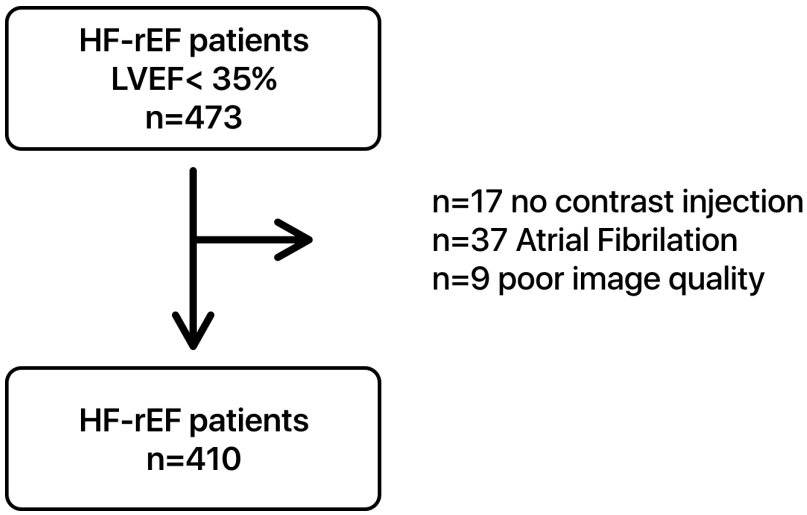

Figure 2 Flowchart of patient inclusion

	All (n=410)	PTT<11 beats (n=322)	PTT≥11 beats (n=88)	P value
Clinical parameters				
Age (years)	61±13	60±13	64±13	**0.21**
Female Sex (n, %)	103 (25%)	88 (27%)	15 (17%)	**0.053**
Ischemic etiology (n, %)	243 (59%)	193 (60%)	50 (56%)	**0.63**
BMI (kg/m2)	25.9±4.8	25.9±4.8	25.9±5.0	**0.83**
BSA (m2)	1.89±0.23	1.88±0.23	1.89±0.22	**0.88**
MAP (mmHg)	87±13	87±13	84±12	**0.06**
Heart rate (beats/min)	76±15	78±14	72±15	**<0.001**
COPD (n, %)	58 (14%)	47 (15%)	11 (13%)	**0.73**
Diabetes (n, %)	105 (26%)	82 (25%)	23 (26%)	**0.89**
NYHA III-IV (n, %)	198 (48%)	141 (44%)	57 (65%)	**<0.001**
GFR (ml/min/1.73m2)	71±22	73±23	63±17	**<0.001**
Hemoglobin (g/dl)	13.5±1.8	13.4±1.8	13.8±1.8	**0.06**
Beta blockers (n, %)	361 (88%)	281 (87%)	80 (91%)	**0.46**
Diuretics (n, %)	267 (65%)	201 (62%)	66 (75%)	**0.032**
ACEi/ARBs/SA-VAL (n, %)	401 (98%)	314 (97%)	87 (99%)	**0.69**
Spironolactone (n, %)	286(70%)	217 (67%)	69 (78%)	**0.05**
MAGGIC HF Score	25±6	25±6	28±7	**<0.001**
Echocardiographic parameters				
E/A ratio	1.50±0.86	1.41±0.83	1.83±0.92	**<0.001**
e/é ratio	17.5±8.5	17.1±8.7	19.2±7.8	**0.06**
TR 2-3 (n, %)	35(9%)	15(5%)	20(24%)	**<0.001**
eSPAP>40mmHg (n, %)	152(37%)	104(32%)	48(55%)	**<0.001**
TAPSE (mm)	18.0±4.8	18.3±4.6	16.8±5.3	**0.02**
FAC (%)	36.5±12.0	37.8±11.6	31.7±12.5	**<0.001**

cMR parameters				
cMR-LV-EDVi (ml/m2)	151±47	146±44	172±54	**<0.001**
cMR-LV-ESVi(ml/m2)	117±44	112±41	138±52	**<0.001**
cMR-LV-SV index (ml/m2)	34±10	34±10	34±12	**0.80**
cMR-LVEF (%)	24±7	24±7	20±7	**<0.001**
cMR-LV-FT-GLS (%)	-6.6±2.7	-6.9±2.6	-5.5±2.5	**<0.001**
CO (L/min/m2)	2.56±0.76	2.63±0.76	2.33±0.68	**0.001**
cMR-RV-EDVi (ml/m2)	85±31	78±27	106±39	**<0.001**
cMR-RV-ESVi (m/m2l)	52±31	47±26	72±39	**<0.001**
cMR-RV- SV indexed (ml/m2)	33±10	33±10	34±11	**0.54**
cMR-RVEF (%)	42±15	44±14	36±16	**<0.001**
cMR-RV- FT GLS (%)	-11.7±4.4	-12.4±4.3	-9.4±4.2	**<0.001**
septal stripe (n, %)	80 (20%)	50 (16%)	30 (34%)	**<0.001**
LV LGE (n, %)	258 (63%)	192 (60%)	66 (75%)	**0.009**
LGE size (%)	3.9[0.4 ;12.0]	3.0[0.4 ;11]	6.0[1.0 ;14]	**0.052**
CMR-PBVi (ml/m2) *	306±254	229±103	596±404	**<0.001**
cMR-PTT (seconds)	11.0±6.3	8.6±2.9	19.9±7.6	**<0.001**
cMR-PTT (heart beats)	8.9±5.5	6.7±2.2	16.9±6.8	**by design**

Table 1 Clinical characteristics of HFrEF patients according to normal and abnormal pulmonary transit time. Across-group P value is for the difference across the PTT cut off value by paired t-test (normal distribution), X2 Wilkoxon U,(non-normal data) or Chi Square test (discrete data) . *: n=261 patients

BMI indicates body mass index; BSA: Body Surface Area; MAP: Mean Arterial Pressure; COPD: Chronic obstructive pulmonary disease; NYHA: New York Heart association functional class, GFR: Glomerual Filtration rate; ACEi/ARBs/SA-VAL or Sacubitril-Valsartan: Angiotensin-Converting-Enzyme Inhibitor/Angiotensin II Receptor Blockers; MAGGIC HF scores: Meta-Analysis Global Group in Chronic Heart Failure Risk score; TR 2-3: Tricuspid Regurgitation moderate ; eSPAP: estimated Systolic Pulmonary Artery Pressure; TASPE: Tricuspid Annular Plane Systolic Excursion; FAC: Fractional Area Change; cMR= cardiac magnetic resonance; LV: Left Ventricular; RV: Right Ventricular; EDVi: End-Diastolic volume Index; ESVi: End-Systolic Volume Index; SVi: Stroke Volume index; EF: Ejection Fraction; FT-GLS: Feature Tracking Global Longitudinal Strain, CO:

Cardiac Output;; LGE: Late Gadolinium Enhancement; PBVi: Pulmonary Blood Volume index and PTT: Pulmonary Transit Time.

Pulmonary transit time

Normal values of cMR PTT in 40 asymptomatic controls (mean age 51±18 years, 51% female, average heart rate 68±11 bpm, systolic blood pressure 127±18 mmHg) were respectively 7±2 beats (95%CI 2.2;11.1 beats) and 6.2±2.2 seconds (95% CI 2.5;11.1 seconds).

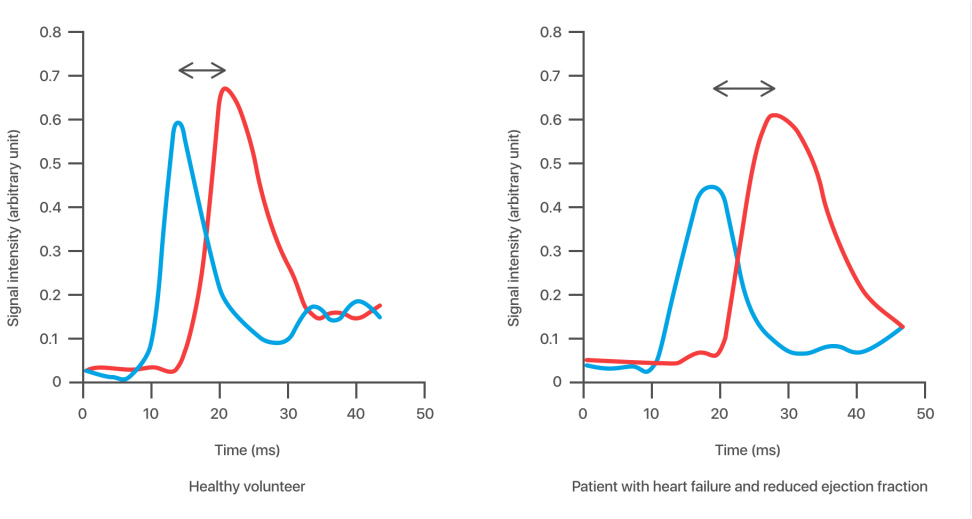

Figure 1 Example of PTT measurements. The blue line represents the bolus peak from the right ventricle and the red line the bolus peak from the left ventricle.

Average PTT in HFrEF patients was significantly higher (9±6 beats or 11.0±6.3 seconds, both p<0.001) relative to volunteers. Based on normal 95% CI of asymptomatic volunteers, patients were stratified into normal (<11 beats) and abnormal (ie ≥11 beats) PTT. As shown in **Table 1**, patients with high PTT were significantly older, had higher NYHA class, worse renal function and higher diuretic use, higher echocardiographic filling pressures as indicated by higher E/A and E/e' ratio, more pulmonary hypertension and worse RV function (lower TAPSE and FAC) by echocardiography. By cMR, they presented larger LV and RV volumes,

lower LV-EF and RV-EF, lower cardiac output and lower LV and RV FT-GLS. Interestingly there was no difference in PTT between patients with ischemic and non-ischemic etiology, however there was higher prevalence of LGE and septal stripe in patients with high PTT. There was also no significant difference in the number of patients with high PTT which underwent ICD or CRT implantation during follow-up (20 vs 19%, p=0.89). To better emphasize these differences, patients were also grouped based on PTT quartiles (**Supplementary Table 1***)*.

As expected, PTT in beats and seconds were highly correlated among each other (r=0.91, p<0.001). **Supplementary Table 2** shows correlation with other hemodynamic parameters, PTT correlated significantly, however moderately, with E/A ratio, cMR LV-EDVi, LV-ESVI, RV-EDVi, RV-ESVi, LV-FT-GLS and RV-FT-GLS. It also correlated inversely but moderately with RVEF and LVEF and the cardiac output. All correlations were higher for PTT in seconds than in beats.

Survival

Follow-up was 100% complete for a median duration of 6 years. During follow-up 28 patients underwent heart transplantation and were censored at the time of transplant. 182 patients died, 152 patients of cardiovascular causes: 72 suddenly, 60 of HF, 11 of cardiogenic shock, 5 of stroke and 4 postoperatively and 30 patients of non-cardiac causes. 101 patients underwent hospitalization for HF. Accordingly, 182 patients reached the primary endpoint of overall mortality, and 200 the secondary endpoint of cardiac death or HF hospitalization.

Predictors of outcomes

As shown in **Figure 3**, overall unadjusted survival in patients with prolonged PTT was significantly reduced.

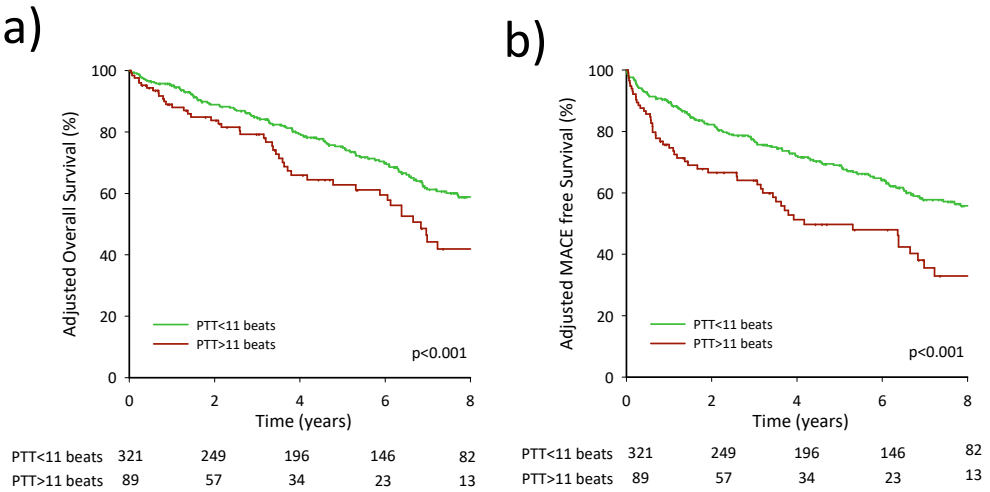

Figure 3 Adjusted survival curves showing overall (a) and MACE (b) free survival according to abnormal / normal PTT.

Table 2 lists univariate cox regression analysis predictors of survival. In Univariate analysis, age, ischemic etiology, arterial hypertension, diabetes, NYHA functional class III-IV, MAGGIC-HF risk score, cMR-LV and RV volumes, EF and FT-GLS, LV LGE, PTT, E/A and e/e' ratio, eSPAP> 40 mm Hg, TAPSE, RV-FAC and GFR were associated with overall mortality. Regarding the secondary composite endpoint, not only the same parameters listed above were associated with cardiovascular mortality and HF hospitalization, but also LVEF by cMR and female sex (**Supplementary Table 3**).

	Alive N=228	Dead N=182	HR (95% CI)	P-value
Clinical characteristics				
Age(years)	57±14	66±11	1.68[1.41 ;2.00]	<0.001
Female sex (n, %)	64 (28%)	39 (21%)	0.82[0.58 ;1.17]	0.27
Ischemic etiology (n, %)	99 (43%)	144 (79%)	2.23[1.55 ;3.19]	<0.001
AHT (n, %)	90 (40%)	109 (60%)	1.53[1.14 ;2.07]	0.004
Diabetes Mellitus (n, %)	46 (20%)	59 (32%)	1.52[1.12 ;2.07]	0.008
NYHA III-IV (n, %)	93 (41%)	105 (60%)	1.72[1.27 ;2.31]	<0.001
Beta-blockers (n, %)	207 (91%)	154 (85%)	0.62[0.41 ;0.92]	0.026
Diuretics (n, %)	135 (59%)	132 (73%)	1.74[1.25 ;2.42]	<0.001
GFR (ml/kg/1.73m²)	74±23	67±21	0.75[0.64 ;0.88]	<0.001
MAGGIC HF Score	24±6	27±6	1.65[1.44 ;1.88]	<0.001
ICD implantation as time-dependent covariate	58 (25%)	21 (11%)	0.88[0.56 ;1.39]	0.59
CRT as time-dependent covariate	45 (20%)	17 (9%)	0.67[0.41;1.11]	0.13
Echocardiographic parameters				
TAPSE (mm)	18.3±4.7	17.8±4.9	0.83[0.07 ;0.96]	0.01
RV-FAC (%)	37±12	36±12	0.84[0.72 ;0.97]	0.018
eSPAP>40mmHg	68 (38%)	84 (46%)	1.74[1.29;2.33]	<0.001
E/a ratio	1.47±0.85	1.52±0.88	1.19[1.02 ;1.39]	0.026
E/e’	16.5±7.9	19.2±9.3	1.32[1.12 ;1.56]	0.001

cMR parameters				
RV-EDVi (ml/m²)	82±32	89±31	1.25[1.09 ;1.44]	0.001
RV-ESVi (ml/m²)	50±31	55±31	1.241[1.09 ;1.42]	0.001
RV-EF (%)	43±14	42±15	0.82[0.71 ;0.95]	0.01
RV-GLS (%)	-12±5	-12±4	1.24[1.04 ;1.39]	0.01
LV-EDVi (ml/m²)	152±49	150±44	1.11[0.96'1.29]	0.14
LV-ESVi (ml/m²)	118±47	116±41	1.12[0.97 ;1.30]	0.11
LV-SVi (ml/m2)	35±11	33±9	0.99[0.85 ;1.15]	0.89
Cardiac output (l/min)	4.8±1.4	4.8±1.5	0.90[0.77 ;1.05]	0.16
LVEF (%)	23.5±7.6	23.5±6.5	0.866[0.74 ;1.00]	0.06
LV-GLS (%)	-7±3	-6±3	1.32[1.13;1.54]	<0.001
Presence of LV scar (n. %)	117 (51%)	141 (78%)	1.87[1.32;2.66]	<0.001
Septal stripe (n, %)	48 (21%)	32 (18%)	1.11[0.76 ;1.64]	0.58
PBVi (ml/m2) *	283±256	335±250	1.31[1.17 ;1.47]	<0.001
PTT in beats	8.2±5.5	10.4±6.6	1.31[1.16 ;1.49]	<0.001
PTT in seconds	9.6±5.5	11.7±5.8	1.47[1.29 ;1.67]	<0.001

Table 2 univariate analysis primary endpoint

AHT, Arterial hypertension; ICD: Implantable Cardioverter Defibrillator; CRT: cardiac resynchronization therapy; CI: Confidence Interval; HR: Hazard Ratio (for standardized value). All other abbreviations as in table 1.

MAGGIC-HF risk score and ischemic etiology were independent predictors of primary and secondary endpoints, and since these are well-known predictors of mortality in HFrEF, they were used as baseline multivariable predictors. **Figure 4 and 5** and **supplementary Table 4 and 5** show the incremental prognostic value of different cMR parameters over MAGGIC-HF risk score and ischemic etiology.

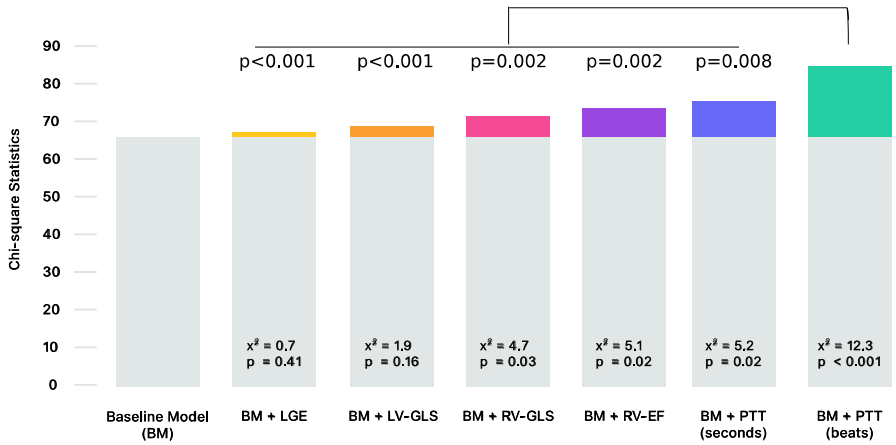

Figure 4 Chi square statistics bar chart: Additional prognostic value of the parameters over a baseline model to predict overall mortality.

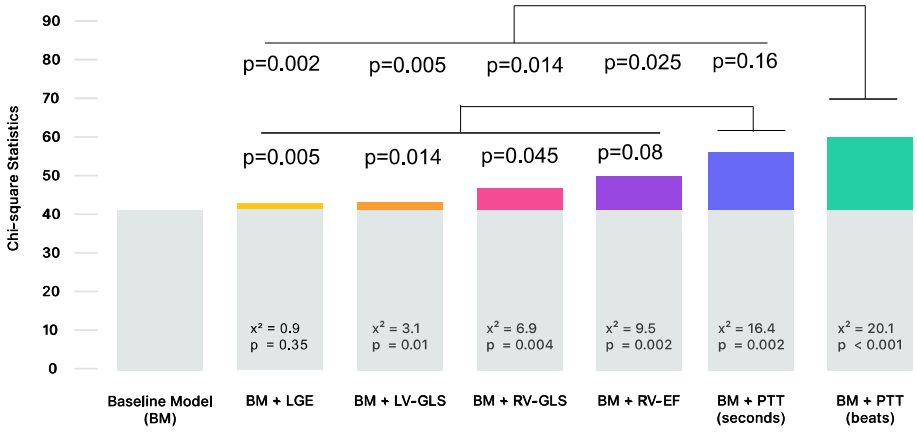

Figure 5 Chi square statistics bar chart: Additional prognostic value of the parameters over a baseline model to predict the secondary end-point of cardiovascular mortality and HF hospitalization.

Importantly, LVEF was not included since statistically non-significant in univariate analysis., The incremental prognostic value of PTT beats was significantly higher than PTT in seconds, cMR-LGE, cMR-RV and LV-FT-GLS, and RVEF for the primary endpoints. For the secondary endpoint both PTT in beats and in seconds had better predictive value than cMR

LGE, RV and LV FT-GLS. PTT in beats but not in seconds had also significantly higher predictive value than RVEF. **Table 3** shows the multivariable model including all cMR parameters for our primary endpoint and **Table 4** for the secondary endpoint accounting for competing risk. In multivariable analysis, PTT either in seconds or beats had additional prognostic value over MAGGIC-HF risk score and ischemic etiology. Interestingly, LV-FT-GLS showed only a significant incremental value in predicting the secondary composite endpoints, but not the primary endpoint. This is well illustrated in **Figure 4 and 5 and Supplementary Table 4 and 5**. Additionally, the incremental prognostic value of PTT > 11 beats was also demonstrated by other discrimination measures. Indeed, the continuous NRI for adding PTT> 11 beats in the baseline model was 0.45 [0.19;0.65] for overall mortality and 0.49[0.26;0.56] for the secondary endpoint at one year ($p<0.001$). The IDI was significantly increased ($p=0.02$) for the secondary endpoint but not for the primary endpoint ($p=0.16$).

Parameter	Partial HR	X^2	P value
MAGGIC HF Score	1.46[1.24;1.71]	23.3	<0.001
Ischemic etiology	2.46[1.59;3.73]	17.3	<0.001
PTT (beats)	1.33[1.12;1.57]	10.55	<0.001
cMR-RVEF	0.88[0.75;1.03]	2.25	0.12
cMR-LV-FT-GLS	1.04[0.87;1.29]	3.87	0.72
cMR-RV-FT-GLS	1.04[0.86;1.27]	0.33	0.66
cMR-LV- LGE	1.06[0.72;1.57]	0.10	0.74

Table 3 Multivariable analysis for primary endpoint**.** Hazard Ratio (HR) of continuous values were standardized. PTT (seconds) and PBV were not entered together, as highly correlated with PTT (beats) Abbreviations as in Table 1.

Parameter	Partial HR	P value
MAGGIC Score	1.28[1.11;1.49]	<0.001
Ischemic etiology	1.59[1.05;2.41]	0.03
PTT (beats)	1.34[1.15;1.57]	<0.001
cMR-RVEF	0.88[0.76;1.02]	0.08
cMR-LVGLS	1.10[0.92;1.30]	0.30
cMR-RVGLS	1.03[0.87;1.22]	0.71
cMR-LGE	1.07[0.72;1.59]	0.73

Table 4: Multivariable analysis for prediction of secondary endpoints.
Hazard ratio (HR) of continuous values were standardized. PTT (seconds) and PBVi were not entered, as highly correlated with PTT (beats). Abbreviations as in Table1

PTT in beats retained its high prognostic value in predicting both endpoints even if eSPAP by echocardiography was considered in the model (X2 to enter 12, p<0.001 and X2=8, p<0.001 respectively).

A sub-analysis was performed in 261 patients who had aortic flow phase data allowing to compute PBVi and the cardiac output. In this subpopulation, 100 patients died, 87 from cardiovascular death. Regarding the univariate analysis, the same parameters than with the entire population were associated with both of the endpoints, with in addition PBVi.

In multivariable analysis using the same baseline model, PTT in beats still had significantly (p=0.02) higher additional value than PBVi. (X^2 to enter 17.6 p<0.001 vs 11.2, p=0.001 respectively)

To better illustrate this increased risk in patient with high PTT, we evaluated hazard ratios relative to PTT (**Figure 6**). This graph show that the risk of mortality starts to exponentially increase when PTT is > 11 beats. This is also demonstrated in the adjusted survival curves stratified by quartiles of PTT (**Supplementary Figure 1**)

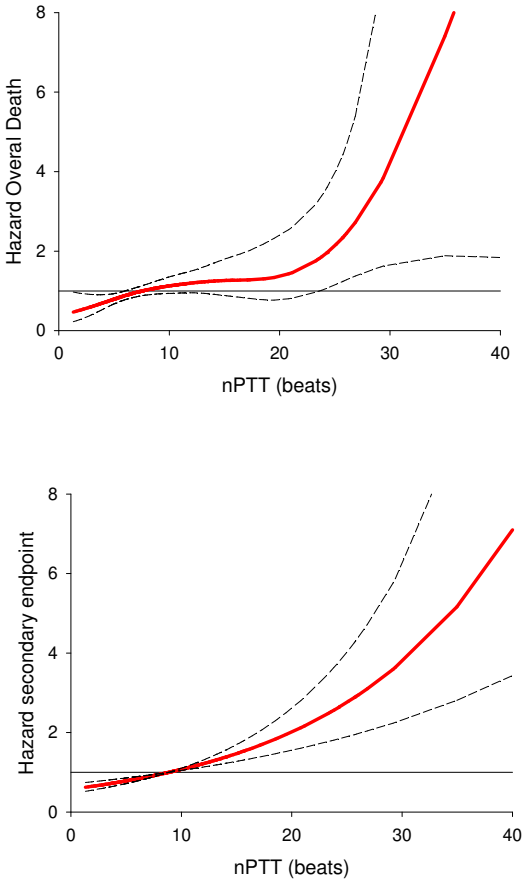

Figure 6 Hazard ratio of overall death and MACE free survival for PTT in beats

Finally, we examined the interaction between RV function and PTT in the prognostic stratification. Therefore, patients were separated according to normal (≤11 beats) and abnormal (>11 beats) PTT and low (<42%) and high median (≥42%) RVEF. Both RVEF<42% (HR:1.68 [1.23;2.31], p<0.001 for overall mortality and HR:1.76 [1.32;2.35], p<0.001 for the combined endpoint) and PTT>11 beats (HR:1.48 [1.04;2.1] with a p= 0.03

and HR 1.65 [1.27;2.32] with a p<0.001 for overall mortality and the combined endpoint respectively) independently predicted primary and secondary outcome over MAGGIC Score and ischemic etiology. **Figure 7** shows adjusted survival curves of overall survival and secondary endpoint stratified by normal/abnormal RVEF and PTT. This figure illustrates clearly that the prognosis of patients is independently influenced by both RVEF and PTT. Indeed, survival was highest when both RVEF and PTT were normal and worst when RVEF was low and PTT was increased. Patients with poor RVEF but preserved PTT or patients with normal RVEF, but increased PTT had intermediate prognosis.

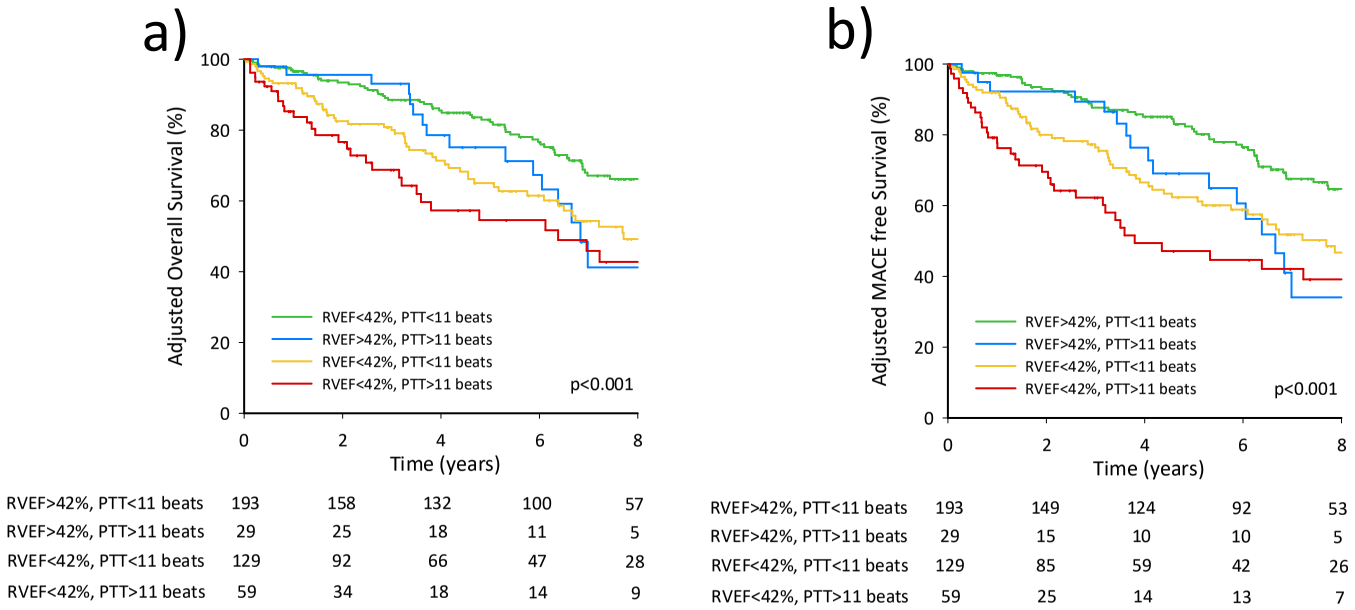

Figure 7 Adjusted survival curves demonstrating interaction between RVEF and PTT for predicting a) overall survival and b) combined endpoint of cardiovascular survival and survival free of heart failure hospitalization.

Reproducibility

Intraobserver and Interobserver reproducibility of PTT measurements was high (ICC=0.99/ 0.98 and CV 3.7%/5.7% respectively). Test-retest reproducibility of PTT resulted in absolute difference measurement on 2 consecutive days of 0±1.2 seconds (95CI: -2.3;2.4 seconds), with a CV of 6.4% and an ICC of 0.84. Interstudy reproducibility of other conventional cMR and FT measurements were recently published(154).

DISCUSSION

The salient findings of our study were:

1. PTT measurements can be easily obtained automatically from analysis of contrast kinetics during routine clinical cMR first pass perfusion scans with high intra-, inter and test-retest reproducibility.

2. PTT was significantly increased in patients with HFrEF as compared to controls, and correlated with NYHA class, cMR-LV and -RV volumes, RV and LV systolic function (EF and FT-GLS), cardiac output and with echocardiographic parameters of diastolic function.

3. PTT both in beats and seconds were independent predictors of overall long-term mortality and combined endpoint of CV mortality and HF hospitalization with significant additional value over a strong baseline model including well-validated parameters in patient with heart failure.

4) Importantly, the additional prognostic value of both PTT in beats and seconds was greater than RV and LV FT-GLS and EF and independent of eSPAP and RVEF in predicting both endpoints.

PTT, defined as the time for a bolus of contrast to pass from the RV to the LV, is a well-known measurement for evaluation of cardiopulmonary status. Indeed circulation time measurements are used since the mid-twentieth century for diagnosis of HF. PTT was first determined using radionuclide tracers(32) then also using other techniques such as contrast enhanced echocardiography and injected CT. Recently, it was proposed that PTT measurements could be derived from first pass perfusion cMR imaging(37-41) such as in our present work.

Several investigators demonstrated that PTT is prolonged both in HFrEF, HFpEF(41) and in isolated pulmonary hypertension(40). According to the indicator dilution theory(42), PTT is directly proportional to pulmonary blood volume and indirectly related to the right ventricular cardiac output(43). Hemodynamic studies(36,40,41,44) confirmed that PTT correlates with RV stroke volume, RV cardiac output(35,41), LVEF and RVEF(37,45,46),

but also importantly with parameters of increased pulmonary congestion(40,41). Indeed, in our previous work(47), we demonstrated a strong correlation between PTT assessed by CT scanner, mean pulmonary artery pressure (r=0.68) and pulmonary artery wedge pressure (r=0.74). PTT was also shown to correlate with N-terminal pro-B natriuretic peptide(35,47) which is an indicative for volume and pressure overload in congestive HF. This is in accordance with our findings. Overall, this suggests that prolonged PTT is a not only a measurement of low cardiac output, but mainly related to increased blood volume and thus, a parameter estimating pulmonary congestion in different types of HF.

In our study, normal values of PTT in healthy volunteers were in line with other reports(39-41,46,151). HFrEF patients had significantly prolonged PTT, however, with considerable overlap of normal PTT values when compared to volunteers. Indeed, only about 20% of HFrEF patients presented significantly prolonged PTT. However, this was clearly associated with more severe left (LVEF and LVGLS) and RV (RVEF, RVGLS, TAPSE and FAC) dysfunction, more severe symptomatic state (NYHA class) and more severe congestion (higher E/e').

Increased PTT predicted independently long-term overall survival and survival free of HF hospitalization and cardiovascular death. Indeed, normalized PTT in beats was the only variable statistically significant in the multivariable models when we allow to simultaneously enter all cMR parameters together with ischemic etiology and MAGICC score parameters. All the cMR parameters who had evident collinearity were not added in the multivariable models in order to avoid issue related to selecting parameters.

We also demonstrated that PTT had higher incremental prognostic value than FT-GLS in predicting not only overall mortality but also the combined endpoint of CV death and HF hospitalization. Additionally, the incremental benefit of PTT over a strong baseline model to predict both the endpoints was illustrated using three measures of discrimination such as the likelihood ratio test which is the uniformly most powerful test for nested models, and also by the NRI and the IDI. Although the NRI increase was modest, it demonstrated clearly a clinical reclassification of patients over a strong baseline model incorporating predictive parameters already well-validated in patients with heart failure.

In this respect, we believe that the specific clinical value of our data is the fact that it demonstrates that HFrEF patients with normal PTT (beats) should be reclassified to a lower risk. Also, PTT was independent and complementary to eSPAP to predict outcomes. This is in agreement with the fact that both clinical and hemodynamic congestion are important predictors of mortality in HF(155-158). While clinical congestion, which is always associated with signs and symptoms of HF, may rapidly resolve with diuretics, hemodynamic congestion may be incomplete despite aggressive treatment. Our study is, to our knowledge, the first to demonstrate the strong independent and additional value of PTT to predict outcome over other cMR derived parameters which are well-known prognostic factors in HFrEF patients, such as RVEF(98) and LV-FT-GLS(88) and RV-FT-GLS(98). Interestingly, the prognostic value of PTT was prolonged and persistent over a median follow up of 6 years. This is remarkable because one could conceive that the degree of pulmonary congestion might change over time in patients with HFrEF with progression of disease, or with treatment changes. A potential explanation could be that patients in our study underwent cMR during stable conditions, thus not during acute congestion, and thus that an increased PTT would reflect an incomplete hemodynamic decongestion which seems to be the main cause of early readmission(159).

CLINICAL IMPLICATION

HFrEF has variable prognosis, and assessment of pulmonary congestion is known to be relevant in HFrEF. Our study shows that cMR-PTT assessment is a simple, robust, and highly reproducible parameter, which might allow detection of pulmonary congestion non-invasively and which had significant and prognostic value over other clinical and cMR parameters such as RVEF in HFrEF both to predict mortality and HF hospitalization. Since PTT can be easily made from routine clinical cMR scans without any additional cost, we believe that PTT should be systematically analyzed during viability studies for risk stratification and identification of HFrEF patients at high risk of death and acute heart failure which potentially could benefit from more intensive monitoring and therapy. Indeed, PTT measurements could potentially be derived automatically from analysis of first pass image intensity, and the parameter could be computed within seconds.

STUDY LIMITATIONS

Our study was a single center retrospective observational study, with a potential referral reference bias to undergo cMR. Limitations related to this retrospective design include no quality control of acquired imaging and potential referral bias as we excluded patients with atrial fibrillation, devices, severe lung disease and renal failure. Therefore, our findings may not apply to these populations. Additionally, only one single observer performed the measurement of PTT. However, PTT measurement was performed automatically. Furthermore, image acquisitions were performed with a sequence with full cardiac coverage and temporal resolution limited to 2 RR intervals and contrast was injected at 3 cc/s. This might have limited the ability to detect the sharpness of the contrast peak and might have limited precision of measurement. Higher temporal resolution and injection speed might allow for more pronounced contrast peaks with more accurate estimates of PTT(160). Absolute difference between the normal and abnormal PTT groups was small representing only 2 beats, which is explained by the fact that majority of patients had normal PTT and only 20-25% of patients had increased PTT. Importantly, we believe that the clinical relevance of a biomarker can only be accurately demonstrated by its effect on patient management and outcomes which need to be confirmed in further prospective studies. Our baseline model was created based on well-validated variable in the outcome in heart failure to add flexibility and robustness to our model. We used software validated for LGE quantification only in ischemic pattern of fibrosis. We also used the same approach for non-ischemic scar since there is no universally recognized quantification strategy to detect focal fibrosis for this population. As our work may have predated the widespread use of ECV, this technique was not evaluated. Since we did not perform phase-contrast measurements of systemic or pulmonary stroke volume in all patients, we were able to compute pulmonary blood volume(151) only in a subgroup of our population. Finally, brain natriuretic peptide and invasive right heart catheterization measurements were not available for all the population and therefore these parameters could not be included in our analysis.

CONCLUSION

In HFrEF, PTT is an integrative marker of hemodynamic congestion, which has significantly additional prognostic value to predict overall mortality, CV death and HF hospitalization over and above other well-known risk factors. Importantly, PTT measurements are highly reproducible since it can be automated and easily made from routine clinical cMR. We therefore suggest that PTT should be integrated in the risk stratification process of HFrEF patients.

SUPPLEMENTARY DATA

Supplementary Table 1: Clinical characteristics of HFrEF patients according to quartiles of pulmonary transit time

	All (n=410)	PTT 1st quartile (n=102)	PTT 2nd quartile (n=103)	PTT 3rd quartile (n=103)	PTT 4th quartile (n=102)	P value
Age (years)	61±13	57±13	61±14	62±12	64±13	0.02
Female Sex (n,%)	103 (25%)	37 (36%)	30 (29%)	15 (15%)	21 (21%)	0.002
Ischemic etiology n,%)	243 (59%)	52 (51%)	59 (57%)	72 (70%)	60 (59%)	0.05
BMI (kg/m2)	25.9±4.8	25.9±5.5	25.8±4.9	26.5±4.1	25.6±4.8	0.60
BSA (m2)	1.89±0.23	1.88±0.23	1.88±0.24	1.90±0.23	1.87±0.21	0.78
MAP (mmHg)	87±13	87±14	88±12	87±12	85±13	0.47
Heart rate (beats/min)	76±15	83±14	79±12	74±15	71±15	<0.001
COPD Gold I or II (n,%)	58 (14%)	16(15%)	15(15%)	14(14%)	13(13%)	0.94
Diabetes (n,%)	105 (26%)	21(21%)	31(30%)	30(29%)	23(23%)	0.31
NYHA III-IV (n,%)	198 (48%)	38(37%)	50(49%)	46(45%)	64(63%)	0.003
GFR (ml/min/1.73m2)	71±22	77±25	73±24	71±21	63±17	<0.001
Hemoglobin (g/dl)	13.5±1.8	13.4±1.7	13.4±1.9	13.5±1.8	13.6±1.9	0.76
Beta blockers (n,%)	361 (88%)	89(87%)	85(83%)	94(91%)	93(91%)	0.17
Diuretics (n,%)	267 (65%)	59(58%)	64(62%)	71(69%)	73(71%)	0.15
ACEi/ARBs/SA-VAL (n(%)	401 (98%)	99(97%)	101(98%)	102(99%)	101(99%)	0.29
Spironolactone (n,%)	286(70%)	68(67%)	69(67%)	69(67%)	80(78%)	0.18
Maggic HF Score	25±6	23±6	25±6	25±5	28±7	<0.001
E/A ratio	1.50±0.86	1.26±0.75	1.37±0.77	1.53±0.95	1.82±0.89	<0.001
e/e' ratio	17.5±8.5	16.3±8.8	17.6±8.3	16.6±8.3	19.6±7.8	0.08
TR 2-3 (n,%)	35(9%)	3(3%)	7(7%)	4(4%)	21(21%)	<0.001
eSPAP>40mmHg (n,%)	152(37%)	22(22%)	42(41%)	37(36%)	51(50%)	<0.001
TAPSE (mm)	18.0±4.8	18.3±4.3	18.6±4.8	18.3±4.8	16.9±5.2	0.07
FAC (%)	36.5±12.0	38.53±11.6	38.7±12.7	36.9±10.0	32.2±12.8	<0.001
cMR-LV-EDVi (ml/m2)	151±47	140±47	143±39	151±42	172±52	<0.001
cMR-LV-ESVi(ml/m2)	117±44	105±41	110±38	117±39	138±51	<0.001
cMR-LV-SVi (ml/m2)	34±10	34±9	34±8	34±11	34±11	0.981
cMR-LV-EF (%)	24±7	26±7	25±7	24±7	20±7	<0.001
cMR-LV-FT-GLS (%)	-6.6±2.7	-7.2±2.7	-6.9±2.5	-6.5±2.6	-5.6±2.6	<0.001
CO(L/min)	4.1±1.3	4.6±1.3	4.4±1.2	4.0±1.2	3.3±1.1	<0.001
cMR-RV-EDVi (ml/m2)	85±31	76±27	76±25	83±25	105±39	<0.001
cMR-RV-ESVi (ml/m2)	52±31	43±25	43±23	51±25	72±39	<0.001
cMR-RV- SVi (ml/m2)	33±10	33±8	34±9	41±15	36±15	<0.001
cMR-RV-EF (%)	42±15	47±12	46±14	41±15	36±15	<0.001
cMR-RV-FT-GLS (%)	-11.7±4.4	-13.3±4.5	-12.2±4.1	-11.6±4.3	-9.8±4.3	<0.001
Septal stripe (n,%)	80 (20%)	15 (14%)	16 (16%)	19 (18%)	30 (29%)	0.03
LV LGE (n,%)	258 (63%)	55(54%)	58(56%)	69(67%)	76(74%)	0.007
cmR-PBVi (ml/m2)	237±157	127±53	194±56	257±88	398±225	<0.001
cMR-PTT (seconds)	11.0±6.3	5.8±1.7	8.5±1.4	10.9±2.3	18.7±7.6	<0.001
cMR-PTT (heart beats)	8.9±5.5	4.2±1.0	6.5±0.6	8.8±0.9	16±6.6	**by design**

Across-group P value is for the difference across the PTT cut off value by the X2 Wilkoxon U or Chi Square test .

BMI indicates Body Mass Index; BSA: Body Surface Area; MAP: mean Blood Pressure; COPD: Chronic Obstructive Pulmonary Disease; NYHA: New York Heart Association functional class, GFR: Glomerual Filtration Rate; ACEi/ARBs/SA-VAL: Angiotensin-

Converting-Enzyme inhibitor/Angiotensin II Receptor Blockers or Sacubitril-Valsartan ; MAGGIC HF scores: Meta-Analysis Global Group in Chronic Heart Failure Risk score; TR 2-3: Tricuspid Regurgitation moderate; eSPAP: estimated Systolic.Pulmonary Artery Pressure; TASPE: Tricuspid Annular Plane Systolic Excursion; FAC: Fractional Area Change; cMR= cardiac Magnetic Resonance; LV: Left Ventricular; RV: Right Ventricular; EDVi: End- Diastolic volume Index; ESVi: End-Systolic Volume Index; SVi: Stroke Volume index; EF: Ejection Fraction; FT-GLS: Feature Tracking Global Longitudinal Strain, CO: Cardiac Output;; LGE: Late Gadolinium Enhancement; PBVi: Pulmonary Blood Volume index and PTT: Pulmonary Transit Time

Supplementary Table 2: correlation of pulmonary transit time with other parameters.

	vs nPTT (beats)		vs PTT (sec)	
	Correlation coefficient	**P value**	**Correlation coefficient**	**P value**
Heart rate	-0.27	<0.001	0.06	NS
NYHA III/IV class	0.30	<0.001	0.17	0.001
E/A ratio (n=357)	0.25	<0.001	0.31	<0.001
E/e' ratio (n=297)	0.14	0.015	0.21	<0.001
cMR-LV-EDVi	0.25	<0.001	0.31	<0.001
cMR-LV-ESVi	0.26	<0.001	0.35	<0.001
cMR-LV-EF	-0.25	<0.001	-0.38	<0.001
cMR-LV-SVi	-0.06	NS	0.08	NS
cMR-AoSVi (n=261)*	0.17	<0.007	0.33	<0.001
cMR-CO	-0.35	<0.001	-0.35	<0.001
cMR-LV-FT-GLS	0.22	<0.001	0.34	<0.001
cMR-RV-EDVi	0.35	<0.001	0.43	<0.001
cMR-RV- ESVi	0.35	<0.001	0.48	<0.001
cMR-RV-EF	-0.26	<0.001	-0.41	<0.001
cMR-RV-SVi	-0.11	<0.05	0.02	NS
cMR- RV-FT -GLS	0.32	<0.001	0.40	<0.001

cMR indicates cardiac magnetic resonance; LV: left Ventricular; EDVi: End-Diastolic Ventricular volume index; ESVi: End-Systolic Volume Index; EF: Ejection Fraction; SVi: Stroke Volume index; AoSvi: Aortic phase-contrast stroke volume index; COi: Cardiac Output;; FT-GLS: Feature Tracking Global Longitudinal Strain; RV: Right ventricular.

*Phase contrast sequences were available only in 261 patients.

Supplementary Table 3: univariate analysis secondary endpoint

	No event N=210	CV death or WHF hospitalization N=200	HR (95% CI)	P-value
Clinical characteristics				
Age(years)	58±13	64±16	1.28[1.08;1.52]	0.004
Female sex (n,%)	65 (31%)	38 (19%)	0.63[0.44;0.89]	0.01
Ischemic etiology (n,%)	98 (47%)	145 (72%)	1.56[1.14;2.13]	0.005
AHT (n,%)	84(40%)	115 (58%)	1.39[1.05;1.83]	0.02
Diabetes Mellitus (n,%)	42(20%)	63 (32%)	1.45[1.08 ;1.95]	0.014
NYHA III-IV (n,%)	82 (39%)	116 (58%)	1.81[1.37;2.38]	<0.001
Beta-blockers(n,%)	189 (90%)	172 (86%)	0.64[0.4;0.94]	0.02
Diuretics(n,%)	120 (57%)	147 (74%)	1.88[1.39;2.56]	<0.001
GFR (ml/kg/1.73m²)	74±24	68±19	0.79[0.69;0.92]	0.002
MAGGIC HF Score	24±5	27±6	1.52[1.33 ;1.75]	<0.001
Echocardiographic parameters				
TAPSE (mm)	18.4±4.8	17.8±4.9	0.86[0.75;0.99]	0.03
RV-FAC (%)	37±12	36±12	0.83[.0.71;0.96]	0.009
eSPAP>40mmHg	58(28%)	94 (47%)	1.83[1.38;2.42]	<0.001
E/a ratio	2.3±0.6	2.4±0.6	1.17[1.01;1.36]	0.04
E/e'	16.8±8.3	18.6±8.7	1.17[1.00;1.36]	0.045
cMR parameters				
RV-EDVi (ml/m²)	79±28	92±33	1.39[1.18;163]	<0.001
RV-ESVi (ml/m²)	47±27	57±33	1.37[1.17;1.61]	<0.001
RVEF (%)	44±14	42±16	0.78[0.67;0.89]	<0.001
RV-GLS (%)	-12±5	-12±4	1.27[1.12;1.44]	<0.001
LV-EDVi (ml/m2)	151±49	152±45	1.14[0.99;1.3]	0.06
LV-ESVi(ml/m2)	116±46	119±42	1.15[1;1.32]	0.04
LV-SVi (ml/m2)	34±10	34±10	0.99[0.86;1.15]	0.97
Cardiac output (L/min)	4.8±1.3	4.8±1.6	0.99[0.86;1.15]	0.95
LVEF (%)	23.8±7.4	23.3±6.9	0.854[0.74;0.98]	0.03
LV-GLS (%)	-7±3	-6±3	1.34[1.17;1.55]	<0.001
Presence of LV scar (n. %)	109 (52 %)	149 (75%)	1.51[1.10;2.52]	0.01
Septal stripe (n,%)	42 (20%)	38 (19%)	1.14[0.79;1.63]	0.48
PBVi (ml/m2)	274±262	340±242	1.28[1.15 ;1.41]	<0.001
PTT in beats	8±5	10±6	1.43[1.26;1.63]	<0.001
PTT in seconds	10±6	12±7	1.39[1.16;1.66]	<0.001

WHF: worsening of heart failure ; CI: Confidence Interval and HR: Hazard Ratio for standardized values. All other abbreviations as in table 1 and 2.

Supplementary Table 4: Stepwise multivariate analysis for prediction of primary endpoint over baseline parameters

Parameter	Partial HR	X^2	P value
MAGGIC HF Score	1.65 [1.42;1.90]	45.2	<0.001
Ischemic Etiology	2.1 [1.46;3.04]	16.1	<0.001
Combined Baseline model		65.9	<0.001

Additional prognostic value	Parameter	X2 to improve	Partial HR	P value
	+ CO*	1.9	0.86[0.69;1.06]	0.16
	+ Heart rate	1.5	0.91[0.77;1.06]	0.22
	+ LGE	0.7	1.18[0.8;1.74]	0.41
	+ cMR LV-EF	0.01	1.01[0.85;1.20]	0.91
	+ cMR-LV-FT-GLS	1.9	1.124 [0.95;1.32]	0.16
	+ cMR-RV-FT-GLS	4.7	1.18 [1.02;1.38]	0.03
	+ cMR-RV-EF	5.1	0.84[0.72;0.98]	0.024
	+ PTT (seconds)	5.2	1.21[1.03;1.41]	0.02
	+ PTT (beats)†	12.3	1.35[1.16;1.58]	<0.001

Hazard ratio (HR) of continuous values were standardized.
Abbreviations as in Table1
*Cardiac output by phase contrast was available only in 261 patients.
† p<0.01 vs PTT seconds, cMR-RVEF and cMR-RVFT-GLS

Supplementary Table 5: multivariate analysis for prediction of secondary endpoints.

Parameter	Partial HR	X^2	P value
MAGGIC HF Score	**1.56 [1.36;1.78]**	**40.7**	**<0.001**
Ischemic Etiology	**1.44 [1.04;1.99]**	**8.55**	**<0.001**
Combined Baseline model		**46.2**	**<0.001**

Additional prognostic value	Parameter	X2 to improve	Partial HR	P value
	+ CO*	0	1.00[0.81;1.24]	0.99
	+ Heart rate	0.7	0.942[0.81;1.09]	0.4
	+ LGE	0.9	1.19[0.83;1.72]	0.35
	+ cMR LV-EF	0.3	0.96[0.81;1.12]	0.57
	+ cMR-LV-FT-GLS	3.1	1.22[1.05;1.41]	0.01
	+ cMR-RV-FT-GLS	6.9	1.22 [1.06 ;1.39]	0.004
	+ cMR-RVEF	9.5	0.79[0.69;0.92]	0.0018
	+ PTT (seconds) †	16.4	1.34[1.11;1.61]	0.002
	+ PTT (beats) ‡	20.1	1.23[1.21;1.60]	<0.001

Hazard ratio (HR) of continuous values were standardized.
Abbreviations as in Table1.
* Cardiac output by phase contrast was available only in 261 patients.
† p<0.05 vs cMR-RVEF and cMR-RV and LVFT-GLS
‡ p<0.01 vs cMR-RVEF and cMR-RV and LVFT-GLS

Supplementary Figure 1 Adjusted survival according to quartiles of PTT. Adjustment for MAGGIC score and ischemic etiology

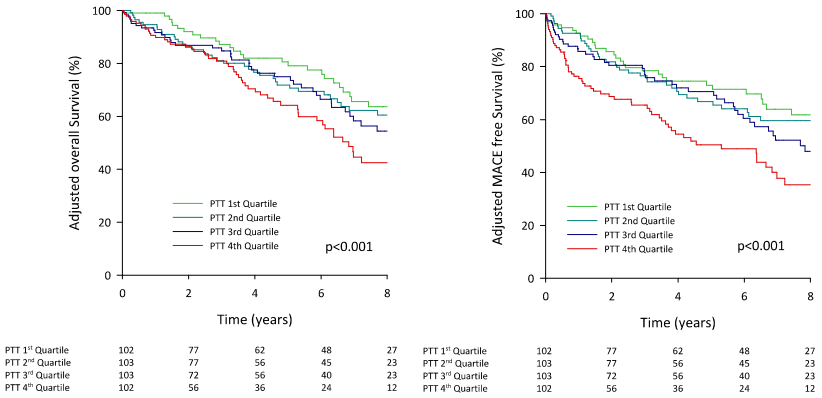

PTT 1st Quartile	102	77	62	48	27
PTT 2nd Quartile	103	77	56	45	23
PTT 3rd Quartile	103	72	56	40	23
PTT 4th Quartile	102	56	36	24	12

PTT 1st Quartile	102	77	62	48	27
PTT 2nd Quartile	103	77	56	45	23
PTT 3rd Quartile	103	72	56	40	23
PTT 4th Quartile	102	56	36	24	12

IV. CONCLUSION AND FUTURE PERSPECTIVES

4.1. FINAL REMARKS AND HIGHLIGHT

The cynic might argue that there is no specific treatment for the right ventricle (RV) and so the presence of RV dysfunction in heart failure and reduced ejection fraction (HF-rEF) would be largely academic and therefore will not improve clinical outcomes.

On the other hand, HF-rEF patients have variable prognosis, and the assessment of right ventricular systolic function is known to be relevant in term of prognosis in these patients. Indeed, HF-rEF patients with RV dysfunction have a higher risk of mortality than those without RV dysfunction. Therefore, risk stratification is crucial in this population of HF in order to provide proper and timely decision regarding aggressive medical treatment, cardiac device therapies and planning cardiac transplantation leading to improve patient survival.

In our first study, we have demonstrated that speckle tracking echocardiography RV- global longitudinal strain (STE- RVGLS) deformation techniques were the most accurate echocardiographic approach for detecting small changes in RV function. It even surpassed the reproducibility of cardiac magnetic resonance (cMR) RV ejection fraction (EF). This suggests that STE-RV-GLS could be used clinically to reliably follow patients for development of subclinical dysfunction in different conditions. Obvious advantages of using STE over cMR are wider availability and lower costs. Nevertheless, STE has potential limitations such as the need of high-quality image, the lack of uniformity in software algorithms(105) and intervendor differences, despite efforts to standardize STE measurements(77).

Simultaneously, we have pointed out the fact that STE-RVGLS was a more robust measure of global deformation that RV free wall longitudinal strain. Indeed, despite the fact that the ventricular septum is mainly a constituent part of the left ventricle (LV), it also true that the ventricular septum contributes importantly to RV systolic performance. Additionally, the presence of spatial and temporal smoothing algorithms makes the global average values more reliable than segmental measurements.

We have also shown that, when taking precautions for uniformity of acquisitions and analysis due to its still unsolved technical issues, STE could also be useful for evaluation of RV systolic function in longitudinal studies with a potentially lower cost than cMR.

By contrast, we did not observe advantages of feature tracking (FT) over conventional cMR, for reproducibility of LV or RV function assessment. Therefore, we cannot currently recommend this technique to limit sample sizes in research studies. Meanwhile, acceptance and analysis of negative findings is an important part of the process of assessing a new technique as it prompts further improvements. Indeed, the reproducibility of FT-cMR strains could be theoretically improved by higher temporal and spatial resolution, either through parallel imaging or iterative reconstruction techniques. Nevertheless, with the compromise of decreasing signal-to-noise ratio leading to more artefacts and consequently to a less good tracking.

STE allows more accurate estimates of strain than cMR-FT, mainly due to the presence of physical markers (speckles) and much higher spatial and temporal resolution(105). Indeed, STE evaluates speckle motion, while cMR-FT doesn't distinguish intramyocardial features, as the grey level distribution in cine SSFP images is relatively homogenous. Indeed, cMR-FT-RVGLS often failed to adequately track the base of the RV especially in subjects with relatively vigorous annular motion or in presence of flow artifacts.

Finally, cMR-FT showed significantly lower strain value than STE. This fact is in accordance with our previous works comparing STE to tagging(121) The most likely explanation for this is that STE software provide more endocardial strain estimates than cMR-FT software which provide mid-ventricular strain. Also, the lower frame rate of FT-cMR could also explain lower strain values than STE(105).

Furthermore, in line with previous publications, we have confirmed in our second study that right ventricular dysfunction is a strong independent predictor of overall and cardiovascular mortality in patients with HFrEF. The use of STE-RV-GLS was the most powerful echocardiographic parameter to assess RV dysfunction and had higher prognostic value than cMR derived RVEF. More importantly, our study strengthens and expands previous studies by showing that RV-GLS by echocardiography may provide similarly or
even better risk prognostic value than cMR-RVEF. This simple echocardiographic measurement, which can easily be performed at bed site, could thus avoid less accessible and more costly cMR exams for risk stratification.

Finally, since the assessment of pulmonary congestion is known to be relevant in HFrEF, we performed our last study assessing the PTT in 410 HF-rEF patients. Indeed, Pulmonary transit time is strongly correlated with pulmonary congestion and left and right ventricular systolic function. However, when applied to HF-rEF patients, PTT is mainly correlated with RV systolic function and pulmonary congestion.

We have demonstrated that cMR-PTT assessment is a simple, robust, and highly reproducible parameter, which might allow detection of pulmonary congestion non-invasively and which had significant and prognostic value over the MAGGIC score, ischemic etiology, estimated pulmonary artery pressure by echocardiography and cMR parameters such as RVEF in HF-rEF both to predict mortality and HF hospitalization.

To argument this statement we highlight the following aspects, representing the core finding of our work:

1: Right ventricular dysfunction is a strong independent predictor of overall and cardiovascular mortality in patients with HFrEF.

2: 2D-STE-RV-GLS had higher test-retest reliability to assess RV systolic function than not only RV-STE- free wall longitudinal strain (FWLS), tricuspid annular plane systolic excursion (TAPSE), RV- fractional area change (FAC), and FT-RV-GLS, but also cMR-RVEF.

3: cMR-FT-RV-GLS do not seems to be a reliable parameter to assess RV systolic function since its test-retest reliability was extremely poor.

4: STE-RV-GLS have a better interstudy-reproducibility and a slightly better predictive value of mortality than RV-FWLS in HFrEF.

5: The predictive value of 2D- STE-RV-GLS was superior to cMR-LVEF, cMR-RVEF, FT-RVGLS, TAPSE and FAC for both overall and cardiovascular mortality.

6: PTT measurements can be easily obtained automatically from routine clinical cMR scans without any additional cost with high intra-, inter and test-retest reproducibility.

7: PTT was independent of eSPAP and RVEF in predicting long-term mortality and a combined endpoint of CV mortality and HF hospitalization with a greater additional additional prognostic value than cMR-FT- RV and LV and RVEF over a strong baseline model including well-validated parameters in patient with heart failure.

In conclusion, 2D-STE-RVGLS is more reproducible and may provide similarly or even better prognostic value than cMR-RVEF in HFrEF. Importantly, it is cheap, fast, reliable and widely available. PTT assessed by cMR can be automated and may also provide a better prognostic value than cMR-RVEF in predicting mortality in HFrEF.
Therefore, from our research experience, RV systolic function by 2D-STE-RVGLS and pulmonary transit time by cardiac magnetic resonance should be systematically analyzed in clinical practice for risk stratification and identification of HFrEF patients at high risk of death and acute heart failure which potentially could benefit from more intensive monitoring and therapy.
Nevertheless, the retrospective design in a single center, as well as the use of a single vendor software for right ventricular strain analysis were our main limitations. Larger, carefully constructed clinical studies should confirm the value of STE-RV-GLS and PTT in such populations in prospective, multicenter design and using different softwares to allow more general recognition of this method for HFrEF patient risk stratification.

4.2. FUTURE PERSPECTIVE

In the 21st century, we have witnessed a massive expansion in the armamentarium of noninvasive imaging technologies capable of providing detailed information about the structure and function of the heart and vasculature. Significant advances in echocardiography, cMR, nuclear imaging and computed tomography have added to our arsenal of improved testing to diagnose disease and improve patient care. Indeed, all imaging technologies have undergone continual improvements to a point that imaging has become essential in both clinical practice and research. Advanced cardiac imaging is and will remain

an integral part of structural heart programs.

Heart failure patients demand constant follow-up with baseline imaging. Indeed, Imaging guides treatment for the improvement of heart failure patients and further significant advances in this field are going to require better selection of treatment for specific patients. Hence, we believe that successful therapy will be dependent on selecting patients with RV dysfunction such as synchronization device therapies, defibrillator and with already some optimism, pulmonary vasodilators because it would seem logical hypothesis to aim more aggressive treatment at these patients.

Therefore, a correct and attentive evaluation of RV morphology and function is mandatory in HFrEF patients, as this might be the key in predicting outcome. One challenge for biomedical engineers is to develop better, non-invasive automatic methods for measuring RV function and efficiency of hemodynamic coupling.

Tissue tracking technology is a continuously developing field and is submitted to intense research hypothesis testing. A large number of tissues tracking technologies are available to assess right ventricular myocardial strain, and while this is clearly a sign of development and progress, it is also an indicator that none of these methods are good enough on its own. Also the large number of alternative methodologies makes it likely that inconsistencies in results will continue to prevail (161). Cross-platform standardization is still needed in order to expand deformation imaging methods beyond the current research-oriented environment.
Indeed, despite the large amount of accumulated data since its early development, myocardial strain quantification has not reached the intended practical application and does not replace or complement the traditional evaluation by EF. Importantly, it is still load dependent.
New promising tool are knocking at the door of clinical practice such as myocardial work with a correction for afterload via blood pressure and three-dimension cMR since it may reduce variability particularly near the apex and base where partial effect leads to large variation. However, quibbling over which is the best measure should not obscure the importance of measuring the RV with something in heart failure.
Overall, the future of cardiac noninvasive imaging looks also toward fully automated measurement and diagnostic using machine learning. The goal will be to improve speed and quality of acquisition, reduce measurement time and allow prompt diagnoses, which in turn

would improve workflow and patient care. Although artificial intelligence (AI) is very exciting, many steps need to be undertaken for this approach to be translated into everyday clinical practice. Indeed, in the near future, the value-adding potential of AI will not be to replace the doctor, but it will be most likely to be an intelligent precision medicine tools for imaging specialists and clinicians. Importantly, I truly believe that the data will be one day in a secured collaboration based-cloud platform.

Finally, but not less importantly, we truly believe that patient target education and close structured follow-up using virtual care will also improve significantly the prognosis of HFrEF patients in modern cardiology.

Therefore, our future research will be certainly focused on evaluating PTT assessed by echocardiography and pulse contour cardiac output; evaluating the feasibility and reproducibility of 3D-STE-RVGLS latest software and comparing the prognostic value of PTT assessed either by echocardiography and cMR with STE-RVGLS in HFrEF.

V: REFERENCES

1. Kanar BGA-Ohoo, Tigen MK, Sunbul M et al. The impact of right ventricular function assessed by 2-dimensional speckle tracking echocardiography on early mortality in patients with inferior myocardial infarction.
2. Freed BH, Tsang W Fau - Bhave NM, Bhave Nm Fau - Patel AR et al. Right ventricular strain in pulmonary arterial hypertension: a 2D echocardiography and cardiac magnetic resonance study.
3. Dell'Italia LJ. The right ventricle: anatomy, physiology, and clinical importance. Curr Probl Cardiol 1991;16:653-720.
4. Haddad F, Hunt Sa Fau - Rosenthal DN, Rosenthal Dn Fau - Murphy DJ, Murphy DJ. Right ventricular function in cardiovascular disease, part I: Anatomy, physiology, aging, and functional assessment of the right ventricle.
5. Konstam Ma Fau - Kiernan MS, Kiernan Ms Fau - Bernstein D, Bernstein D Fau - Bozkurt B et al. Evaluation and Management of Right-Sided Heart Failure: A Scientific Statement From the American Heart Association.
6. Naeije R, Badagliacca R. The overloaded right heart and ventricular interdependence.
7. Lahm T Fau - Douglas IS, Douglas Is Fau - Archer SL, Archer Sl Fau - Bogaard HJ et al. Assessment of Right Ventricular Function in the Research Setting: Knowledge Gaps and Pathways Forward. An Official American Thoracic Society Research Statement.
8. Sanz J, Sanchez-Quintana D, Bossone E, Bogaard HJ, Naeije R. Anatomy, Function, and Dysfunction of the Right Ventricle: JACC State-of-the-Art Review.
9. Buckberg GD, Hoffman JI, Coghlan HC, Nanda NC. Ventricular structure-function relations in health and disease: Part I. The normal heart.
10. Meier Gd Fau - Bove AA, Bove Aa Fau - Santamore WP, Santamore Wp Fau - Lynch PR, Lynch PR. Contractile function in canine right ventricle.
11. Vonk Noordegraaf A, Westerhof BE, Westerhof N. The Relationship Between the Right Ventricle and its Load in Pulmonary Hypertension.
12. Bleasdale Ra Fau - Frenneaux MP, Frenneaux MP. Prognostic importance of right ventricular dysfunction.
13. Ponikowski P Fau - Voors AA, Voors Aa Fau - Anker SD, Anker Sd Fau - Bueno H et al. 2016 ESC Guidelines for the diagnosis and treatment of acute and chronic heart failure: The Task Force for the diagnosis and treatment of acute and chronic heart failure of the European Society of Cardiology (ESC). Developed with the special contribution of the Heart Failure Association (HFA) of the ESC.
14. Setaro JF, Cleman Mw Fau - Remetz MS, Remetz MS. The right ventricle in disorders causing pulmonary venous hypertension.
15. Klima UP, Guerrero Jl Fau - Vlahakes GJ, Vlahakes GJ. Myocardial perfusion and right ventricular function.
16. Venkatachalam S, Wu G, Ahmad MA-O. Echocardiographic assessment of the right ventricle in the current era: Application in clinical practice.
17. Lang RM, Badano LP, Mor-Avi V et al. Recommendations for cardiac chamber quantification by echocardiography in adults: an update from the American Society of Echocardiography and the European Association of Cardiovascular Imaging. Eur Heart J Cardiovasc Imaging 2015;16:233-70.
18. Maffessanti F, Muraru D Fau - Esposito R, Esposito R Fau - Gripari P et al. Age-, body size-, and sex-specific reference values for right ventricular volumes and

ejection fraction by three-dimensional echocardiography: a multicenter echocardiographic study in 507 healthy volunteers.
19. Larrazet F, Czitrom D Fau - Laborde F, Laborde F Fau - Bouabdallah K, Bouabdallah K Fau - Folliguet T, Folliguet T. Decreased right ventricular lateral wall velocities early after cardiac surgery.
20. Tei C, Dujardin Ks Fau - Hodge DO, Hodge Do Fau - Bailey KR et al. Doppler echocardiographic index for assessment of global right ventricular function.
21. Rudski LG, Lai WW, Afilalo J et al. Guidelines for the echocardiographic assessment of the right heart in adults: a report from the American Society of Echocardiography endorsed by the European Association of Echocardiography, a registered branch of the European Society of Cardiology, and the Canadian Society of Echocardiography. Journal of the American Society of Echocardiography : official publication of the American Society of Echocardiography 2010;23:685-713; quiz 786-8.
22. Leibundgut G, Rohner A Fau - Grize L, Grize L Fau - Bernheim A et al. Dynamic assessment of right ventricular volumes and function by real-time three-dimensional echocardiography: a comparison study with magnetic resonance imaging in 100 adult patients.
23. Bellenger NG, Grothues F Fau - Smith GC, Smith Gc Fau - Pennell DJ, Pennell DJ. Quantification of right and left ventricular function by cardiovascular magnetic resonance.
24. Grothues F, Moon Jc Fau - Bellenger NG, Bellenger Ng Fau - Smith GS, Smith Gs Fau - Klein HU, Klein Hu Fau - Pennell DJ, Pennell DJ. Interstudy reproducibility of right ventricular volumes, function, and mass with cardiovascular magnetic resonance.
25. Clarke CJ, Gurka Mj Fau - Norton PT, Norton Pt Fau - Kramer CM, Kramer Cm Fau - Hoyer AW, Hoyer AW. Assessment of the accuracy and reproducibility of RV volume measurements by CMR in congenital heart disease.
26. Maceira AM, Prasad Sk Fau - Khan M, Khan M Fau - Pennell DJ, Pennell DJ. Reference right ventricular systolic and diastolic function normalized to age, gender and body surface area from steady-state free precession cardiovascular magnetic resonance.
27. Semelka RC, Tomei E Fau - Wagner S, Wagner S Fau - Mayo J et al. Normal left ventricular dimensions and function: interstudy reproducibility of measurements with cine MR imaging.
28. Lorenz CH, Walker Es Fau - Morgan VL, Morgan Vl Fau - Klein SS, Klein Ss Fau - Graham TP, Jr., Graham TP, Jr. Normal human right and left ventricular mass, systolic function, and gender differences by cine magnetic resonance imaging.
29. Grothues F, Smith Gc Fau - Moon JCC, Moon Jc Fau - Bellenger NG et al. Comparison of interstudy reproducibility of cardiovascular magnetic resonance with two-dimensional echocardiography in normal subjects and in patients with heart failure or left ventricular hypertrophy.
30. Suinesiaputra A, Bluemke DA, Cowan BR et al. Quantification of LV function and mass by cardiovascular magnetic resonance: multi-center variability and consensus contours.
31. Hudsmith LE, Petersen Se Fau - Francis JM, Francis Jm Fau - Robson MD, Robson Md Fau - Neubauer S, Neubauer S. Normal human left and right

ventricular and left atrial dimensions using steady state free precession magnetic resonance imaging.
32. Blumgart HL, Weiss S. CLINICAL STUDIES ON THE VELOCITY OF BLOOD FLOW: IX. The Pulmonary Circulation Time, the Velocity of Venous Blood Flow to the Heart, and Related Aspects of the Circulation in Patients with Cardiovascular Disease. The Journal of clinical investigation 1928;5:343-77.
33. Slutsky Ra Fau - Bhargava V, Bhargava V Fau - Higgins CB, Higgins CB. Pulmonary circulation time: comparison of mean, median, peak, and onset (appearance) values using indocyanine green and first-transit radionuclide techniques.
34. Muller HM, Tripolt Mb Fau - Rehak PH, Rehak Ph Fau - Groell R, Groell R Fau - Rienmuller R, Rienmuller R Fau - Tscheliessnigg KH, Tscheliessnigg KH. Noninvasive measurement of pulmonary vascular resistances by assessment of cardiac output and pulmonary transit time.
35. de Lepper AGW, Herold IHF, Saporito S et al. Noninvasive pulmonary transit time: A new parameter for general cardiac performance. Echocardiography 2017;34:1138-1145.
36. Choi BG, Sanai R, Yang B et al. Estimation of cardiac output and pulmonary vascular resistance by contrast echocardiography transit time measurement: a prospective pilot study. Cardiovascular ultrasound 2014;12:44.
37. Shors SM, Cotts WG, Pavlovic-Surjancev B, Francois CJ, Gheorghiade M, Finn JP. Heart failure: evaluation of cardiopulmonary transit times with time-resolved MR angiography. Radiology 2003;229:743-8.
38. Francois CJ, Shors SM, Bonow RO, Finn JP. Analysis of cardiopulmonary transit times at contrast material-enhanced MR imaging in patients with heart disease. Radiology 2003;227:447-52.
39. Swift AJ, Telfer A, Rajaram S et al. Dynamic contrast-enhanced magnetic resonance imaging in patients with pulmonary arterial hypertension. Pulmonary circulation 2014;4:61-70.
40. Skrok J, Shehata ML, Mathai S et al. Pulmonary arterial hypertension: MR imaging-derived first-pass bolus kinetic parameters are biomarkers for pulmonary hemodynamics, cardiac function, and ventricular remodeling. Radiology 2012;263:678-87.
41. Cao JJ, Li L, McLaughlin J, Passick M. Prolonged central circulation transit time in patients with HFpEF and HFrEF by magnetic resonance imaging. European heart journal cardiovascular Imaging 2018;19:339-346.
42. Meier P, Zierler KL. On the theory of the indicator-dilution method for measurement of blood flow and volume. Journal of applied physiology 1954;6:731-44.
43. Grodins FS. Basic concepts in the determination of vascular volumes by indicator-dilution methods. Circulation research 1962;10:429-46.
44. Defreitas FM, Faraco EZ, Nedel N, Deazevedo DF, Zaduchliver J. Determination of Pulmonary Blood Volume by Single Intravenous Injection of One Indicator in Patients with Normal and High Pulmonary Vascular Pressures. Circulation 1964;30:370-80.
45. Anavekar NS, Skali H, Bourgoun M et al. Usefulness of right ventricular fractional area change to predict death, heart failure, and stroke following

myocardial infarction (from the VALIANT ECHO Study). Am J Cardiol 2008;101:607-12.
46. Hansch A, Heyne JP, Jung C, Wolf G, Pfeil A. Quantitative first pass perfusion in cardiovascular magnetic resonance for determination of peak ventricular transit time--a technique for evaluation of heart function. European journal of radiology 2012;81:e996-1001.
47. Colin GC, Pouleur AC, Gerber BL et al. Pulmonary hypertension detection by computed tomography pulmonary transit time in heart failure with reduced ejection fraction. European heart journal cardiovascular Imaging 2019.
48. Zerhouni EA, Parish Dm Fau - Rogers WJ, Rogers Wj Fau - Yang A, Yang A Fau - Shapiro EP, Shapiro EP. Human heart: tagging with MR imaging--a method for noninvasive assessment of myocardial motion.
49. D'Hooge J, Heimdal A Fau - Jamal F, Jamal F Fau - Kukulski T et al. Regional strain and strain rate measurements by cardiac ultrasound: principles, implementation and limitations.
50. Urheim S, Edvardsen T Fau - Torp H, Torp H Fau - Angelsen B, Angelsen B Fau - Smiseth OA, Smiseth OA. Myocardial strain by Doppler echocardiography. Validation of a new method to quantify regional myocardial function.
51. Pedrizzetti G, Claus P, Kilner PJ, Nagel EA-OX. Principles of cardiovascular magnetic resonance feature tracking and echocardiographic speckle tracking for informed clinical use.
52. Kukulski T, Hubbert L Fau - Arnold M, Arnold M Fau - Wranne B, Wranne B Fau - Hatle L, Hatle L Fau - Sutherland GR, Sutherland GR. Normal regional right ventricular function and its change with age: a Doppler myocardial imaging study.
53. Badano LP, Kolias TJ, Muraru D et al. Standardization of left atrial, right ventricular, and right atrial deformation imaging using two-dimensional speckle tracking echocardiography: a consensus document of the EACVI/ASE/Industry Task Force to standardize deformation imaging.
54. Cameli M, Lisi M Fau - Righini FM, Righini Fm Fau - Tsioulpas C et al. Right ventricular longitudinal strain correlates well with right ventricular stroke work index in patients with advanced heart failure referred for heart transplantation.
55. Lisi M, Cameli M, Righini FM et al. RV Longitudinal Deformation Correlates With Myocardial Fibrosis in Patients With End-Stage Heart Failure.
56. Santamore WP, Dell'Italia LJ. Ventricular interdependence: significant left ventricular contributions to right ventricular systolic function.
57. Yamaguchi S, Li Ks Fau - Harasawa H, Harasawa H Fau - Santamore WP, Santamore WP. Acute alterations in systolic ventricular interdependence-mechanical dependence of right ventricle on left ventricle following acute alteration of right ventricular free wall.
58. Lu KJ, Chen JX, Profitis K et al. Right ventricular global longitudinal strain is an independent predictor of right ventricular function: a multimodality study of cardiac magnetic resonance imaging, real time three-dimensional echocardiography and speckle tracking echocardiography.
59. Park JH, Negishi K, Kwon DH, Popovic ZB, Grimm RA, Marwick TH. Validation of global longitudinal strain and strain rate as reliable markers of right ventricular dysfunction: comparison with cardiac magnetic resonance and outcome.

60. Fine NM, Chen L Fau - Bastiansen PM, Bastiansen Pm Fau - Frantz RP et al. Outcome prediction by quantitative right ventricular function assessment in 575 subjects evaluated for pulmonary hypertension.
61. Muraru D, Onciul S, Peluso D et al. Sex- and Method-Specific Reference Values for Right Ventricular Strain by 2-Dimensional Speckle-Tracking Echocardiography. Circ Cardiovasc Imaging 2016;9:e003866.
62. Morris DA, Krisper M, Nakatani S et al. Normal range and usefulness of right ventricular systolic strain to detect subtle right ventricular systolic abnormalities in patients with heart failure: a multicentre study. Eur Heart J Cardiovasc Imaging 2017;18:212-223.
63. Fine NM, Chen L Fau - Bastiansen PM, Bastiansen Pm Fau - Frantz RP et al. Reference Values for Right Ventricular Strain in Patients without Cardiopulmonary Disease: A Prospective Evaluation and Meta-Analysis.
64. Guendouz S, Rappeneau S, Nahum J et al. Prognostic significance and normal values of 2D strain to assess right ventricular systolic function in chronic heart failure. Circ J 2012;76:127-36.
65. Ichikawa K, Dohi K Fau - Sugiura E, Sugiura E Fau - Sugimoto T et al. Ventricular function and dyssynchrony quantified by speckle-tracking echocardiography in patients with acute and chronic right ventricular pressure overload.
66. Liu B, Dardeer AM, Moody WE, Edwards NC, Hudsmith LE, Steeds RP. Reference ranges and reproducibility studies for right heart myocardial deformation by feature tracking cardiovascular magnetic resonance imaging.
67. Kempny A, Fernandez-Jimenez R Fau - Orwat S, Orwat S Fau - Schuler P et al. Quantification of biventricular myocardial function using cardiac magnetic resonance feature tracking, endocardial border delineation and echocardiographic speckle tracking in patients with repaired tetralogy of Fallot and healthy controls.
68. Gertz RJ, Lange T, Kowallick JT et al. Inter-vendor reproducibility of left and right ventricular cardiovascular magnetic resonance myocardial feature-tracking.
69. Augustine D, Lewandowski Aj Fau - Lazdam M, Lazdam M Fau - Rai A et al. Global and regional left ventricular myocardial deformation measures by magnetic resonance feature tracking in healthy volunteers: comparison with tagging and relevance of gender.
70. Schuster A, Stahnke VC, Unterberg-Buchwald C et al. Cardiovascular magnetic resonance feature-tracking assessment of myocardial mechanics: Intervendor agreement and considerations regarding reproducibility.
71. Smiseth OA, Torp H, Opdahl A, Haugaa KH, Urheim S. Myocardial strain imaging: how useful is it in clinical decision making?
72. Tadic M, Pieske-Kraigher E, Cuspidi C et al. Right ventricular strain in heart failure: Clinical perspective. Arch Cardiovasc Dis 2017;110:562-571.
73. Langeland S, Wouters Pf Fau - Claus P, Claus P Fau - Leather HA et al. Experimental assessment of a new research tool for the estimation of two-dimensional myocardial strain.
74. De Craene M, Marchesseau S Fau - Heyde B, Heyde B Fau - Gao H et al. 3D strain assessment in ultrasound (Straus): a synthetic comparison of five tracking methodologies.

75. Bijnens BH, Cikes M Fau - Claus P, Claus P Fau - Sutherland GR, Sutherland GR. Velocity and deformation imaging for the assessment of myocardial dysfunction.
76. Pavlopoulos H, Nihoyannopoulos P. Strain and strain rate deformation parameters: from tissue Doppler to 2D speckle tracking.
77. Voigt JU, Pedrizzetti G, Lysyansky P et al. Definitions for a common standard for 2D speckle tracking echocardiography: consensus document of the EACVI/ASE/Industry Task Force to standardize deformation imaging. European heart journal cardiovascular Imaging 2015;16:1-11.
78. Mada RO, Lysyansky P, Daraban AM, Duchenne J, Voigt JU. How to define end-diastole and end-systole?: Impact of timing on strain measurements.
79. Zornoff LA, Skali H, Pfeffer MA et al. Right ventricular dysfunction and risk of heart failure and mortality after myocardial infarction. Journal of the American College of Cardiology 2002;39:1450-5.
80. Ghio S, Recusani F Fau - Klersy C, Klersy C Fau - Sebastiani R et al. Prognostic usefulness of the tricuspid annular plane systolic excursion in patients with congestive heart failure secondary to idiopathic or ischemic dilated cardiomyopathy.
81. Chockalingam A, Gnanavelu G Fau - Alagesan R, Alagesan R Fau - Subramaniam T, Subramaniam T. Myocardial performance index in evaluation of acute right ventricular myocardial infarction.
82. Eidem BW, O'Leary Pw Fau - Tei C, Tei C Fau - Seward JB, Seward JB. Usefulness of the myocardial performance index for assessing right ventricular function in congenital heart disease.
83. Gulati A, Ismail TF, Jabbour A et al. The prevalence and prognostic significance of right ventricular systolic dysfunction in nonischemic dilated cardiomyopathy. Circulation 2013;128:1623-33.
84. Sabe MA, Sabe SA, Kusunose K, Flamm SD, Griffin BP, Kwon DH. Predictors and Prognostic Significance of Right Ventricular Ejection Fraction in Patients With Ischemic Cardiomyopathy. Circulation 2016;134:656-65.
85. Damy T, Viallet C, Lairez O et al. Comparison of four right ventricular systolic echocardiographic parameters to predict adverse outcomes in chronic heart failure. Eur J Heart Fail 2009;11:818-24.
86. Puwanant S, Priester Tc Fau - Mookadam F, Mookadam F Fau - Bruce CJ, Bruce Cj Fau - Redfield MM, Redfield Mm Fau - Chandrasekaran K, Chandrasekaran K. Right ventricular function in patients with preserved and reduced ejection fraction heart failure.
87. MacNee W. Pathophysiology of cor pulmonale in chronic obstructive pulmonary disease. Part One.
88. Romano S, Judd RM, Kim RJ et al. Feature-Tracking Global Longitudinal Strain Predicts Death in a Multicenter Population of Patients With Ischemic and Nonischemic Dilated Cardiomyopathy Incremental to Ejection Fraction and Late Gadolinium Enhancement. JACC Cardiovasc Imaging 2018;11:1419-1429.
89. Bourantas CV, Loh Hp Fau - Bragadeesh T, Bragadeesh T Fau - Rigby AS et al. Relationship between right ventricular volumes measured by cardiac magnetic resonance imaging and prognosis in patients with chronic heart failure.

90. Pouleur AC, Rousseau MF, Ahn SA et al. Right Ventricular Systolic Dysfunction Assessed by Cardiac Magnetic Resonance Is a Strong Predictor of Cardiovascular Death After Coronary Bypass Grafting. Ann Thorac Surg 2016;101:2176-2184.
91. Mikami Y, Jolly U, Heydari B et al. Right Ventricular Ejection Fraction Is Incremental to Left Ventricular Ejection Fraction for the Prediction of Future Arrhythmic Events in Patients With Systolic Dysfunction. LID - e004067 [pii] LID - 10.1161/CIRCEP.116.004067 [doi].
92. Vizzardi E, D'Aloia A Fau - Bordonali T, Bordonali T Fau - Bugatti S et al. Long-term prognostic value of the right ventricular myocardial performance index compared to other indexes of right ventricular function in patients with moderate chronic heart failure.
93. Guendouz S, Rappeneau S Fau - Nahum J, Nahum J Fau - Dubois-Rande J-L et al. Prognostic significance and normal values of 2D strain to assess right ventricular systolic function in chronic heart failure.
94. Cameli M, Righini Fm Fau - Lisi M, Lisi M Fau - Bennati E et al. Comparison of right versus left ventricular strain analysis as a predictor of outcome in patients with systolic heart failure referred for heart transplantation.
95. Rouleau JL, Talajic M, Sussex B et al. Myocardial infarction patients in the 1990s--their risk factors, stratification and survival in Canada: the Canadian Assessment of Myocardial Infarction (CAMI) Study. Journal of the American College of Cardiology 1996;27:1119-27.
96. Buxton AE, Lee KL, DiCarlo L et al. Electrophysiologic testing to identify patients with coronary artery disease who are at risk for sudden death. Multicenter Unsustained Tachycardia Trial Investigators. N Engl J Med 2000;342:1937-45.
97. Rihal CS, Nishimura RA, Hatle LK, Bailey KR, Tajik AJ. Systolic and diastolic dysfunction in patients with clinical diagnosis of dilated cardiomyopathy. Relation to symptoms and prognosis. Circulation 1994;90:2772-9.
98. Houard L, Benaets MB, de Meester de Ravenstein C et al. Additional Prognostic Value of 2D Right Ventricular Speckle-Tracking Strain for Prediction of Survival in Heart Failure and Reduced Ejection Fraction: A Comparative Study With Cardiac Magnetic Resonance. JACC Cardiovascular imaging 2019;12:2373-2385.
99. Bonow RO, Lakatos E, Maron BJ, Epstein SE. Serial long-term assessment of the natural history of asymptomatic patients with chronic aortic regurgitation and normal left ventricular systolic function. Circulation 1991;84:1625-35.
100. Enriquez-Sarano M, Tajik AJ, Schaff HV, Orszulak TA, Bailey KR, Frye RL. Echocardiographic prediction of survival after surgical correction of organic mitral regurgitation. Circulation 1994;90:830-7.
101. Bohbot Y, de Meester de Ravenstein C, Chadha G et al. Relationship Between Left Ventricular Ejection Fraction and Mortality in Asymptomatic and Minimally Symptomatic Patients With Severe Aortic Stenosis. JACC Cardiovascular imaging 2019;12:38-48.
102. Calkins H, Corrado D, Marcus F. Risk Stratification in Arrhythmogenic Right Ventricular Cardiomyopathy. Circulation 2017;136:2068-2082.
103. Plana JC, Galderisi M, Barac A et al. Expert consensus for multimodality imaging evaluation of adult patients during and after cancer therapy: a report from the American Society of Echocardiography and the European Association of

Cardiovascular Imaging. European heart journal cardiovascular Imaging 2014;15:1063-93.
104. Grothues F, Smith GC, Moon JC et al. Comparison of interstudy reproducibility of cardiovascular magnetic resonance with two-dimensional echocardiography in normal subjects and in patients with heart failure or left ventricular hypertrophy. The American journal of cardiology 2002;90:29-34.
105. Amzulescu MS, De Craene M, Langet H et al. Myocardial strain imaging: review of general principles, validation, and sources of discrepancies. European heart journal cardiovascular Imaging 2019;20:605-619.
106. Heiberg E, Ugander M, Engblom H et al. Automated quantification of myocardial infarction from MR images by accounting for partial volume effects: animal, phantom, and human study. Radiology 2008;246:581-8.
107. Grothues F, Moon JC, Bellenger NG, Smith GS, Klein HU, Pennell DJ. Interstudy reproducibility of right ventricular volumes, function, and mass with cardiovascular magnetic resonance. American heart journal 2004;147:218-23.
108. Moody WE, Edwards NC, Chue CD et al. Variability in cardiac MR measurement of left ventricular ejection fraction, volumes and mass in healthy adults: defining a significant change at 1 year. Br J Radiol 2015;88:20140831.
109. Moon JC, Lorenz CH, Francis JM, Smith GC, Pennell DJ. Breath-hold FLASH and FISP cardiovascular MR imaging: left ventricular volume differences and reproducibility. Radiology 2002;223:789-97.
110. Nosir YF, Lequin MH, Kasprzak JD et al. Measurements and day-to-day variabilities of left ventricular volumes and ejection fraction by three-dimensional echocardiography and comparison with magnetic resonance imaging. The American journal of cardiology 1998;82:209-14.
111. Otterstad JE, Froeland G, St John Sutton M, Holme I. Accuracy and reproducibility of biplane two-dimensional echocardiographic measurements of left ventricular dimensions and function. Eur Heart J 1997;18:507-13.
112. Thavendiranathan P, Grant AD, Negishi T, Plana JC, Popovic ZB, Marwick TH. Reproducibility of echocardiographic techniques for sequential assessment of left ventricular ejection fraction and volumes: application to patients undergoing cancer chemotherapy. Journal of the American College of Cardiology 2013;61:77-84.
113. Baron T, Berglund L, Hedin EM, Flachskampf FA. Test-retest reliability of new and conventional echocardiographic parameters of left ventricular systolic function. Clinical research in cardiology : official journal of the German Cardiac Society 2019;108:355-365.
114. Barbier P, Mirea O, Cefalu C, Maltagliati A, Savioli G, Guglielmo M. Reliability and feasibility of longitudinal AFI global and segmental strain compared with 2D left ventricular volumes and ejection fraction: intra- and inter-operator, test-retest, and inter-cycle reproducibility. European heart journal cardiovascular Imaging 2015;16:642-52.
115. Kleijn SA, Aly MF, Terwee CB, van Rossum AC, Kamp O. Reliability of left ventricular volumes and function measurements using three-dimensional speckle tracking echocardiography. European heart journal cardiovascular Imaging 2012;13:159-68.

116. Onishi T, Saha SK, Delgado-Montero A et al. Global longitudinal strain and global circumferential strain by speckle-tracking echocardiography and feature-tracking cardiac magnetic resonance imaging: comparison with left ventricular ejection fraction. Journal of the American Society of Echocardiography : official publication of the American Society of Echocardiography 2015;28:587-96.
117. Aurich M, Keller M, Greiner S et al. Left ventricular mechanics assessed by two-dimensional echocardiography and cardiac magnetic resonance imaging: comparison of high-resolution speckle tracking and feature tracking. European heart journal cardiovascular Imaging 2016;17:1370-1378.
118. Singh A, Steadman CD, Khan JN et al. Intertechnique agreement and interstudy reproducibility of strain and diastolic strain rate at 1.5 and 3 Tesla: a comparison of feature-tracking and tagging in patients with aortic stenosis. Journal of magnetic resonance imaging : JMRI 2015;41:1129-37.
119. Graham-Brown MP, Gulsin GS, Parke K et al. A comparison of the reproducibility of two cine-derived strain software programmes in disease states. European journal of radiology 2019;113:51-58.
120. Morton G, Schuster A, Jogiya R, Kutty S, Beerbaum P, Nagel E. Inter-study reproducibility of cardiovascular magnetic resonance myocardial feature tracking. Journal of cardiovascular magnetic resonance : official journal of the Society for Cardiovascular Magnetic Resonance 2012;14:43.
121. Amzulescu MS, Langet H, Saloux E et al. Head-to-Head Comparison of Global and Regional Two-Dimensional Speckle Tracking Strain Versus Cardiac Magnetic Resonance Tagging in a Multicenter Validation Study. Circulation Cardiovascular imaging 2017;10.
122. Hudsmith LE, Petersen SE, Francis JM, Robson MD, Neubauer S. Normal human left and right ventricular and left atrial dimensions using steady state free precession magnetic resonance imaging. Journal of cardiovascular magnetic resonance : official journal of the Society for Cardiovascular Magnetic Resonance 2005;7:775-82.
123. Negishi K, Negishi T, Hare JL, Haluska BA, Plana JC, Marwick TH. Independent and incremental value of deformation indices for prediction of trastuzumab-induced cardiotoxicity. Journal of the American Society of Echocardiography : official publication of the American Society of Echocardiography 2013;26:493-8.
124. Tilemann LM, Heckmann MB, Katus HA, Lehmann LH, Muller OJ. Cardio-oncology: conflicting priorities of anticancer treatment and cardiovascular outcome. Clinical research in cardiology : official journal of the German Cardiac Society 2018;107:271-280.
125. Buckert D, Cieslik M, Tibi R et al. Longitudinal strain assessed by cardiac magnetic resonance correlates to hemodynamic findings in patients with severe aortic stenosis and predicts positive remodeling after transcatheter aortic valve replacement. Clinical research in cardiology : official journal of the German Cardiac Society 2018;107:20-29.
126. Leibundgut G, Rohner A, Grize L et al. Dynamic assessment of right ventricular volumes and function by real-time three-dimensional echocardiography: a comparison study with magnetic resonance imaging in 100 adult patients. Journal of the American Society of Echocardiography : official publication of the American Society of Echocardiography 2010;23:116-26.

127. Meyer P, Filippatos GS, Ahmed MI et al. Effects of right ventricular ejection fraction on outcomes in chronic systolic heart failure. Circulation 2010;121:252-8.
128. de Groote P, Fertin M, Goeminne C et al. Right ventricular systolic function for risk stratification in patients with stable left ventricular systolic dysfunction: comparison of radionuclide angiography to echoDoppler parameters. European heart journal 2012;33:2672-9.
129. Mor-Avi V, Lang RM, Badano LP et al. Current and evolving echocardiographic techniques for the quantitative evaluation of cardiac mechanics: ASE/EAE consensus statement on methodology and indications endorsed by the Japanese Society of Echocardiography. European journal of echocardiography : the journal of the Working Group on Echocardiography of the European Society of Cardiology 2011;12:167-205.
130. Felker GM, Shaw LK, O'Connor CM. A standardized definition of ischemic cardiomyopathy for use in clinical research. J Am Coll Cardiol 2002;39:210-218.
131. Amzulescu MS, Rousseau MF, Ahn SA et al. Prognostic Impact of Hypertrabeculation and Noncompaction Phenotype in Dilated Cardiomyopathy: A CMR Study. JACC Cardiovascular imaging 2015;8:934-46.
132. Pocock SJ, Ariti CA, McMurray JJ et al. Predicting survival in heart failure: a risk score based on 39 372 patients from 30 studies. Eur Heart J 2013;34:1404-13.
133. Rahimi K, Bennett D, Conrad N et al. Risk prediction in patients with heart failure: a systematic review and analysis. JACC Heart failure 2014;2:440-6.
134. Ghio S, Recusani F, Klersy C et al. Prognostic usefulness of the tricuspid annular plane systolic excursion in patients with congestive heart failure secondary to idiopathic or ischemic dilated cardiomyopathy. The American journal of cardiology 2000;85:837-42.
135. Polak JF, Holman BL, Wynne J, Colucci WS. Right ventricular ejection fraction: an indicator of increased mortality in patients with congestive heart failure associated with coronary artery disease. Journal of the American College of Cardiology 1983;2:217-24.
136. Shah PK, Maddahi J, Staniloff HM et al. Variable spectrum and prognostic implications of left and right ventricular ejection fractions in patients with and without clinical heart failure after acute myocardial infarction. The American journal of cardiology 1986;58:387-93.
137. Juilliere Y, Barbier G, Feldmann L, Grentzinger A, Danchin N, Cherrier F. Additional predictive value of both left and right ventricular ejection fractions on long-term survival in idiopathic dilated cardiomyopathy. European heart journal 1997;18:276-80.
138. La Vecchia L, Zanolla L, Varotto L et al. Reduced right ventricular ejection fraction as a marker for idiopathic dilated cardiomyopathy compared with ischemic left ventricular dysfunction. American heart journal 2001;142:181-9.
139. Longobardo L, Suma V, Jain R et al. Role of Two-Dimensional Speckle-Tracking Echocardiography Strain in the Assessment of Right Ventricular Systolic Function and Comparison with Conventional Parameters. J Am Soc Echocardiogr 2017;30:937-946 e6.
140. Cameli M, Righini FM, Lisi M et al. Comparison of right versus left ventricular strain analysis as a predictor of outcome in patients with systolic heart failure

referred for heart transplantation. The American journal of cardiology 2013;112:1778-84.
141. Carluccio E, Biagioli P, Alunni G et al. Prognostic Value of Right Ventricular Dysfunction in Heart Failure With Reduced Ejection Fraction: Superiority of Longitudinal Strain Over Tricuspid Annular Plane Systolic Excursion. Circulation Cardiovascular imaging 2018;11:e006894.
142. Iacoviello M, Citarelli G, Antoncecchi V et al. Right Ventricular Longitudinal Strain Measures Independently Predict Chronic Heart Failure Mortality. Echocardiography (Mount Kisco, NY) 2016;33:992-1000.
143. Motoki H, Borowski AG, Shrestha K et al. Right ventricular global longitudinal strain provides prognostic value incremental to left ventricular ejection fraction in patients with heart failure. Journal of the American Society of Echocardiography : official publication of the American Society of Echocardiography 2014;27:726-32.
144. Cameli M, Bernazzali S, Lisi M et al. Right ventricular longitudinal strain and right ventricular stroke work index in patients with severe heart failure: left ventricular assist device suitability for transplant candidates. Transplantation proceedings 2012;44:2013-5.
145. Santamore WP, Dell'Italia LJ. Ventricular interdependence: significant left ventricular contributions to right ventricular systolic function. Progress in cardiovascular diseases 1998;40:289-308.
146. Yamaguchi S, Li KS, Harasawa H, Santamore WP. Acute alterations in systolic ventricular interdependence-mechanical dependence of right ventricle on left ventricle following acute alteration of right ventricular free wall. Basic Res Cardiol 1993;88:350-61.
147. Sachdev A, Villarraga HR, Frantz RP et al. Right ventricular strain for prediction of survival in patients with pulmonary arterial hypertension. Chest 2011;139:1299-1309.
148. Schmidt B, Dick A, Treutlein M et al. Intra- and inter-observer reproducibility of global and regional magnetic resonance feature tracking derived strain parameters of the left and right ventricle. European journal of radiology 2017;89:97-105.
149. Slutsky RA, Bhargava V, Higgins CB. Pulmonary circulation time: comparison of mean, median, peak, and onset (appearance) values using indocyanine green and first-transit radionuclide techniques. American heart journal 1983;106:41-5.
150. Roy C, Slimani A, de Meester C et al. Age and sex corrected normal reference values of T1, T2 T2* and ECV in healthy subjects at 3T CMR. Journal of cardiovascular magnetic resonance : official journal of the Society for Cardiovascular Magnetic Resonance 2017;19:72.
151. Ricci F, Barison A, Todiere G et al. Prognostic value of pulmonary blood volume by first-pass contrast-enhanced CMR in heart failure outpatients: the PROVE-HF study. European heart journal cardiovascular Imaging 2018;19:896-904.
152. Pocock SJ, Ariti CA, McMurray JJ et al. Predicting survival in heart failure: a risk score based on 39 372 patients from 30 studies. Eur Heart J 2013;34:1404-13.
153. Montant P, Chenot F, Goffinet C et al. Detection and quantification of myocardial scars by contrast-enhanced 3D echocardiography. Circulation Cardiovascular imaging 2010;3:415-23.
154. Houard L, Militaru S, Tanaka K et al. Test-retest reliability of left and right ventricular systolic function by new and conventional echocardiographic and

cardiac magnetic resonance parameters. European heart journal cardiovascular Imaging 2020.
155. Binanay C, Califf RM, Hasselblad V et al. Evaluation study of congestive heart failure and pulmonary artery catheterization effectiveness: the ESCAPE trial. JAMA 2005;294:1625-33.
156. Unverferth DV, Magorien RD, Moeschberger ML, Baker PB, Fetters JK, Leier CV. Factors influencing the one-year mortality of dilated cardiomyopathy. The American journal of cardiology 1984;54:147-52.
157. Stevenson LW, Tillisch JH, Hamilton M et al. Importance of hemodynamic response to therapy in predicting survival with ejection fraction less than or equal to 20% secondary to ischemic or nonischemic dilated cardiomyopathy. The American journal of cardiology 1990;66:1348-54.
158. Zile MR, Bennett TD, St John Sutton M et al. Transition from chronic compensated to acute decompensated heart failure: pathophysiological insights obtained from continuous monitoring of intracardiac pressures. Circulation 2008;118:1433-41.
159. Voors AA, Ter Maaten JM. Tackling Early Heart Failure Deaths and Readmissions by Estimating Congestion. JACC Heart failure 2015;3:894-5.
160. Claussen CD, Banzer D, Pfretzschner C, Kalender WA, Schorner W. Bolus geometry and dynamics after intravenous contrast medium injection. Radiology 1984;153:365-8.
161. Reichek N. Myocardial Strain: Still a Long Way to Go. LID - e007145 [pii] LID - 10.1161/CIRCIMAGING.117.007145 [doi] FAU - Reichek, Nathaniel.